UC Berkeley
UC Berkeley Electronic Theses and Dissertations

Title

Embryonic and Adult Stem Cells Explored through Microfluidics and Biological Manipulation

Permalink

https://escholarship.org/uc/item/3nw4g804

Author

Jabart, Eric Benjamin Pierre

Publication Date

2013

Peer reviewed|Thesis/dissertation

Embryonic and Adult Stem Cells Explored through Microfluidics and Biological Manipulation

by

Eric Benjamin Pierre Jabart

A dissertation submitted in partial satisfaction of the

requirements for the degree of

Joint Doctor of Philosophy
with University of California, San Francisco

in

Bioengineering

in the

Graduate Division

of the

University of California, Berkeley

Committee in charge:

Professor Lydia L. Sohn, co-Chair
Professor Irina M. Conboy, co-Chair
Professor Tejal A. Desai
Professor Matthew B. Francis

Fall 2013

Abstract

Embryonic and Adult Stem Cells Explored through Microfluidics and Biological Manipulation

by

Eric Benjamin Pierre Jabart

Doctor of Philosophy in Bioengineering

University of California, Berkeley

Professors Lydia L. Sohn and Irina M. Conboy, co-Chairs

Part I - A Microfluidic Method for the Selection of Undifferentiated Human Embryonic Stem Cells and *in Situ* Analysis

Conventional cell-sorting methods such as FACS or MACS can suffer from certain shortcomings such as lengthy sample preparation time, cell modification through antibody labeling, and exposure to high shear forces or metallic microparticles. In light of these drawbacks, we have recently developed a novel, label-free, microfluidic platform that can not only sort cells with minimal sample preparation but also enable analysis of cells *in situ*. In contrast to MACS or FACS, cells sorted by our method have very high viability (~90%). In this part of my thesis, I first describe existing antibody-functionalized microfluidic devices for cell sorting as well those designed for human embryonic stem cell (hESC) sorting. I then demonstrate the utility of our platform to sort undifferentiated human embryonic stem cells (hESCs) from a heterogeneous population, achieving ~60% average purity of the cells expressing a marker of interest. I also discuss future strategies to improve sorting efficiency. Overall, our platform technology could be applied to other cell types beyond hESCs and to a variety of heterogeneous cell populations.

Part II – Attenuation of TGF-β Signaling via Incorporation of a Dominant-negative TGF-β Type II Receptor Promotes Improved Muscle Regeneration in Murine Skeletal Myoblasts

Skeletal muscle stem cells known as satellite cells are responsible for muscle regeneration. Upon muscle injury or exercise, quiescent satellite cells become activated, proliferate as myogenic precursors, differentiate into myoblasts, and ultimately fuse into new, multinucleated myofibers. Unfortunately, this paradigm breaks down with aging and multiple factors contribute to a build-up of scar tissue instead of new muscle. Among these negative contributors are some members of the TGF-β family of signaling molecules. After an introduction to muscle regeneration and satellite cells, the adult skeletal muscle stem cells, I will discuss how biomaterials can help improve muscle regeneration and recent advances in combating TGF-β-induced impairment in muscle repair. I will then discuss the work I have done in improving skeletal muscle repair by attenuating the effects of TGF-β signaling via incorporation of a dominant-negative TGF-β type II receptor.

I'd like to dedicate this dissertation to my parents, for their un-ending nagging, questioning of what I'm doing, for the number of times they asked me when I'd graduate – I mean I'd like to thank them for all their support (as I'm sure it seems like they have been supporting me for a long, long, long, long, time). The goal for my next 7.5 years may be to explain to them what in fact I have been doing and to convince them that it was all worthwhile.

There are too many people I need to thank here so I apologize in advance if I leave out someone's name – it's only because I've been around so long and am old and I'm losing my memory – not because you're easily forgettable.

Thanks to my family, my parents, my sister, my aunts and uncles and cousins for their encouragement.

Thanks to my peers: the ICE COLD class of 2006, Anuj, Sam, Jeff, An-Chi, Haroldo, Eugene, Jennifer, Karl, Zach, Lane, Josh, Vi, Jonathan. Thanks to my peers from other years – Ally, Lukasz, Alec, Maria, Emma, Alexis, Kim, Elena, Paul, Martha, Monica, Rebekah, Rich, Deb, John, Ray, Kyle, Tim, Eric, Jeff, Mark, Justyn, Joey.

I'd like to dedicate this thesis in part to our neighbor Martin Graaf who will be missed at graduation.

To Dr. Daniel Py for his warm, overconfidence in me, and his encouragement to not settle for less.

To Amy, Wiktor, and Terry (and everyone else) for helping me launch Big BEAR and bringing some more fun into my time here.

Thank you to Dr. Justin Hanes and the Hanes Lab at Johns Hopkins University for getting me hooked on research and being a great mentor and role model. To all my peers from Hopkins for the support and encouragement (Tim, Tom, Ben, Kaoru, Jung Soo, Junghae, Matt, Nit, Rich, Glenna, Melissa). To Dr. Becky Vonakis for allowing me my first foray into scientific research. To Dr. David Schaffer and Kwang-Il for my first Berkeley research experience. To Dr. Kevin Healy and the Healy lab.

To my countless friends from the I-House from my 4 years there and to the lifelong friends I've made there: Valentine, Nelda, Laurel, Clemency, Matt, Adam, Luis, Nono, Goose, Jeremy, Liv, Virve, JR, Kit, Benji, Julian, Jeff - will be hard to list a few hundred people here! A special thanks to Sheridan and Betsey Warrick for welcoming me into Berkeley and into their home, for great conversations and dinners, and introducing me to the I-House.

Thank you to the GoT and food crowds: Gary, Jess, Greg, Morgan, Andro and our crazy food nights.

To the (board)-gamers: James, DC, Tom and Tom.

To everyone I've played soccer with since returning (over 50 teams since 2006).

Special shout-out to the California wine country for its moral support.

To my partners in Wine: Albs, Jen, Lindsey, Kelly, John, Tenzing, Lowry, Aleks, Renee

To my bro JT for sticking with it and rocking it.

To my friends Sam and Renee for keeping the good times rolling.

To Frankie and our as-of-yet non-existent rock band, and awesome phone messages in French

To D-Co, for his constant harassment and attempts at convincing me that I'm actually successful. Miao, plots, bof, games, ports, Belgian Tuesdays, and whatever's next.

To my roommates: Randall (and Fatima ☺), Sofo Pofo, Sarah, Mike – good food, good company, good times.

To Miss Webster, for her well-intentioned "encouragement".

To my Hopkins crowd and close friends – Leon and Grace, Marina and Adam, Elizabeth and Dan, Danielle, Dave and Jill, Susan, Sarah, and Sarah.

To lifelong FASNY friends: Sebby G, Phil, Simsim, Nico, Alex, Jo, Pierre

To the Madrid crowd: Kitkat and Croquettes, Alfonso and Erika.

To Wendy and Christian for both their scientific support and friendship, and hopefully my future job. Team France all the way!

To Lydia for her constant support and for always looking out for me.

TABLE OF CONTENTS

LIST OF FIGURES

APPENDIX

List of Tables

Acknowledgements

I would like to take this opportunity to thank everyone who has made the work I completed possible.

To my qualifying exam members Drs. Ting Xu, Tejal Desai, Amy Herr, and Song Li thank you for your advice and guidance.

To my committee members Matt Francis and Tejal Desai, thank you for your support and guidance on my projects and through the program.

Thank you to Mary West from the Berkeley Stem Cell Center for training and assistance with microscopy.

Thank you to my labmates in the Conboy Lab: Haroldo, JuLi, Preeti, Jaemin, Sean, Michelle, Rajiv, Amir, Mike for their help, advice, assistance, and making the lab a fun place to be.

Thank you to my labmates in the Sohn Lab: Karthik, Matthew, Matthew, Mustafa, Ally for their advice and and help.

Thank you to all the undergraduate students who have worked with me and been instrumental in helping me complete my work and becoming a better mentor: Sachin for all his hard work, especially on flow cytometry and microfluidic device running, Jimmy for his work on COMSOL modeling, Rui, Bo, and Anad for their great effort in getting their project off the ground, Dina for her persistence and western blotting work, and Vince and Katherine.

A big thank you to Bobby and Corinne for their work on the microfluidic project and for training me in microfabrication.

Another big thanks to Dr. Brett Helms for all his efforts in helping me develop my qualifying exam project and for the training, advice, and guidance he gave me during my time working at the Lawrence Berkeley National Lab's Molecular Foundry.

Thank you to Dr. Irina Conboy for accepting me into her lab, and providing guidance and support during my graduate career.

A huge thank you to Drs. Wendy Cousin and Christian Elabd for being great mentors, teachers, and friends and without whom this work would have been a much less fun experience and probably may not have even been completed.

And to Dr. Lydia Sohn, for her unending support, mentorship, and guidance, for always looking out for me and providing me with the best opportunities for success. Thank you.

Part I

Microfluidic Devices for Cell Sorting –

Sorting of Human Embryonic Stem Cells and in Situ Analysis
Using a Microfluidic Channel

Chapter 1

Microfluidic Devices for Cell Sorting

Introduction

       Fluorescence-activated cell sorting (FACS) and magnetic-activated cell sorting (MACS) have long been the standard for sorting large populations of cells[1]. However, FACS and MACS suffer from a number of shortcomings that can ultimately damage cells. Both FACS and MACS can directly modify cells: FACS through high shear flow rates and antibody conjugation to cell-surface antigens and MACS through conjugation of magnetic Microbeads. These direct conjugation methods can modify cell signaling and fate and affect further analyses on sorted cells[2–6]. The drawbacks associated with FACS and MACS have paved the way for microfluidic devices to address a number of unmet needs and modalities in cell sorting ranging from in-the-field diagnostics to sorting of rare blood cells to manipulation of low-volume, small-cell-number samples[1,7–9]. Microfluidic devices are compact (unlike FACS), often portable, low-cost, simple to create and modify per application, and can be label-free (no direct modification or labeling of cells, e.g. with antibodies). They are thus poised to tackle a wide range of applications. Part I of my thesis will discuss recent advances in microfluidic cell sorting. In Chapter 1, I will introduce antibody-functionalized microdevices for cell sorting and microdevices for human embryonic stem cell sorting. In Chapter 2, I will discuss my work in developing a microfluidic cell sorter for human embryonic stem cells.

1.1 Recent Advances in Microfluidic Devices for Cell Sorting

       Part of the power of microfluidic cell sorting is its ability to tackle sorting problems with a variety of modalities[10]. While microfluidic sorting devices similar to FACS and MACS already exist[1,11–13], hydrodynamic sorting based on particle size and shape[14,15], dielectrophoretic sorting using cell polarity[16,17], and acoustophoretic sorting employing high-intensity sound waves[18] are just a few of the other sorting modalities[1] upon which the community has focused. Of particular interest to the work discussed here are 1) microdevices that employ antibody-functionalized surfaces and 2) those that aim to sort embryonic stem cells. The following sections will describe recent work in these areas.

1.1.1 Antibody-functionalized Microdevices for Cell Sorting

       Unlike FACS and MACS, antibody-functionalized microdevices for cell sorting (AMCS) incorporate the antibody into the microdevices, thereby precluding the initial need to label cells. The removal of traditional labeling steps can save significant time in sample preparation, decrease the time cells spend in suspension (especially if they are negatively affected by being in suspension or dissociated as single cells), and avoid possible negative side effects of labeling cells with antibodies, such as induction of cell signaling or cell death (which is critical for rare samples)[3–6,19]. Such microdevices are also very versatile and can be modified in various ways to improve sorting based on specific applications.

When implementing AMCS, a number of decisions must be made. Most importantly, it is necessary to decide whether positive or negative selection of cells is needed. In positive selection (Figure 1.1a), sorted target cells from a heterogeneous cell population will interact or be capture by the microdevice's functionalized antibodies. In this case, it is important that the target cell-antibody interactions are specific and that non-specific or background interactions are low[1]. With high specificity and affinity antibodies, high capture efficiency can be achieved. Minimizing non-specific interactions (i.e. non-specific capture of non-target cells) will increase the purity of the captured cell population. For positive selection, the highest purity of sorted cells is desired, as non-target cells can confound or make subsequent analyses more difficult. While higher efficiency is obviously better, it may not always be necessary and can sometimes be sacrificed for higher purity. Other issues with positive selection using AMCS include possible activation of cell signaling due to prolonged interactions with functionalized antibodies, or difficulties and complications in the collection of target cells, to name only a few.

As expected, in negative selection (Figure 1.1b), non-target cells are captured and target cells in heterogeneous populations flow through AMCS. In this case, as specific interactions increase, purity increases; as non-specific interactions decrease, efficiency increases. Whereas it may be easier to achieve higher purities with positive selection (to the possible detriment of efficiency), increasing efficiency (percent of total target cells collected) in negative selection (to the detriment of purity) is easier to achieve. Negative selection also has the advantage of not promoting antibody-target cell binding, thereby reducing the possible negative effects of antibody binding and allowing direct collection of target cells for further analysis.

3
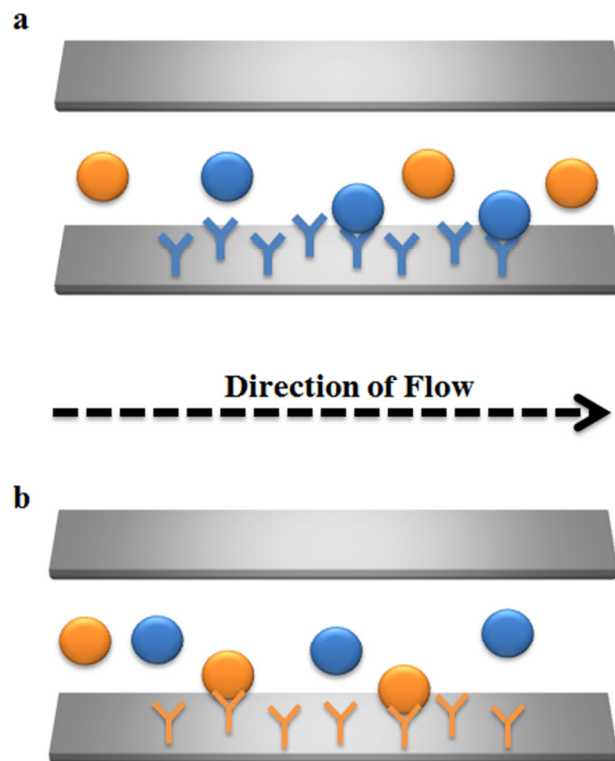
Figure 1.1 a) Target cells (blue) are positively selectively and captured in the AMCS. Negative cells (orange) flow through the channel without capture. b) Non-target cells (orange) are capture in negative selection, and target cells (blue) are collected at the output.

1.1.2 Improving Sorting Efficiency of AMCS

Increasing the efficacy of AMCS to sort cells is of great importance – many such microdevices are often limited by a ~60-70% sorting efficiency[20]. Control of ligand type and orientation, conjugation method, ligand density, and fluid flow through the microdevice are the main avenues for improving efficiency. In terms of ligand type, the choice of antibody (its specificity and affinity) will affect efficiency. Antibody isotypes (e.g. IgG or IgM) have different sizes, conformations, and number of antigen-binding sites and can therefore alter efficiency (see Chapter 2). Replacing antibodies with other ligands such as peptides, proteins, or aptamers is another option[1]. The conjugation method, or how the antibody is attached to the surface, can affect not only the functionality of the antibody, but also its orientation and therefore the display of the antigen-binding sites. By modifying the conjugation strategy (e.g. passive adsorption, conjugation to a silane, conjugation to Protein G, and controlling antibody orientation, increased capture can be achieved[19,21–23]. In order to increase the density of antibodies, several groups have incorporated antibody-coated microposts or other antibody-decorated topographical features and controlled fluid flows to increase antibody-cell interactions[24,25].

In late 2007, a seminal study by Toner et al. showed successful clinical implementation of an antibody-functionalized microfluidic device for rare (1 in 10^9 cells in blood) circulating tumor cell (CTC) sorting[24]. This microdevice used anti-EpCAM-coated microposts and control of fluid flow to increase interactions of CTCs with functionalized antibodies. The optimal flow rate (which affects shear stress and influences cell-antibody adhesion) and the flow profile (optimizing the size and spacing of microposts within the flow to promote cell-antibody interactions) were controlled. The researchers achieved 65% efficiency in spiked samples in phosphate-buffered saline and succeeded in detecting CTCs in 115/116 cancer-patient blood samples. They also showed that their CTC counts correlated well with disease progression of the various cancers they analyzed. Many subsequent AMCS for CTC or other cell sorting have been sprung forth from this study[26].

As discussed above, many groups have struggled with improving sorting efficiency of AMCS above 60-70% for rare-cell populations. This efficiency number, however, should always be correlated with throughput (e.g. the number of cells in a given volume of blood that can be sorted in a specified time). Increasing throughput of AMCS is of critical importance, especially if they are to rival FACS, where throughput can reach upwards of 70,000 cells/s[27–30]. A recent publication by Mittal et al.[20] describes a novel microdevice that incorporates a fluid-permeable antibody-functionalized surface to capture cells at high flow rates (100 µL/min), 20-fold higher than most solid-surface AMCS. In many AMCS, there is no fluid flow mixing, and as cells move farther along devices, they become less likely to interact with antibodies, leading to decreased

4

capture or sorting later in the device. In Mittal et al.'s device, the streamlines direct the flowing cells towards the fluid-permeable antibody-functionalized surface, thereby promoting cell-antibody interactions and increasing capture efficiency compared to solid-surface devices operated at low flow rates (5 µL/min). Furthermore, the use of their fluid-permeable system leads to decreased shear stress at the antibody-functionalized surface, promoting cell rolling, and further enabling efficient cell capture[31,32]. Higher shear stresses, characteristic of solid surfaces (vs. permeable surfaces) lead to greater bond dissociation and therefore a decrease in capture/sorting efficiency[24,33]. While Mittal et al.'s capture efficiency at high-flow rates remains only 60% (when adjusted for non-specific binding) and 55% at low flow rates (accounting for 20% non-specific binding), their new design will likely lead to improved throughput for many AMCS.

1.1.3 Concerns with AMCS

Increasing purity, throughput, and efficiency of AMCS are clearly important tasks, and recent breakthroughs should help improve these numbers. However, the effects of AMCS on cell fate and cell survival are also critical. High shear stresses can damage cells and in certain cases activate signaling pathways[4,34]. Different cell retrieval methods after capture (e.g. increased flow rate/shear, enzymatic release) can also negatively affect cell fate. In AMCS, cells are either captured by antibodies or interact with them transiently, possibly leading to activation of cell signaling pathways. This activation could, in turn, confound downstream analysis of sorted cells. For this reason, AMCS that do not activate cell signaling pathways are clearly advantageous.

1.1.4 A Label-free Antibody-Functionalized Microfluidic Device for Sorting Single Satellite Cells

A recent publication from the Sohn Lab at UC-Berkeley showcases a novel AMCS to analyze the heterogeneity of skeletal muscle stem cells, termed satellite cells[2]. As I contributed to the work and it is relevant here, I will discuss it in more detail.

The AMCS in this case consists of a narrow, antibody-functionalized pore (similar to that described in Figure 1.1) that connects two reservoirs of a polydimethylsiloxane (PDMS)-on-glass microdevice (Figure 1.2a). Using a technique called resistive-pulse sensing (RPS)[21,22,35–37], the current through the pore is recorded. As a cell moves from reservoir to pore back to reservoir, a current pulse is observed (Figure 1.2b). The pulse height corresponds to the size of the cells and the duration of the pulse represents the length of time the cell transits the pore. The microdevice pores were functionalized with either antibodies specific to known/supposed cell-surface markers of satellite cells or their corresponding isotype control (non-specific) antibodies. Cells that expressed surface receptors corresponding to the functionalized antibodies underwent transient interactions with the antibodies leading to longer recorded transit times through the pore. The use

of an AMCS in this case had several advantages over conventional sorting methods. As we demonstrated, the microfluidics employed were better equipped to handle small volumes and small cell numbers and satellite cells represent a rare cell population (only 3-11% of cells within the contour of muscle fibers)[38]. Furthermore, our work was able to directly correlate the myogenic potential of the sorted satellite cells – their ability to form new muscle – with their surface marker expression, all at the single-cell level. Importantly, the advantage of this label-free method was demonstrated as it was also shown that the transient interactions between the cell-surface receptors and the functionalized antibodies did not lead to downstream activation of cell signaling. Future work on this device aims to analyze multiple surface markers at once using a single device[5,39].
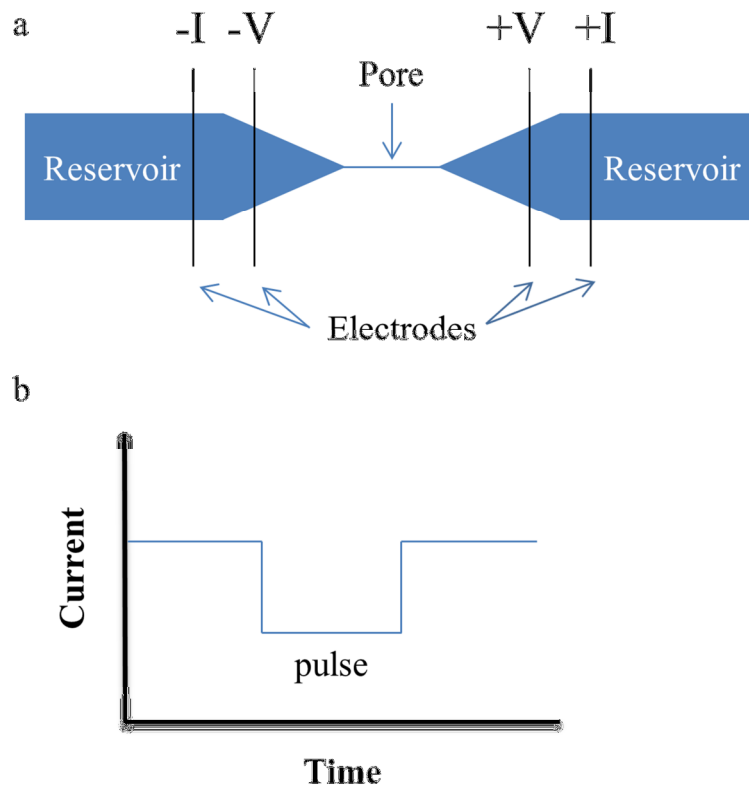
Figure 1.2 a) Schematic of pore device. An antibody-functionalized pore separates two reservoirs. Cells transit from one reservoir to the other through the pore under pressure-driven flow. The current in the channel is monitored via a four-point electrode measurement. Unlike the device described in Figure 1.1, cells are not captured here and only transient interactions with antibodies occur. b) As a cell transits the pore, a current pulse is recorded: the height of the pulse is related to the cell size and the width to the length of time the cell spends in the pore; longer pulse times imply greater interaction between the functionalized antibodies and the cell-surface receptors of the transiting cell.

6

1.1.5 Microdevices for Human Embryonic Stem Cell Sorting

Embryonic stem cells (ESCs) are pluripotent – they have the ability to become any type of cell in our bodies[40]. Repairing degenerating organs or creating new ones is the promise of ESCs[41,42]. Along with this promise, however, come associated concerns: tissue rejection and ethical concerns – that are being addressed by induced pluripotent stem cell (iPSC) research[43,44] – and teratoma (tumor) formation or the creation of ESC-based tumors after implantation[45]. Implanting as few as 500-1,000 undifferentiated ESCs or iPSCs can lead to the formation of a tumor. Numerous protocols have already been developed to differentiate ESCs and iPSCs into a variety of cell types (e.g. neurons, blood, muscle, etc.)[46] and efficient differentiation of potential teratoma-forming cells is therefore essential if the promise of ESC- or iPSC-based tissue engineering applications are to become a reality. Increasing differentiation efficiencies to 100 % or sorting of differentiated stem cell populations – either negatively or positively – are the two main avenues for ensuring the safety of stem-cell-based therapies.

Along with FACS and MACS, microfluidic devices have also sought to tackle the issue of hESC sorting. A recent paper used a combination microfluidic device and optical tweezers to sort fluorescently-labeled hESCs[47]. OCT4-driven Green Fluorescence Protein (GFP)-expressing hESCs flowed into a channel along with GFP$^-$ cells via syringe pump. The microdevice included a mercury lamp and CCD camera in order to excite and detect GFP$^+$ cells. If a GFP$^+$ hESC was detected, optical tweezers were used to displace the cells towards the collection outlet of the microdevice. GFP$^-$ cells would flow through the microdevice and exit through a waste outlet. Using this method, the researchers achieved a 90% recovery rate and 90% purity out of a starting 210 cells. Although efficient, this method required enzymatic release and digestion of hESCs into single cells in addition to fluorescent labeling of the cells. Furthermore a 90% recovery rate, although high, may not be sufficient if large numbers of cells need to be recovered, especially for tissue engineering applications. Since as little as 500-1,000 undifferentiated hESCs can lead to teratoma formation, then after sorting only 10,000 cells, this method would no longer be viable for transplantation therapies. Throughput therefore becomes important as enough cells need to be collected for the specific application while maintaining the number of undifferentiated cells below the critical threshold. At slower flow rates, recovery rates and purity can increase, but only to the detriment of collection times. Longer collection times can have negative effects on cell survival, especially when dealing with hESCs. A happy medium between purity and collection time will have to be struck or other methods of dealing with leftover undifferentiated cells, such as removing them post-sorting[48].

A more recent label-free microdevice used adhesion strength to differentially sort hESCs, iPSCs, partially reprogrammed cells, somatic cells, and differentiated cells derived from hESC or IPSCs[49]. Cell surface-marker expression varies based on the differentiation stage of a cell; in essence, as cells adopt a more dedifferentiated or pluripotent state, surface-marker expression shifts from favoring cell-extracellular matrix (ECM) interactions to favoring cell-cell interactions. This shift in marker expression correlates with a visible reduction in cell spreading

on surfaces: fully-differentiated cells adopt single-cell, spread conformations, whereas hESCs adopt large, compact, colony conformations. Therefore, hESCs and more undifferentiated cells display lower adhesion strengths to ECM-coated surfaces than do differentiating or differentiated cells. The researchers were able to successfully enrich hESCs and iPSCs to 95-99% purity with >80% survival with a mixed population including a fibroblast cell line. They also successfully purified >97% of hESCs and iPSCs when co-cultured with between 6-70% of non-pluripotent cells at various stages of differentiation. This microfluidic technique allowed purification of hESCs without the need to dissociate into single cells (unlike FACS or MACS), which decreases cell survival, and without the use of enzymatic digestion (e.g. trypsin) which has been shown to lead to karyotypic abnormalities[50]. By increasing shear rates, the researchers could release all the undifferentiated cells (although this would increase their proportion of contaminating, differentiated cells), meaning this device could likely serve as a method for removing all undifferentiated, teratoma-forming cells from a heterogeneous culture of hESCs.

Conclusion

While hESCs have been analyzed using microfluidic devices for a variety of applications (2-D or 3-D culture, differentiation, EB formation, biomaterial interactions, etc.)[10], few groups address the issue of sorting. Chapter 2 will discuss a novel, label-free microfluidic device that I have worked on that aimed to positively or negatively sort heterogeneous populations of cells, including hESCs.

Chapter 2

A Microfluidic Method for the Selection of Undifferentiated Human Embryonic Stem Cells and *in Situ* Analysis

Abstract

Conventional cell-sorting methods such as FACS or MACS can suffer from certain shortcomings such as lengthy sample preparation time, cell modification through antibody labeling, and cell damage due to exposure to high shear forces or to attachment of superparamagnetic Microbeads[1–5]. In light of these drawbacks, we have recently developed a novel, label-free, microfluidic platform that can not only select cells with minimal sample preparation but also enable analysis of cells *in situ*. We demonstrate the utility of our platform by successfully isolating undifferentiated human embryonic stem cells (hESCs) from a heterogeneous population based on a particular stem-cell marker. Importantly, we show that, in contrast to MACS or FACS, cells isolated by our method have very high viability (~90%). Overall, our platform technology could be applied to other cell types beyond hESCs and to a variety of heterogeneous cell populations.

Introduction

Conventional cell-sorting methods such as fluorescence-activated cell sorting (FACS) or magnetic-activated cell sorting (MACS) are often used to purify cells from heterogeneous populations using established cell-surface markers[1,5,6]. Both FACS and MACS, however, can require large numbers of cells and, in some cases, adversely affect cells through either required exogenous labeling procedures or the use of high shear flows. Examples of adverse effects include cell death, modification of growth kinetics, or undesired initiation of cell signaling[1,3,7–9]. While FACS and MACS are routinely utilized in sorting hESCs[8–13], there is no doubt that, given their limitations, new technologies would be of strong interest as alternatives to sorting hESCs and other cell types. One viable and obvious candidate for hESC sorting is microfluidics because of its ability to handle/process small sample volumes and the low shear forces to which samples are exposed. Few groups, however, have pursued this direction. Wang et al. used optical tweezers within a microfluidic device to sort OCT4-GFP+ hESCs[14]. More recently, Singh et al. employed extracellular-matrix-coated microfluidic channels to sort undifferentiated and differentiated hESCs based on adhesion strength[8]. They showed that microfluidics-sorted cells had >80% survival vs. FACS-sorted cells, which only had 40% survival.

Here, we showcase a low-shear, label-free, microfluidic platform for isolating a targeted sub-population of cells (in this case, hESCs) from a heterogeneous population. Cell mixtures are passed through an antibody-functionalized microfluidic channel: cells positive for the antibody target remain bound to the channel, while cells that are negative flow through the channel and are collected at the output. Through a Live/Dead® assay, we show that channel-bound cells that are subsequently collected have significantly higher viability than those sorted with either MACS or FACS. Furthermore, we demonstrate our ability to analyze cells *in situ* by immunostaining the hESCs in-channel for a specific marker.

2.1 Materials and Methods

Device fabrication

Figure 2.1a-b shows an image of our platform, which consists primarily of a polydimethylsiloxane (PDMS) mold permanently bonded to a glass substrate. The PDMS mold is created using standard soft-lithography techniques. Briefly, a silicon wafer is spin-coated with SU-8 2100 photoresist (3000 rpm for 30 sec), UV-exposed to a mask to pattern the resist, and then developed with SU-8 developer, thereby creating an 80-µm high negative-relief master. For the results we present here, we utilize the serpentine geometry shown in Figure 2.1b; however, in general, a variety of geometries could be used. De-gassed Sylgard 184 (10:1 prepolymer:curing agent) is then poured onto the master wafer and cured at $80^{\circ}C$ for 2 hours. The PDMS mold is then sliced and removed from the silicon master, cored at the inlet and outlet ports, exposed to oxygen plasma (200 mTorr, 80 W, 30 seconds), and bonded to a clean glass slide that is also exposed to oxygen plasma. The completed device is then heated to $150^{\circ}C$ for 30 minutes to complete permanent bonding.
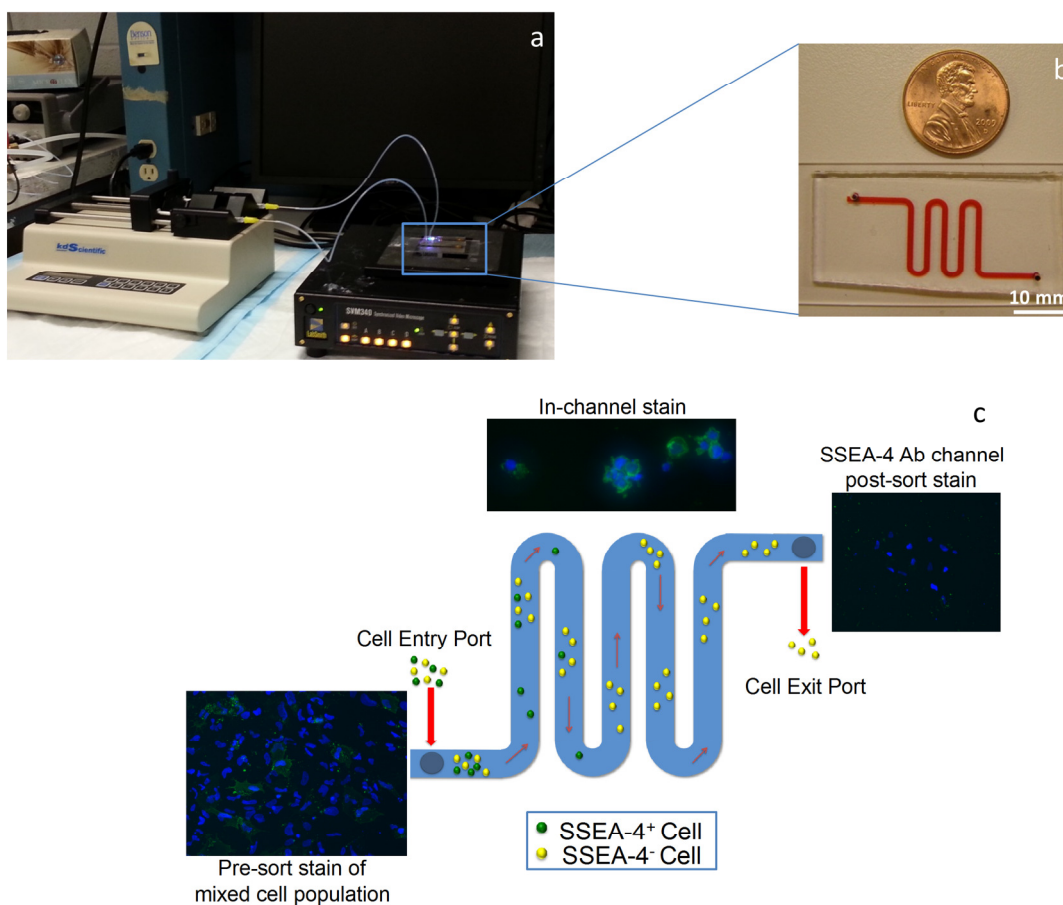
Figure 2.1 a) Two serpentine channels can be run in parallel hooked up to one syringe pump. b) Image of the serpentine channel. The (94 mm x 1 mm x 80 µm) (L x W x H) channel is cored at both ends for inlet and outlet ports. c) A schematic of the device method, using an anti-SSEA-4-functionalized-antibody channel as an example (although any antibody of choice can be used). A mixed population of cells is added at the cell inlet port. The cell outlet port is connected to a syringe pump via plastic tubing. As the cells traverse the device, SSEA-4^{+} cells become bound to the functionalized antibodies and SSEA-4^{-} pass through the device and are collected in the

11

syringe. At the end of the run, the device is washed thoroughly with media to retrieve any unbound cells. Control cells (i.e. those not injected into the channel) and cells passed through the channel and not captured are plated, allowed to adhere to Matrigel-coated plates, fixed, and immunostained for either SSEA-4^{+} or OCT4^{+}. Captured cells are stained and imaged in-channel. The percentage of SSEA-4^{+} or OCT4^{+} captured and not captured cells is then determined.

Device functionalization

Completed devices are initially filled with 1 M NaOH for 10 minutes, rinsed with 18 MΩ de-ionized (DI) water, and dried on a hotplate for 10 minutes at 150°C. The glass surface enclosed by the microfluidic channel is silanized in a humid chamber using N-(3-triethoxysilylpropyl)-4-hydroxybutyramide (Gelest, Morrisville, PA), diluted in a stock solution of 0.01% acetic acid in 95% ethanol and 5% DI water for 4 hours at room temperature (RT), as done previously[1,15]. Channels are then rinsed with stock solution and DI water and subsequently dried and cured for 2 hours at 120°C. Silane-coated serpentine channels are incubated with the homo-bifunctional amine crosslinker sulfo-EGS (Pierce, Rockford, IL) at 3 mg/mL in PBS for 20 minutes at RT. Protein G (1.00 mg/mL) or Protein L (1.66 mg/mL) (Pierce) is then crosslinked to the silanized surface by incubation for 4 hours in a humid chamber. Finally, antibodies (SSEA-1, SSEA-4, mouse IgG₃, mouse IgM, Tra-1-81 – all obtained from Biolegend, San Diego, CA), diluted to 1.33 µM for IgG isotype antibodies (which are bound by Protein G) and to 556 nM for IgM isotype antibodies (undiluted stock concentration, which are bound by Protein L), are linked to the surface by overnight incubation at 4°C.

COMSOL modeling of shear rates in microchannel

The shear rates in the microfluidic channel were modeled using the COMSOL microfluidics module (COMSOL Inc., Palo Alto, CA). Laminar flow was assumed, and the channel was simulated using input flow rates of 2, 5, and 10 µL/min. Since shear increases closer to the edges of the microchannel (within the first 10 µm), the mesh resolution was selected in order to highlight the effects in the boundary layer.

Cell Culture

hESCs

H9 human embryonic stem cells (hESCs) (WiCell Research Institute, Madison, WI) were cultured on BD Matrigel hESC-qualified Matrix (BD Biosciences, San Jose, CA) in mTeSR1 basal medium with 5X supplement (STEMCELL Technologies, Vancouver, Canada). Cells were routinely passaged, as per the manufacturer's protocol. For single-cell dissociation of colonies, H9s were washed briefly with PBS, incubated at 37°C for 12 minutes with 2 mM EDTA in PBS (Invitrogen, Carlsbad, CA), and gently triturated. Cells were sedimented and re-suspended as single cells in fresh medium before passing through the microchannels (final concentration 2,000-2,500 cells/µL).

A549s

A549 lung carcinoma cells (ATCC, Manassus, VA) were cultured in DMEM supplemented with 10% FBS and 1 X penicillin/streptomycin and routinely passaged, as per the manufacturer's protocol. A549s were dissociated by treatment with 0.25% trypsin/EDTA for 3 min at 37°C, neutralized with media, sedimented, and re-suspended at 500 cells/µL before passing through microchannels.

mESCs

Murine embryonic stem cells (J1 mESCs: J1s, ATCC # SCRC-1010) previously maintained on a murine embryonic fibroblast layer were cultured for 3-4 passages on 0.1% gelatin (in PBS) in DMEM (high glucose) (Invitrogen, Carlsbad, CA), supplemented with 2 mM GlutaMAX-I Supplement (Invitrogen), 1 mM MEM Sodium Pyruvate Solution (Invitrogen), 0.1 mM MEM Non-Essential Amino Acids Solution (Invitrogen), 1 X penicillin/streptomycin Dual Antibiotic Solution (Fisher, Pittsburgh, PA), 55 µM 2-Mercaptoethanol (Invitrogen), 15% FBS (KO SR, Invitrogen) and 1000 U/mL ESGRO LIF (Millipore, Billerica, MA). mESCs were dissociated into single cells by incubation with 0.25% trypsin/EDTA for 3 minutes at 37°C, sedimented, and re-suspended at 2,500 cells/µL before passing through prepared microchannels.

Device operation

Antibody-functionalized microchannels were brought to RT, rinsed once with PBS, and then equilibrated in the appropriate media for 30 minutes. Homogeneous or heterogeneous cell populations were diluted to 2,500 cells/µL in their respective media at an equal ratio to the cell distribution (e.g. a 4:1 mixture of hESCs: A549s contained 2,000 cells/µL hESCs and 500 cells/µL A549s in 80% mTeSR1/20% DMEM media). 35 µL of the cell suspension (~87,500 cells) flowed through the channels at 2 µL/min via a syringe pump and collected for further analysis (Figure 2.1b). The channels were then washed with 15 µL of media at 5 µL/min and then 30 µL of media at 10 µL/min to remove unbound cells. A visual inspection of the entire microchannel ensured that all unbound cells were removed.

Immunostaining

Control cells (i.e. cells that did not run through the channels), channel flow-through cells, and channel-bound hESCs were immunostained for SSEA-4 and OCT4, two markers of undifferentiated stem cells. Briefly, cells were washed once with PBS, fixed for 15 minutes at RT in 4% paraformaldehyde, washed three times with staining buffer (SB: 1% bovine growth serum, 1 mg/mL sodium azide in 1X PBS), permeabilized (for internal staining only) with 0.25% Triton X-100 in SB, washed three times in SB, and labeled with primary antibodies for 2-4 hours at RT or overnight at 4°C at manufacturer-recommended dilutions. Cells were then washed 3 times with SB, incubated for one hour in the dark at RT with fluorophore-conjugated secondary antibodies (Molecular Probes) and Hoechst at 2 µM, washed three times with SB, and either imaged (for the in-channel staining) or mounted with Fluoromount (Sigma-Aldrich, St. Louis, MO) for imaging. Images were taken using a fluorescent microscope.

MACS

J1 mESCs were sorted using MACS anti-IgM or anti-SSEA-1 Microbeads (Miltenyi, Auburn, CA). Following the manufacturer's protocol for MACS preparation, single-cell J1s were

centrifuged at 300 g for 10 minutes and re-suspended in 80 µL of MACS buffer per 10^7 cells (or the total amount of cells if less than 10^7). 20 µL of anti-IgM or anti-SSEA-1 Microbeads were then added and incubated with the cells for 15 minutes at 4°C. The cells were then washed twice with 2 mL of MACS Buffer and re-suspended in 500 µL of MACS Buffer. After magnetic-column preparation, cells were added. Flow-through cells were collected by gravity; bound cells were collected by manually applying pressure via a 5 mL syringe plunger. A Live/Dead® viability assay was immediately performed with the collected cells (see Viability assay).

FACS

FACS for the SSEA-1 antigen on J1 mESCs was completed using established protocols for indirect immunofluorescence[16]. J1 mESCs were washed and incubated with 0.25% trypsin/EDTA for 3 min at 37°C, washed with PBS, and re-suspended in a PBS solution with 10% FBS at a concentration of 10^6 cells/mL. 100 µL of the suspension was incubated with either anti-SSEA-1 or the corresponding IgG control antibody for 30 minutes at RT. The suspension was then collected and washed 3 times by centrifugation at 400 g for 5 minutes and resuspended in the PBS solution with 10% FBS. Cells were then incubated with fluorescently-labeled secondary antibodies for 30 minutes at RT in the dark, and again washed 3 times. On the final wash, cells were resuspended in PBS and collected for FACS. Although higher cell viability is often achieved by keeping cells on ice during a staining procedure, we did not observe any negative effects by staining at RT. In fact, attempts to stain cells on ice led to poor fluorescent signal, which was increased only upon staining at RT. Our results are consistent with published literature on the poor ESC cell survival after FACS sorting[8,17].

J1 mESCs were sorted in a MoFlo Legacy (2002) high-performance cell sorter (Beckman Coulter, Miami, FL) equipped with a Coherent Inc. Innova 90 argon ion-gas laser (Santa Clara, CA) tuned for 488 nm light emission and running at 200 mW. PE fluorescence was directed to a PMT detector using a 605 nm dichroic short pass filter and a 555 nm dichroic long-pass to a 580 nm band-pass optical filter with a bandwidth of 30 nm (Omega Optical, Brattleboro, VT). The MoFlo cell sorter ran at a pressure of 50 psi with a 70 µM flow-cell tip. Samples were maintained at 4°C while being sorted.

Viability assay

Unsorted and sorted (via MACS, FACS, or microchannel) mESCs were analyzed by Live/Dead® Assay (Invitrogen, Carlsbad, CA), per the manufacturer's protocol and as previously described[18–23]. Collected cells from each assay were sedimented by centrifugation for 5 minutes at 300 g, washed once with PBS, spun again for 5 minutes at 300 g, and re-suspended in 1 mL of PBS. A 150 µL aliquot of cells was then allowed to settle briefly on a cover slip. 150 µL of Live/Dead® reagent (2 µM calcein AM and 4 µM ethidium homodimer 1 in PBS) was added to the cover slip and incubated in the dark for 45 minutes at RT. The cover slip was then flipped onto a glass slide and imaged as previously described. Live (green) and dead (red) cells were counted. Over 2000 cells were counted in each case. For FACS-sorted cells, distinguishing dead cells (ethidium homodimer 1, red) vs. SSEA-1-labeled cells (PE) was readily achieved based on the greater intensity of the fluorescent signal for dead cells, the clear nuclear localization of the signal and the absence vs. presence of green fluorescence (Figure 2.2).

14
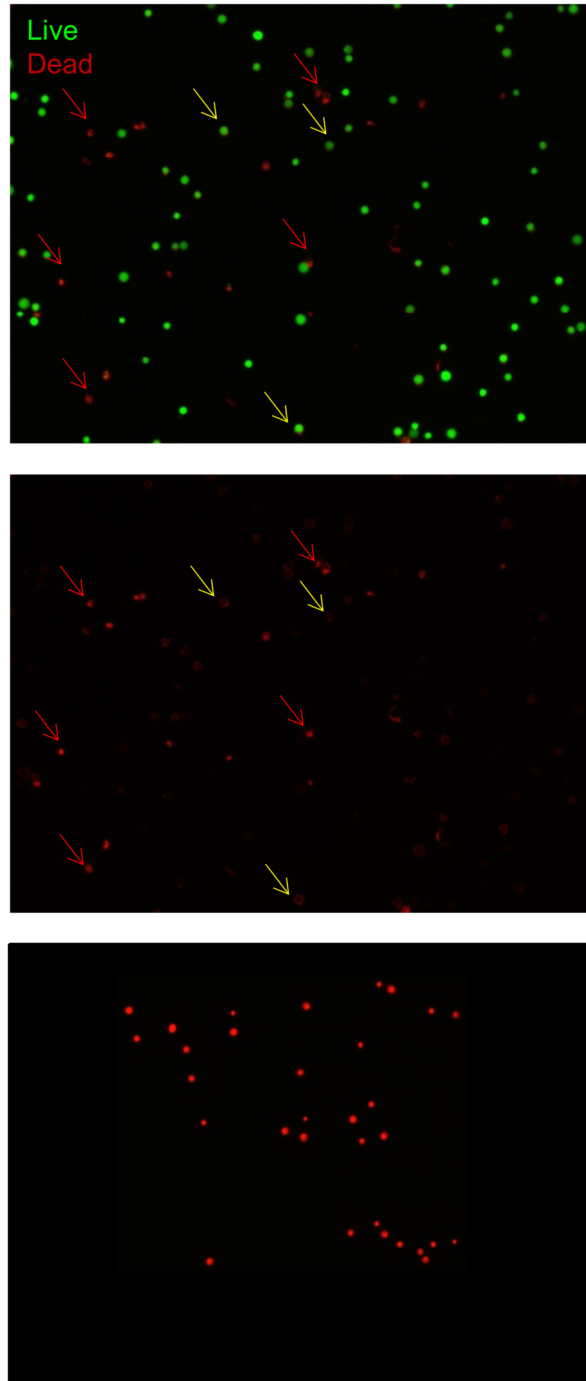
Figure 2.2 Fluorescent images of Live (green) / Dead (red) cells after SSEA-1$^+$ FACS sorting. Cells labeled with PE (yellow arrows) show only faint, background fluorescence, along the cell membrane and are robustly green, i.e. live, whereas dead cells (red arrows) are bright and nuclear stain is clear, while the green, live signal is undetectable. The dead cell control image shows that ethidium homodimer 1 stained cells (red) do not have background levels of staining and are always bright and nuclearly-stained.

15

2.2 Results

Flow-through and bound cells from anti-SSEA-1 Microbeads show decreased survival

Figure 2.3a shows the effects of MACS sorting on mESC cell viability. Cells from the anti-IgM Microbead flow-through showed no significant decrease in viability after MACS sorting. Intriguingly, cells incubated with anti-SSEA-1 Microbeads, whether from the flow-through or the bound fraction, showed a significant 30% decrease in cell survival as compared to the control condition in repeated experiments.

SSEA-1-labeled cells also show a decrease in survival via FACS

Figure 2.3b shows the percentage of cell survival after FACS normalized to unsorted cells maintained in media. Cells incubated with IgM or cells negative for SSEA-1 that had been incubated with anti-SSEA-1 antibodies and sorted by FACS showed a small decrease in viability (16% and 12%, respectively). However, SSEA-1$^+$ cells labeled with anti-SSEA-1 antibodies and sorted by FACS had an almost 45% decrease in cell survival as compared to the control cells maintained in media. This decrease in cell viability might be explained by the possible negative effects of antibody binding[1–5].

Positively-selected cells show increased survival

While both MACS and FACS showed a decrease in the survival of SSEA-1-selected cells, positively-selected cells in our serpentine channel (i.e. collected bound cells) showed an approximate 90% viability as compared to control cells (i.e. cells that did not run through the channels) (Figure 2.3c), indicating the channels preferentially bind viable cells. Cells that flowed through IgM-coated microchannels showed a 10% decrease in viability as compared to control cells, suggesting that running cells through channels may lead to a slight drop in viability. Cells that ran through anti-SSEA-1-functionalized channels showed a 47% decrease in viability. However, while it is unavoidable that some cell death occurs in our microfluidic channels (as shown by our IgM control channel results), a portion of the significant decrease in viability here may also be attributed to the capture of live cells by the anti-SSEA-1 channel, thereby leading to a reduced ratio of viable to dead cells in the overall flow-through population. This decrease would be dependent on the number of viable cells captured in the channel relative to the total population. Future work focusing on the total number of viable cells captured in the channels and those collected at the output could quantitatively determine the contribution of captured viable cells to the overall decrease in viability observed in the SSEA-1 flow-through case. As well, such future work could also determine whether running cells through an anti-SSEA-1 channel is more detrimental to cell viability than control channels. Nonetheless, the important result here is that the viability of positively-selected cells in the channel is very high and greater than that using either FACS or MACS.

Improved capture of hESCs with anti-SSEA-4-functionalized channels

When mixed populations of 4:1 hESCs and A549s were passed through anti-SSEA-4-functionalized channels, >90% of the cells captured in the channel were SSEA-4$^+$, as confirmed by in-channel staining of either OCT4 or SSEA-4 (Figure 2.4). Their SSEA-4 expression was

similar to stained control hESCs (data not shown). The percentage of hESCs in the mixed population before running was compared to the percentage of hESCs in the

a
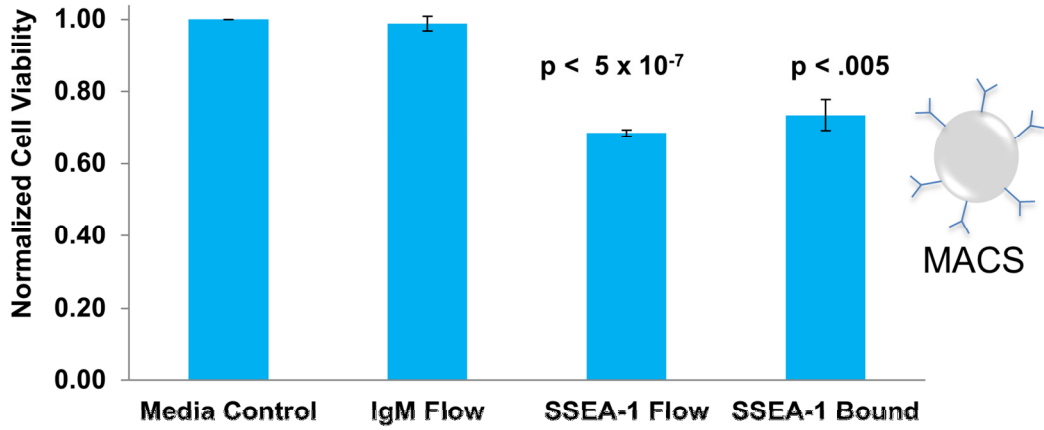
b
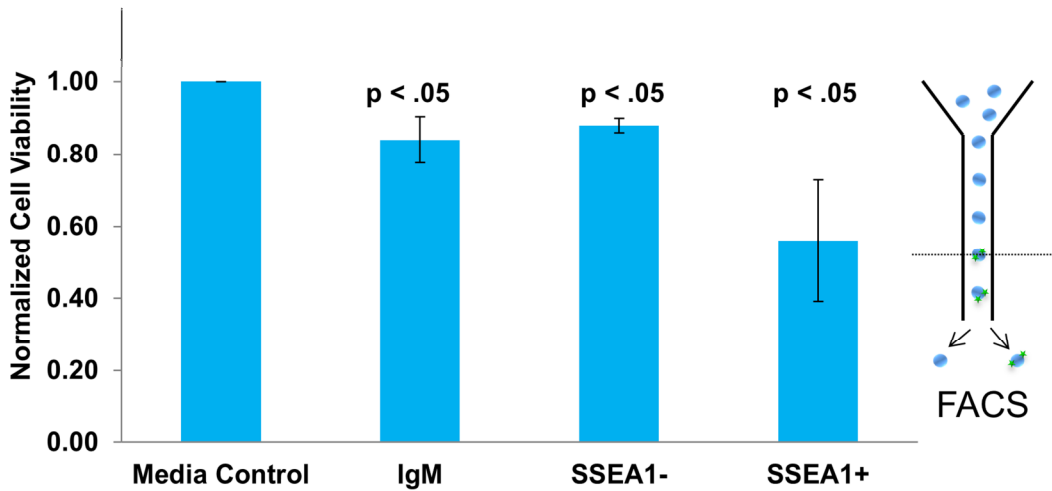
c
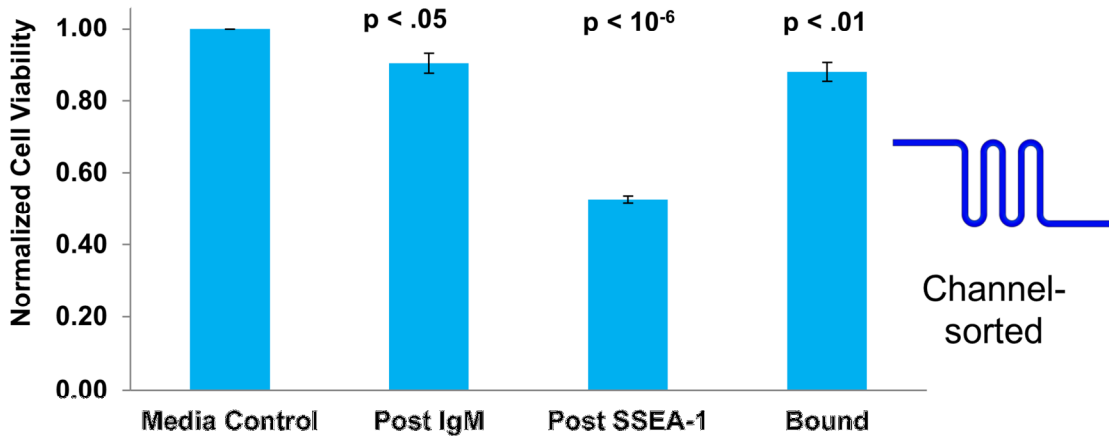
Figure 2.3 Comparison of cell viability using MACS, FACS, and our microfluidics-based method. J1 mESCs cells were employed in all three methods and assayed for viability using a Live/Dead® assay. Average values from 3 independent experiments were normalized to results from cells that were maintained in media. Error bar corresponds to standard error. A) MACS: Assayed cells were collected under the following conditions: anti-IgM Microbeads (flow-through) and anti-SSEA-1 Microbeads (both flow-through and bound fractions). B) FACS: Assayed cells were those incubated with anti-IgM and those positively and negatively sorted for SSEA-1. C) Microfluidic isolation: Assayed cells were those that traversed anti-IgM- or anti-SSEA-1-functionalized antibody channels, as well as bound cells recovered from anti-SSEA-1-functionalized channels.
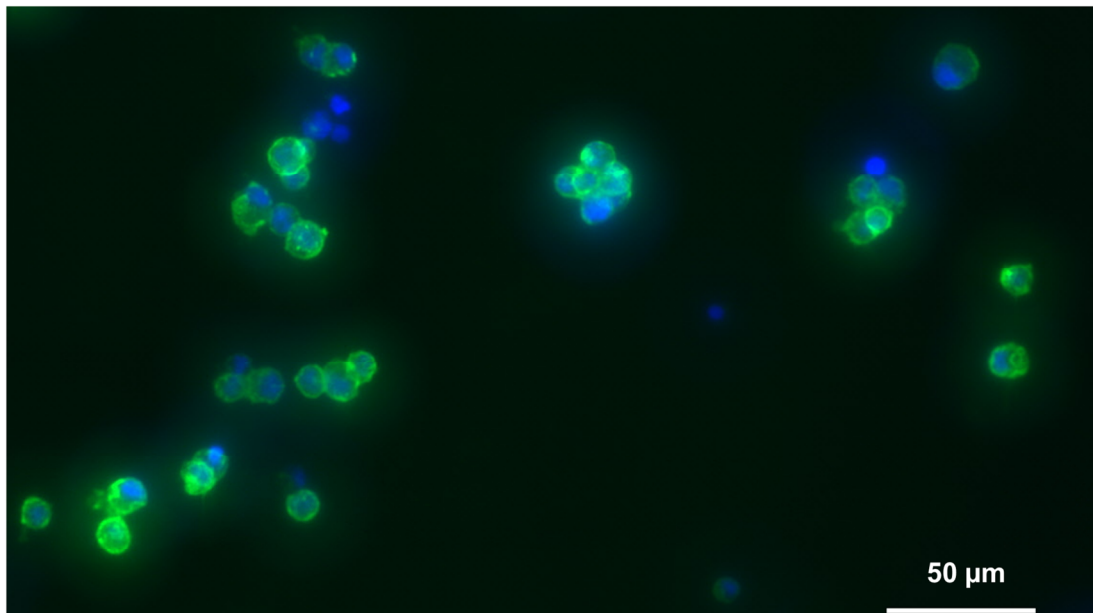
Figure 2.4 hESCs bound inside an anti-SSEA-4-functionalized channel were stained for SSEA-4 (green) and Hoechst (blue). More than 90% of cells stained positive for SSEA-4.

cell population collected after the microchannel run (either through IgG- or anti-SSEA-4-coated channels), based on either SSEA-4 or OCT4 expression. This difference was normalized over the various runs to generate Figures 2.5a-b. Overall, we demonstrate a 60% reduction in the number of hESCs in our mixed population. Improvements in cell capture could increase this efficiency. A visual inspection of all the isotype control antibody channels showed that no cells bind at any time during sorting. Thus, binding in the specific antibody channels is indeed based on specific interactions between the SSEA-4 antibodies and the hESC cell-surface SSEA-4 antigen.

Capture of hESCs with anti-Tra-1-81-functionalized channels

hESCs were mixed at a 4:1 ratio with A549 cells and passed through serpentine channels functionalized with anti-Tra-1-81, another marker of undifferentiated hESCs. Cell mixtures were immunostained for the undifferentiated hESC marker OCT4 and the percent of hESCs in the pre-channel and post-channel cell populations was determined. As shown in Figure 2.5c, only a 32%

reduction in the percentage of hESCs was obtained using Tra-1-81. This lower capture efficiency is explained in Discussion.
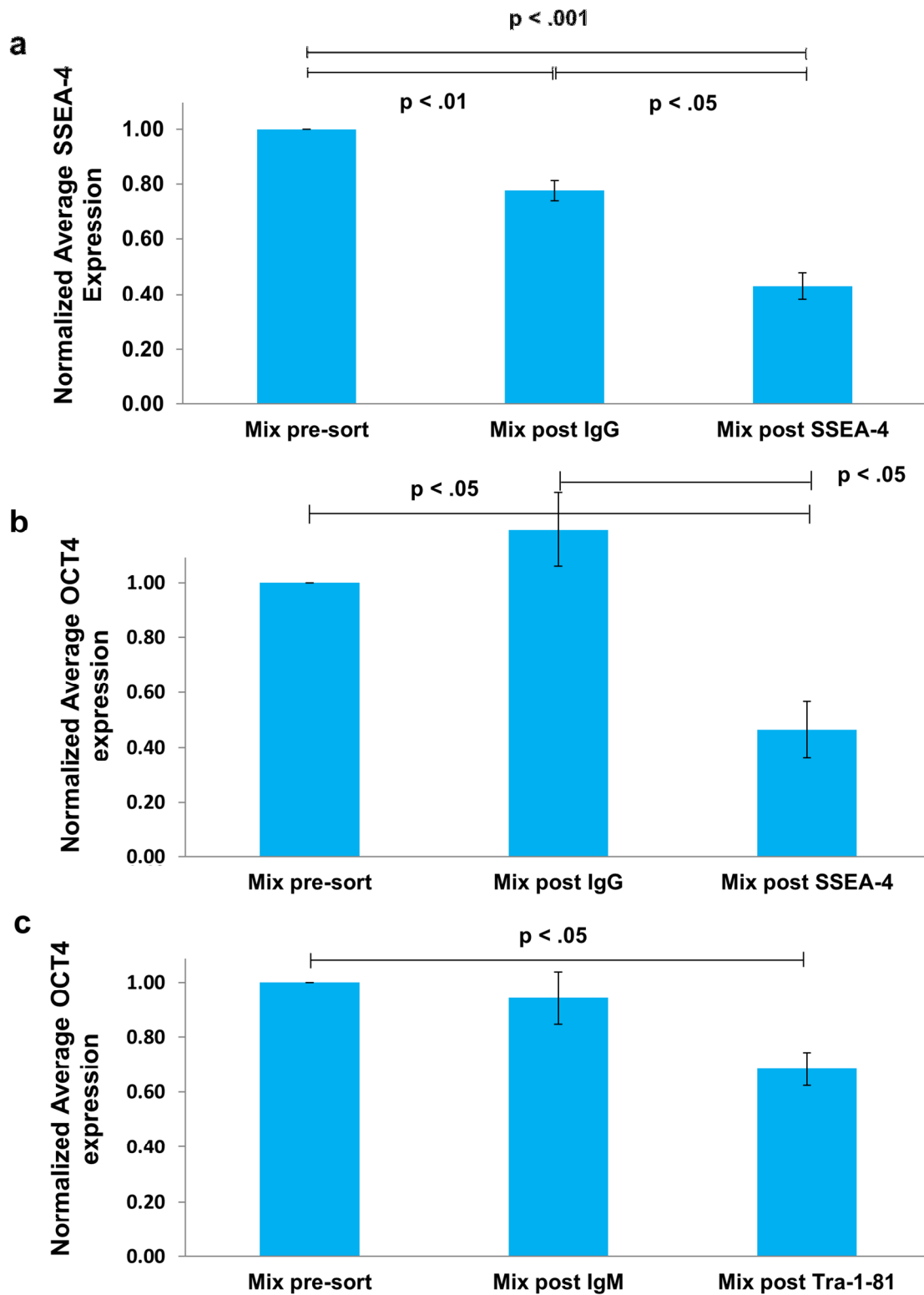
Figure 2.5 a) Normalized average SSEA-4 expression for microchannel runs. A 4:1 ratio of hESCs to A549 were passed through either anti-IgG or anti-SSEA-4-functionalized channels. Control cells (those that do not run through any channel), and cells recovered after traversing either through anti-IgG channels or anti-SSEA-4 channels were plated and stained for the undifferentiated hESC marker, SSEA-4. Average values from 5 independent experiments were normalized to the fraction of SSEA-4 positive control cells. Error bars represent standard error. b) Normalized average OCT-4 expression for microchannel runs. A 4:1 ratio of hESCs to A549 were passed through either anti-IgG or anti-SSEA-4-functionalized channels. Control cells, cells recovered after anti-IgG channels, and cells recovered after anti-SSEA-4 channels were plated and stained for the undifferentiated hESC antigen OCT4. Average values from 4 independent experiments were normalized to the fraction of SSEA-4 positive control cells. Error bars represent standard error. c) Normalized average OCT4 expression for microchannel runs. A 4:1 ratio of hESCs to A549 was passed through either anti-IgM or anti-Tra-1-81-functionalized channels. Control cells, cells recovered after anti-IgM channels, and cells recovered after anti-Tra-1-81 channels were plated and stained for the undifferentiated hESC marker OCT4. Average values from 3 independent experiments were normalized to the fraction of OCT4 positive cells in the control cells. Error bars represent standard error.

Shear rate modeling in microchannels using COMSOL

Shear rates in the device were modeled using COMSOL (Figure 2.6). At our running flow rate of 2 µL/min, the average shear rate was 14.9 s^{-1}, increasing up to 37.3 s^{-1} at 5 µL/min and 74.6 s^{-1} at 10 µL/min during washes. At 2 µL/min, the shear rate increases to 27 s^{-1} for cells along the edges of the device; in the curves, the shear rate ranges from 21 s^{-1} to 36 s^{-1} from the exterior to the interior. Likewise, at 5 µL/min the peak shear rate is 91 s^{-1} toward the interior of the curves and at 10 µL/min the maximum is 183 s^{-1}. The shear rates experienced by cells are all on the lower end of what are typically experienced in microcirculation[24].
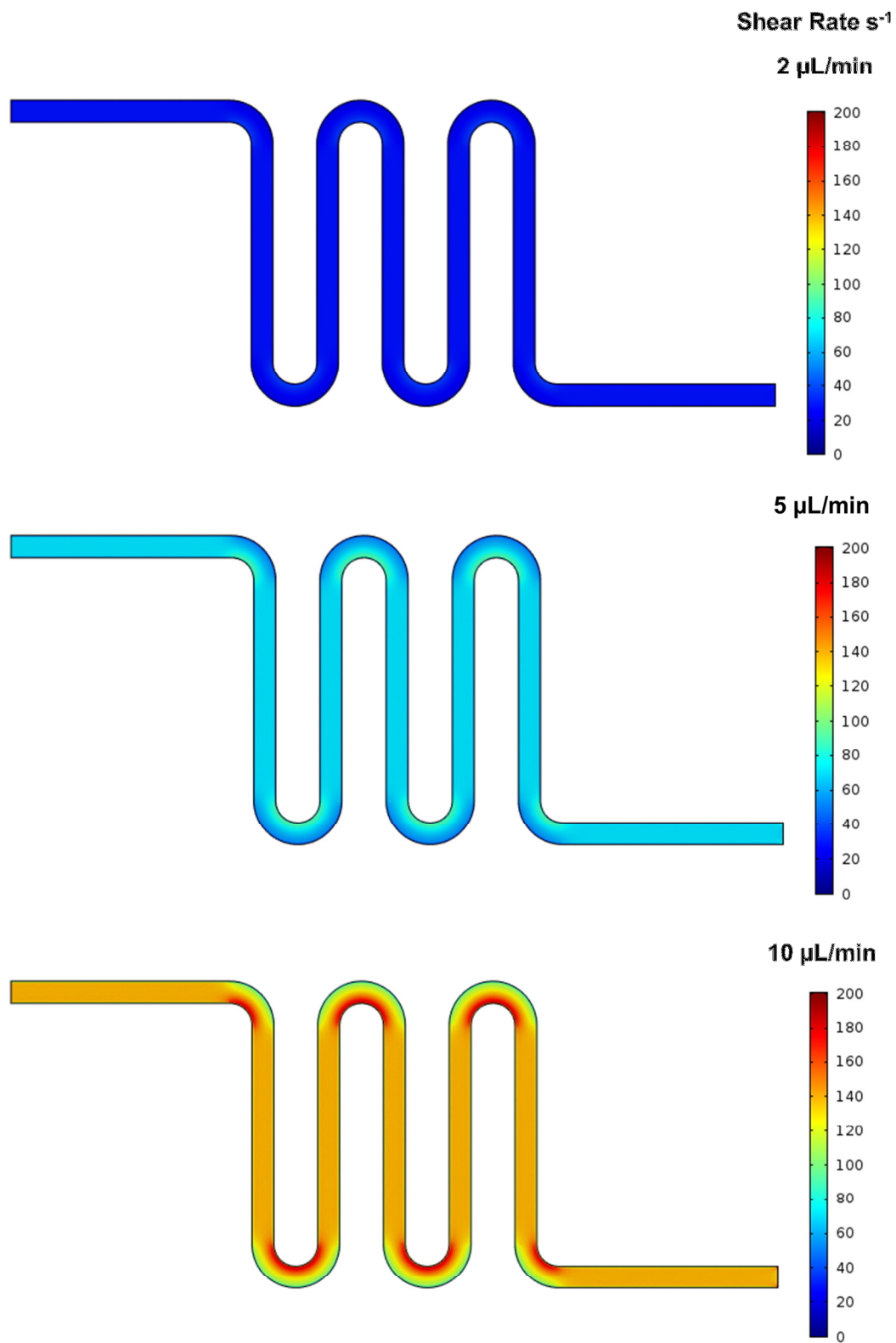
Figure 2.6 COMSOL-modeled shear rates in the microfluidic device at the running flow rate of 2 µL/min and the two washing flow rates, 5 µL/min and 10 µL/min.

Discussion

FACS and MACS have long been the standard for numerous cell-sorting applications. However, their associated constraints – the preference for large numbers of cells, exogenous labeling, high-shear stresses, high cost (for FACS), and interaction with superparamagnetic Microbeads (for MACS) – have paved the way for microfluidics to address cell sorting in novel ways. The microfluidic method we described here can be used to positively select cells from a mixed population. Moreover, our method requires little sample preparation, as cells can be sorted under low shear forces, without any labeling, and either analyzed *in situ* by immunostaining in the microchannel, or retrieved for subsequent analysis.

Our microfluidic method provides a number of advantages over conventional sorting methods such as FACS and MACS. Once cells are dissociated into single cells, they are ready to be injected into the device. Unlike FACS and MACS, sample preparation does not require direct labeling of cells with antibodies or superparamagnetic Microbeads. The only preparation involved is dissociating and collecting the cells, a step common to all three sorting methods. Running two microdevices simultaneously takes only 30 minutes, with only 30 minutes of cell sample preparation time, as just described; for MACS, cell labeling with Microbeads takes up to 1.5 hours, followed by over an hour of sorting; for FACS, cell preparation time is up to 3 hours followed by 2 hours of sorting. The percentage of live cells retrieved after being captured in our device is also greater than that achieved with either MACS or FACS, suggesting a gentler treatment of cells. This is an especially important feature when there is a need to sort/isolate cells which are few in number or are negatively affected by lengthy processing times in suspension. Moreover, our device also allows for further *in situ* analysis of our selected cells (e.g. in-channel staining for cell-surface markers). Although MACS and FACS have greater throughput, running parallel arrays of prepared microfluidic channels could greatly augment throughput of our method. In addition, in situations where cell numbers are limited and starting populations are minute (e.g. analysis of ESC populations from pre-implantation embryos), our microfluidic-based cell separation and analysis could become very valuable.

Selected cell capture with anti-Tra-1-81 vs. anti-SSEA-4-functionalized channels

Both Tra-1-81 and SSEA-4 are expressed in hESCs[25–27]. However, as shown in Figure 2.5, the anti-Tra-1-81 channels show a decreased efficiency in hESC capture. This decrease may be explained by the combination of several factors: 1) decreased antibody surface density, 2) less favorable antigen-binding-site display – both of which are correlated with the antibody isotype used for functionalization; and 3) heterogeneity of hESC surface-marker expression and localization of receptors on the cell surface.

To understand the effects of antibody surface density on capture efficiency, we estimated the functionalized-antibody density in the channels, N_{Ab}[15,28] to be,

$$N_{Ab} = 0.7 \, [Ab] \, V_p \left(\frac{A_v}{A_p M_w} \right)$$

where [*Ab*] is the antibody concentration used to functionalize the channels, V_p is the total channel volume, A_v is Avogadro's number, A_p is the total glass surface area that is

functionalized, and M_w is the molecular weight of the antibody. As previously described by Cozens-Roberts et al. and Clausen, we also assume that only 70% of antibodies bind to the surface[28,29]. For the channels functionalized with IgG-isotype antibodies and IgM-isotype antibodies, we therefore obtain N_{Ab} ~ 4.5 x 10^4 antibodies/µm^2 and N_{Ab} ~ 1.87 x 10^4 antibodies/µm^2, respectively. Considering that IgG antibodies and IgM antibodies have a hydrodynamic radius of 5.29 nm and 12.65 nm, respectively[30], then the maximum theoretical antibody coverage we could obtain in a single antibody layer would be 1.14 x 10^4 antibodies/µm^2 and 1.99 x 10^3 antibodies/µm^2, respectively. We are therefore functionalizing our devices at saturating concentrations. In addition, based on these calculations, we estimate that IgM-isotype-functionalized channels have ~6-fold fewer antibodies than their IgG-isotype-functionalized counterparts. Although IgM-isotype antibodies have 5-times more antigen-binding sites than their IgG counterparts, not all sites will bind cells thereby reducing the capture efficiency in the anti-Tra-1-81 channels (IgM-isotype).

In regard to the effects of antigen-binding-site display, the functionalization differences between IgG- and IgM-isotype antibodies may also contribute to reduced capture efficiency. In the functionalization strategy, IgG-isotype antibodies (such as SSEA-4) were conjugated to the surface via Protein G, which has two Fc-binding domains. The SSEA-4 antigen-binding sites, which are far from the Fc region, are then free to bind SSEA-4 receptors on the hESCs. For the IgM-isotype antibodies (such as Tra-1-81), Protein L has four immunoglobulin-binding domains per protein. However, Protein L interacts with the kappa light chain on antibodies, which is closer to the antigen-binding site than the Fc region. The IgM antibodies, pentamers of IgGs, which have a significantly larger hydrodynamic radius (12.65 nm as compared to 5.29 nm for IgG)[30] may then present a less favorable display of the binding sites for Tra-1-81 on hESCs, and consequently contribute to our lower capture efficiency.

Although undifferentiated hESC markers are well-characterized, it is also clear that there exists significant heterogeneity between hESC lines and even within pluripotent hESC populations from the same line[27,31–33]. Pluripotent hESCs have the potential to become any type of cell in our body, but all pluripotent cells may not have the same expression level of the various stem cell markers[31]. For example, Qiu et al. demonstrated that expression of Tra-1-81 receptors varies significantly even among stem cells from the same line[27]. Future experiments to determine expression level of receptors on the surface could help determine whether this as a potential source of the difference in capture efficiency.

Antibody-functionalized microfluidic devices

Several recent papers have addressed the topic of using antibody-functionalized microdevices for isolating specific sub-populations from a heterogeneous population[3,34]. Isolating specific immune cells or rare cells such as circulating tumors cells are among the most common applications[35–40]. Three main challenges arise when designing antibody-based capture microdevices: directing cells to the antibody-coated surface, increasing the effective area of interaction, and designing with shear-stress considerations.

In microchannels with no mixing, cells will, over time, move more and more along streamlines. If these streamlines do not promote cell interaction with the antibody-functionalized surface, then the amount of time cells are able to spend interacting – and potentially binding – to

functionalized antibodies decreases, thus decreasing the overall capture efficiency[34,41]. Our device most likely suffers from this situation as most binding was observed early on in the device, progressively decreasing as cells moved farther along into the channel. In addition, as cells move through the device and fail to interact with the antibody-coated surface, we observed cells beginning to clump, further decreasing the possibility of capture. In order to increase cell-antibody interactions, one could incorporate a herringbone design to promote mixing[34,42,43] or increase the effective surface area, for example, by incorporating antibody-functionalized microposts in addition to a functionalized solid surface[36,44,45].

The capture efficiency of our device could be improved on several fronts. Running collected cells through a second or multiple rounds of devices should be a straightforward method to improved capture efficiency. Control of the presentation of antibodies, such as their orientation, the amount of surface coverage, or selection of antibodies with greater affinity, can promote cell-antibody interactions and cell rolling[46,47], ultimately leading to increased cell capture[48]. While we do partially control antibody orientation via Protein G, including some of the aforementioned modifications (e.g. flow control to induce mixing/increase cell-antibody interaction or increasing effective surface area with microposts) should boost the capture efficiency of our device.

Conclusion

We demonstrate a new design of an antibody-functionalized PDMS microfluidic channel that is capable of positively selecting cells from a mixed population for *in situ* immunofluorescence or subsequent retrieval and analysis of cells with high viability. To our knowledge, this is the first time antibody-functionalized microdevices have been used to capture and select a sub-population of hESCs. The use of a microfluidic device with the ability to isolate cells such as hESCs with short sample preparation time, low shear stress, and no labeling, provides a platform technology with advantages over FACS and MACS. With improved capture efficiency, these devices could allow for isolating cell populations that would not be feasible with FACS or MACS (e.g. low cell numbers, sensitive cell samples) and allow analysis of bound single cells *in situ*.

Acknowledgements

Part II

Attenuation of TGF-β Signaling via Incorporation of a Dominant-negative TGF-β Type II Receptor Promotes Improved Muscle Regeneration in Murine Skeletal Myoblasts

Chapter 3

Introduction to Skeletal Muscle Regeneration, Aging, and Repair Mechanisms

Introduction

Skeletal muscle stem cells known as satellite cells are responsible for muscle regeneration. Upon muscle injury or exercise, quiescent satellite cells become activated, proliferate as myogenic precursors, differentiate into myoblasts, and ultimately fuse into new, multinucleated myofibers. Unfortunately, this paradigm breaks down with aging and multiple factors contribute to a build-up of scar tissue instead of new muscle. Among these negative contributors are some members of the TGF-β family of signaling molecules. After an introduction to muscle regeneration and satellite cells, the adult skeletal muscle stem cells, we will discuss how biomaterials can help improve impaired muscle regeneration and recent advances in combating TGF-β-induced impairment in muscle repair. We will then discuss the work I have done in improving skeletal muscle repair by attenuating the effects of TGF-β signaling via incorporation of a dominant-negative TGF-β type II receptor.

3.1 Skeletal Muscle is Regenerated and Maintained by Muscle Stem Cells

After exercise or upon injury our muscles regenerate, restoring functionality and maintaining structural integrity[1]. Adult skeletal muscle stem cells, known as satellite cells are responsible for this regeneration. Discovered in frog tibialis anticus muscle fibers in 1961[1,2], satellite cells were named based on their physiological location, between the basement membrane and the plasma membrane of the muscle fiber (Figure 1). Their purpose was already hinted at back then, but it was not until ten years later that their role as myogenic precursors was definitely established[3]. Satellite cells with thymidine-labeled nuclei were observed to undergo cell division and contribute to elongation of muscle fibers. A few years later, proof that satellite cells generate fusion-competent myoblasts was determined through isolated muscle fiber analysis[4-6]. Furthermore, not only did these satellite cells differentiate into myoblasts, they also replenished the satellite cell pool[7-8] identifying them as adult skeletal muscle stem cells.
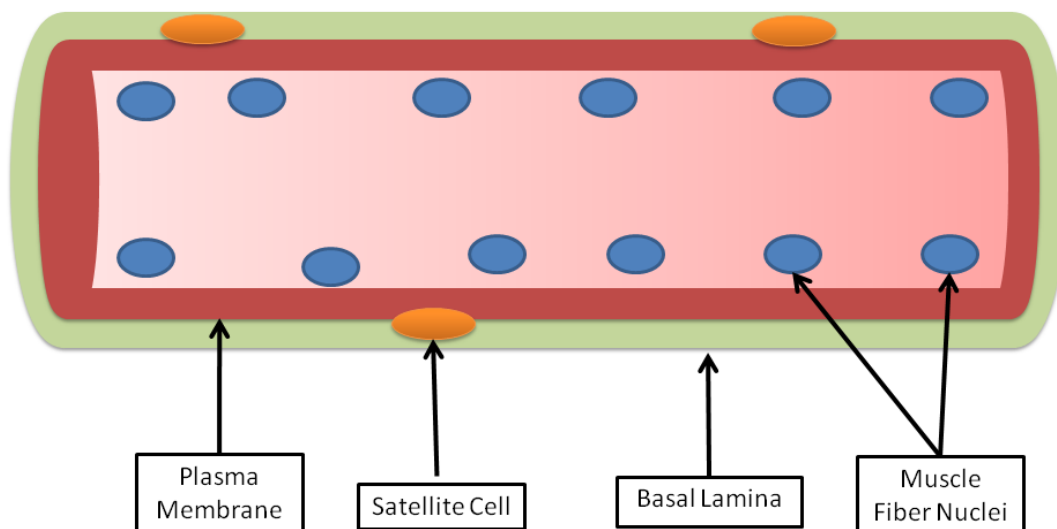
Figure 3.1 The Skeletal Muscle Fiber. Skeletal muscle satellite cells reside between the plasma membrane of myofibers and the basal lamina. Mature muscle nuclei are located towards the periphery of the fiber.

The skeletal muscle regeneration process is now reasonably-well understood. Upon muscle injury, quiescent satellite cells are activated by Notch/Delta signaling[9] and proliferate. Subsequent signaling through the Wnt pathway induces their differentiation and fusion into new myofibers[10] (Figure 2). Importantly, recent studies have shown that in the 'aged' skeletal muscle niche, this signaling cascade is disrupted by increased TGF-β1 signaling and satellite cell activation is impaired upon injury[11]. Promising studies designed to combat the effects of aging on muscle regeneration have been recently conducted[11,12].
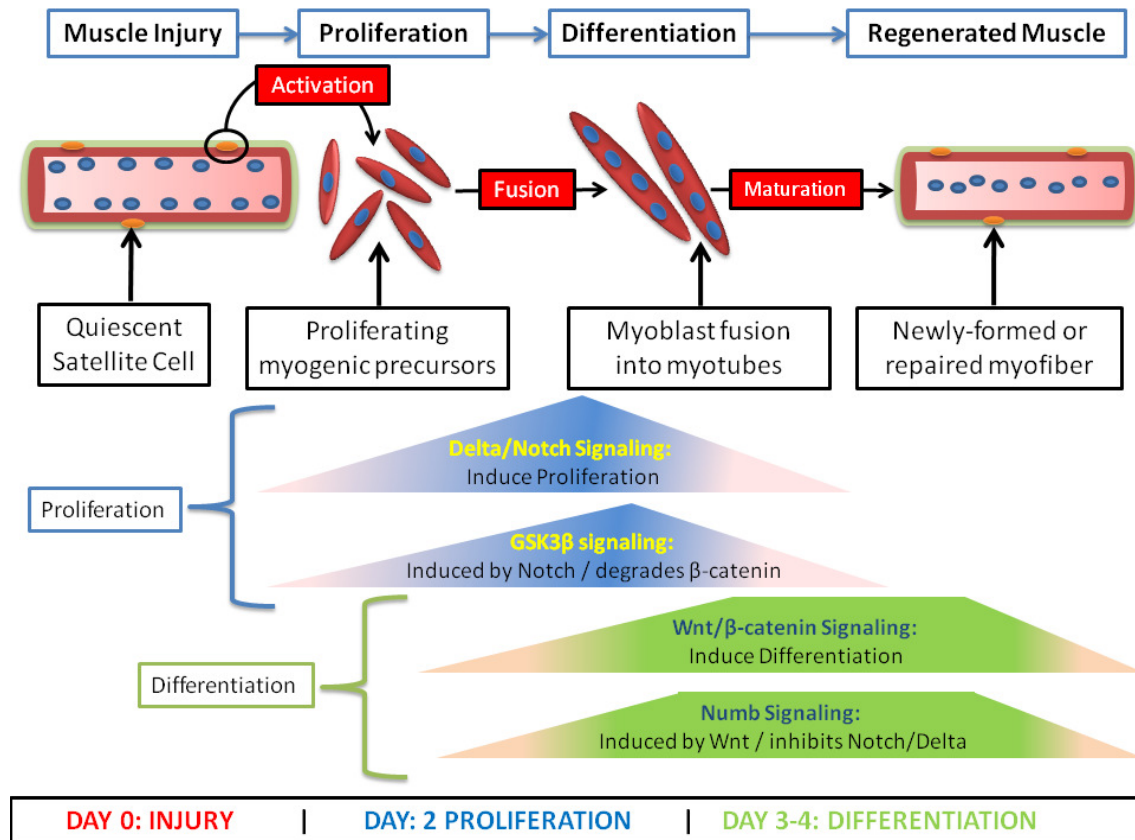
Figure 3.2 Regeneration Timeline and Signaling in Normal Skeletal Muscle Repair. Upon muscle injury, quiescent satellite cells become activated and proliferate in response to Delta/Notch signaling. Downregulation of Delta/Notch signaling via Numb inhibition leads to increased Wnt signaling and differentiation of myogenic precursors. Fusion of myoblasts into myotubes is followed by maturation into myofibers with centrally located nuclei

3.1.1 Delta/Notch Signaling Leads to Activation and Proliferation of Satellite Cells

As many stem cell regenerative pathways – including muscle regeneration – are known to recapitulate embryonic organogenesis[13] and Notch signaling was known to affect cell proliferation and differentiation during embryogenesis as well as tissue repair[14-17], Notch was a logical target of study in skeletal muscle regeneration[9]. While Notch signaling can be involved in differentiation[18-20] or cell proliferation, Notch signaling in murine C2C12 myoblasts was shown to lengthen the time myoblasts remained undifferentiated, observed through lack of expression of differentiation markers MyoD and myogenin[14,21]. After initial studies to induce satellite cell activation *ex vivo*[22] further work demonstrated that during sat-

27

ellite cell proliferation and activation Notch is active, and that the Notch antagonist Numb may play an important role in signaling for myogenic precursor differentiation[9]. Activated Notch levels were elevated during the first few days after injury, when satellite cells are highly proliferative, whereas Numb levels initially decreased. As Numb levels increased again, loss of the satellite cell marker CD34 and higher expression of the myoblast markers desmin and M-cadherin were observed. This work thus showed that Notch signaling is important in the early days of skeletal muscle regeneration by contributing to the rapidly increasing population of myogenic progenitors.

3.1.2 Wnt Signaling Cues Myogenic Progenitor Cells to Differentiate

The Notch pathway interacts with many other signaling pathways (e.g., Transforming Growth Factor (TGF)/Bone Morphogenetic Protein (BMP), Wnt) that are implicated in tissue regeneration[14, 23-26]. For skeletal muscle regeneration specifically, the balance between the Notch and Wnt signaling networks defines the transition from proliferation of myogenic precursors to the differentiation into fusion-competent myoblasts and *de novo* multinucleated muscle fiber formation[10].

In the same way it was known that Notch signaling was implicated in myogenesis and postnatal repair mechanisms, previous studies had shown that Wnt signaling also played a major part in muscle formation and myogenesis[10, 27-30]. Mononucleated muscle cells from regenerating muscle fibers isolated from TOPGAL mice, which express beta-galactosidase based on LEF/TCF or beta-catenin activity[31], demonstrated Wnt signaling activity through beta-galactosidase expression at days 2 and 5 of regeneration[10]. More convincingly, a study of the downstream Wnt regulator GSK3β and its phosphorylation profile at tyrosine 216 revealed a dynamic regulation that works in concert with Notch signaling. A dephosphorylated tyrosine 216 allows GSK3β to phosphorylate β-catenin, a hallmark of canonical Wnt signaling[32,33]. Tyrosine 216 phosphorylation was high early on in muscle regeneration (when Notch signaling was high[9]), but decreased at later times, indicative of activation by Wnt. qRT-PCR studies on 4-day-cultured myofiber explants showed increased transcription of the Wnt3a ligand and the Wnt receptors Frizzled-1 and Frizzled-2, in addition to the downstream target Axin-2.

In order to study the role of Wnt signaling in muscle regeneration, mononucleated cells isolated from single muscle fibers were treated with recombinant Wnt3a or a GSK3β inhibitor. Upon treatment of myogenic progenitors, increased β-catenin activation and nuclear localization was observed, in addition to a close to 70% increase in the number of myogenic precursors expressing desmin after 2 days in culture over untreated cells[10].

In vivo work using recombinant Wnt3a treatment on regenerating muscle led to premature differentiation of myogenic precursors into *de novo* myofibers. This was accompanied by an increase in the size of the regenerated myotubes in addition to an increased number of nascent myotubes early on in regeneration (days 2-3). However by days 4-5, the number of nascent myotubes in untreated samples was still increasing, whereas Wnt3a-treated samples showed no new myotube formation and remaining injured areas of muscle, due to a depletion in myogenic progenitors[10].

Conversely, inhibition of Wnt signaling during the differentiation phase, both *in vitro* and *in vivo*, resulted in decreased number and size of *de novo* myotubes, confirming the importance of Wnt signaling in cell fate commitment of myogenic progenitors.

A deeper analysis of the crosstalk between the Notch and Wnt pathways showed that inhibition of Notch led to an earlier progression towards terminal myogenic differentiation, evidenced by an early increase in Wnt signaling. Inhibition of Notch during the differentia-

tion phase had little effect. However, if Notch was exogenously activated during the differentiation phase, a decrease in nuclear β–catenin was observed, indicating inhibition of Wnt signaling. The intimacy of the Notch/Wnt crosstalk was then confirmed to occur via GSK3β, which is maintained in an active form by Notch but is inhibited by Wnt.

Skeletal muscle regeneration therefore depends on an intricately-regulated crosstalk between the Notch and Wnt signaling pathways. Myogenic precursors rapidly proliferate in response to a perceived injury under the effects of Notch signaling, and then undergo differentiation and fusion into *de novo* myofibers due to both an activation of Wnt signaling and an inhibition of Notch signaling (itself mediated through Wnt activation).

3.2 The Aged Skeletal Muscle Niche Impairs Normal Regeneration: TGF-β1 Signaling Promotes Satellite Cell Quiescence and Leads to Scar Tissue Formation

There is some evidence that the number of skeletal muscle satellite cells in different muscles and species decreases with aging[34-39]. However, the regenerative potential of 'aged' satellite cells *in vitro* is robustly maintained[1,11,12,40]. Nevertheless, in an aged niche, satellite cells fail to efficiently regenerate upon muscle injury and in some areas scar tissue is formed in the place of new myofibers[37,41]. Transforming Growth Factor Beta 1 (TGF-β1), a cytokine involved in many cell functions such as growth, proliferation, differentiation, and apoptosis, disrupts the dynamic Notch/Wnt crosstalk essential to myogenic proliferation and differentiation and has been implicated in this decline in muscle regeneration in aging[11,42-44] (Figure 3a).
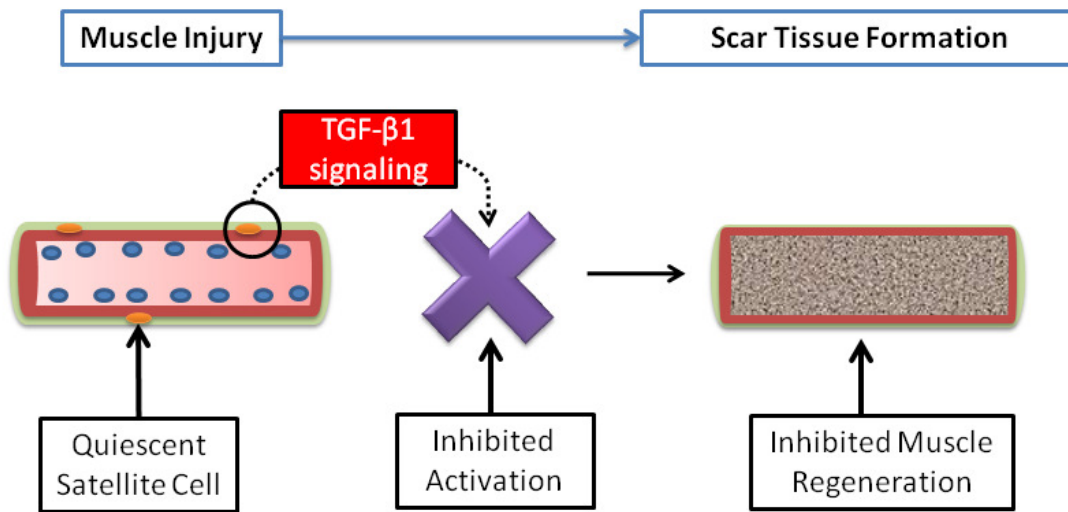
Figure 3.3a Increased TGF-β1 Signaling Inhibits Proper Muscle Regeneration in the Aged Niche. Upon injury to muscle in the 'aged' niche, increased active TGF-β1 levels inhibit activation of quiescent satellite cells. Proliferation and differentiation steps of normal muscle regeneration are inhibited and few new myotubes are formed, leading to scar tissue formation in lieu of new muscle formation

The regenerative potential of skeletal muscle satellite cells is very robust. Early on, Studitsky showed that functional, new muscle could be formed from minced, explanted muscle[45]. Cycles of degeneration and regeneration of muscle using toxins further showed that satellite cells are able to heartily contribute to the formation of new muscle even after 50 sets of induced injury-regeneration cycles[46,47].

Although it is debated whether the satellite cell population may decline with aging[41,48-52], the lack of muscle regeneration with aging is likely not due to exhaustion of the satellite cell population[1]. The balance of Notch/Wnt signaling is central to muscle regeneration and shifting the balance via Notch/Wnt inhibition or activation has been shown to have significant impacts on the efficacy of regeneration[9,10,30,49]. Slight variations in the skeletal muscle niche that affect these pathways and their crosstalk can have a major effect on regeneration.

We saw earlier that Notch activation after injury was essential for proliferation of myogenic precursors[49] and that inhibition of Notch led to fewer nascent myotubes and overall poorer regeneration. In the aged environment it was shown that satellite cell proliferation was reduced, but that exogenous Notch activation reestablished the satellite cells' proliferative capacity (similar to a young environment). In recent work, Notch activation was shown to be important for the regenerative capacity of human satellite cells and to decline in old human muscle[53]. Notably, activation of Notch by its ligand Delta is likely to be positively regulated through MAPK and interestingly, both MAPK and active Notch become diminished with age in the human muscle compartment[53]. In addition to assessing that in this case satellite cell numbers remained constant during a lifetime, the report demonstrated that the Notch ligand Delta failed to become upregulated in aged satellite cells, thus leading to the observed decrease in proliferation. But was this due to an intrinsic aging of satellite cells? Or was it caused by other extrinsic effects?

Earlier publications had shown that transplantation of young muscle into an aged niche impaired regeneration, but that transplantation of aged muscle into a young niche resulted in regeneration[54,55]. It was therefore clear that the muscle stem cells present in the aged niche were still capable of regeneration, but that the niche itself was somehow preventing their activation. This led researchers to question what elements of the aged niche were contributing to impairment of muscle regeneration.

Using a method called heterochronic parabiosis[56], where the circulatory systems of young and aged rats are surgically linked, it was further confirmed that the aged niche caused the decline in satellite cell regeneration and that exposure of 'old' satellite cells to a young circulatory system can restore their regenerative capacity[54]. Delta signaling of Notch in old satellite cells was upregulated, leading to upregulation of Notch signaling, and enhanced proliferation *in vitro*. The cause of muscle regeneration impairment was thus narrowed down to either activating factors in the young circulation, inhibiting factors in the aged circulation, or both. Furthermore, this work supported the idea that 'aged' satellite cells may be able to maintain muscle homeostasis if the niche can be properly regulated[57].

In order to determine whether positive or negative regulation of muscle stem cell growth was occurring, further work demonstrated that the inhibition of young satellite cell activation or the activation of 'aged' satellite cells could be achieved *in vitro* with old and young serum alone, respectively[40]. More importantly, the study showed that culture of young satellite cells in old sera led to inhibition of regeneration, pointing towards the existence of a negative regulator of muscle regeneration in aged sera. A year later transcription growth factor beta 1 (TGF-β1) was identified as an inhibitory culprit[11]. Specifically, TGF-β1 levels were shown to be higher in the aged niche, leading to increased signaling via pSmad3, and antagonizing of Notch signaling. Increased pSmad3 signaling upregulated expression of the cyclin-dependent kinase inhibitors p15, p16, p21, and p27, thus preventing satellite cell activation and proliferation (Figure 3b). Inhibition of TGF-β1 activity via antibody directed to its receptor allowed satellite cells in an 'aged' niche to regenerate muscle similarly to 'young' satellite cells. A subsequent paper dug deeper into the TGF-β1 signaling pathway and established its

evolutionary conserved role (between mouse and human) in the inhibition of muscle repair [12].
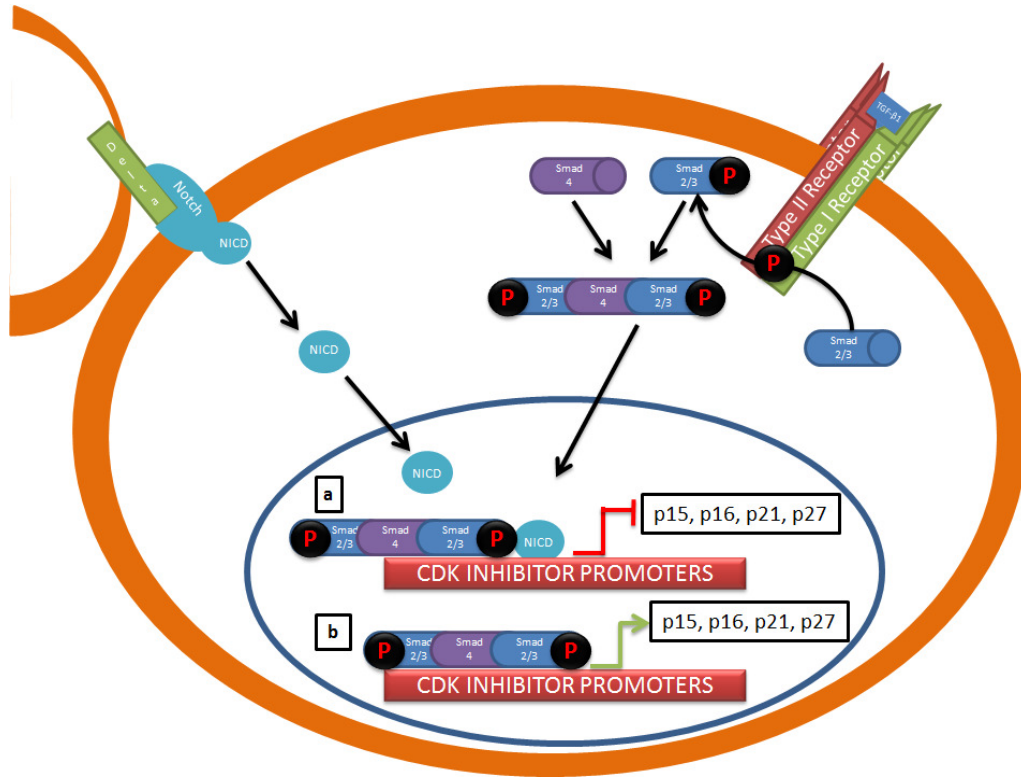
Figure 3.3b Notch and TGF-β1 Signaling Cross-talk in the Aged Niche. In young muscle, interaction of Delta with Notch receptor leads to release of Notch Intracellular Domain (NICD) which enters the nucleus and promotes satellite cell proliferation. TGF-β1 signaling through Type II and Type I TGF-β receptor heterotetramer leads to phosphorylation of Smad2/3 (pSmad3) and subsequent complex formation with Smad4. This complex enters the nucleus to affect transcription of various genes. In the aged muscle niche, increased active levels of TGF-β1 (and decreased levels of active Notch) lead to increased pSmad3 signaling and expression of cyclin-dependent-kinase inhibitors p15, p16, p21, and p27 which maintain satellite cell quiescence (B). In the young niche TGF-β1 levels are low and Delta levels are high, so satellite cell activation is not maintained. However, forced activation of Notch in the aged niche (high active TGF-β1 levels) restores skeletal muscle regeneration after injury through antagonism of TGF-β1/pSmad3 signaling (A)

In sera, TGF-β1 is present in both active and inactive forms[12,58,59] while in plasma only the inactive form is present. Total and active TGF-β1 on the other hand is secreted by platelets and CD4^{+} T lymphocytes[58]. According to a recent study[12] *in vitro* inhibition of muscle regeneration is likely caused by TGF-β1 released from platelet activation during sera collection. However, neither systemically-administered TGF-β neutralizing antibodies nor TGF-β decoys were able to restore muscle regeneration to aged mice. TGF-β levels in addition to TGF-β receptor expression are increased 3-4 fold in aged satellite cells[11], but it is unlikely that TGF-β1 acts as an endocrine inhibitor of satellite cells. Aged satellite cells expressing a dominant-negative TGF-β receptor[60,61] were activated, proliferated, and differentiated in the presence of old serum. *In vivo*, systemic TGF-β receptor I kinase inhibitor[62,63] was able to

promote muscle regeneration in the aged niche, whereas TGF-β neutralizing antibody or the extracellular component of TGF-β Receptor II proved ineffective[12].

In summary, skeletal muscle regeneration is an intricately regulated process that depends on the crosstalk between several essential signaling pathways (Notch/Wnt/TGF-β1). In the 'young' niche, muscle stem (satellite) cells, respond rapidly to injury and proliferate in response to Notch signaling, before differentiating and fusing into new myotubes under Wnt signaling. In the 'aged' niche, TGF-β1 signaling antagonizes Notch signaling and inhibits satellite cell activation, leading to scar tissue creation in lieu of *de novo* myofiber formation. Restoring youthful regeneration capacity to 'aged' satellite cells is an attractive prospect for myogenic therapies. While many advances have been made in *in vitro* skeletal muscle regeneration strategies, very few have yet to take into account the effects of aging on the satellite cell niche *in vivo*. The next two sections will thus analyze what has been accomplished so far in this regard, analyzing either purely biological or biomaterial methods to promote efficient regeneration of skeletal muscle satellite cells under adverse extrinsic conditions.

3.3 Toolbox to Combat TGF-β1-induced Aging of Satellite Cell Niche

Now that some of the signaling pathways behind muscle regeneration have been elucidated, including the inhibitory regulation, it is possible to deconstruct and modify these regulatory pathways in order to enhance muscle tissue engineering constructs and combat the effects of aging and pathology on the satellite cell niche. As described previously, forced activation of Notch[49] or inhibition of TGF-β1 signaling – either through blocking the interaction of TGF-β1 with its receptor, inhibiting the receptor itself, or through siRNA against Smad3[11,12,64] – can lead to 'young' regeneration of satellite cells in an aged niche. However, TGF-β-neutralizing antibody or siRNA against Smad3 might require multiple daily injections, raising concerns with efficiency and safety if these techniques were ever to be considered in clinical applications.

Alternative methods to regulate TGF-β1 levels in the aged niche are currently being pursued in the hopes of improving efficiency (fewer injections) and tuning the TGF-β1 levels precisely. Not only will changes in TGF-β1 levels affect other signaling pathways, but overly- long-term downregulation or complete elimination of TGF-β1 has been recently shown to negatively affect regeneration[12]. In fact, there is a defined window of active TGF-β1 levels that are necessary for proper regeneration before hitting a threshold above which active TGF-β1 levels become inhibitory.

The calibration of TGF-β signaling to young levels has broader implications in tissue engineering and regenerative medicine and raises an issue that has still been poorly addressed – although we may eventually be able to engineer tissues or organs *in vitro*, they will someday be engrafted into humans. However, the aged or elderly population, which will most likely have greater need for these tissues and organs, are unfortunately hosts to 'aged' tissue and organ niches. Few *in vitro* and *in vivo* tissue engineering constructs take the implications of an 'aged' niche into consideration and this could undermine performance of methods that have worked well in the non-aged environments. As has been observed in the adult muscle stem cell niche, the potential of the stem cells to regenerate does not decrease over the lifetime of the organism, but the niche conditions of the aged host prevent the satellite cells from proper function[40,54,57,65,66]. Therefore it is necessary not only to succeed in creating tissues and organs, but to also deal with the issues inherent in aged niches that may prevent proper stem cell regeneration.

When referring to the aged muscle stem cell niche, it was shown that TGF-β1 sera levels are increased over those from the young niche[11,12], indicating a possible first location to target TGF-β1 inhibition. However, systemic TGF-β1 is mostly confined to platelets and exists mainly in its latent form[12,67-69]. Furthermore, a recent study has shown that endocrine TGF-β1 likely has no anti-myogenic activity *in vivo*[12]. Systemic targeting of TGF-β1 for inhibition may not therefore be a viable application. It is possible that endogenous TGF-β1 secretion by the aged tissue (such as myofibers) is responsible for the impaired regeneration [12].

In the adult skeletal muscle niche, activation of TGF-β1 occurs in the extracellular matrix (ECM) around muscle fibers[11,70] and TGF-β1 co-localizes specifically with the laminin component of the ECM[71]. This is therefore an area in which TGF-β1 can be targeted for inhibition. Specifically, it is possible to inhibit the signaling of active TGF-β1 in the muscle niche through local addition of anti-TGF-β1 neutralizing antibody, TGF-β receptor I kinase inhibitor (systemically- or locally-administrated), or through a decoy[11,12].

However, it is likely that greater efficiency in TGF-β1 regulation can be achieved and long-term therapies would be required to tackle chronic 'conditions' such as those imposed by aging of the muscle stem cell niche. Therefore, future work may consider methods to target TGF-β1 inhibition either systemically or in the local muscle niche (or both), in order to improve adult muscle stem cell regeneration in the aged niche. Several purely biological methods have already shown that downregulating TGF-β1 levels below a certain threshold (~1-5 ng/mL[12]) has significant effects on regeneration. The use of biomaterials may facilitate the development of more effective methods to rejuvenate the muscle niche. We will analyze some of the current biomaterial methods being used to modify the adult skeletal muscle niche and will suggest a few directions which may benefit muscle regeneration further.

3.4 Biomaterials to the Rescue: Proposed Strategies for Adult Skeletal Muscle Regeneration

Skeletal muscle tissue engineering aims to create functional muscle *in vitro* followed by engraftment *in vivo* for the replacement or repair of missing or pathological tissue in various dystrophies or myopathies. Biomaterials have rapidly become central to these regeneration efforts and numerous repair strategies already exist. However, optimization of these biomaterial platforms in order to more fully mimic the *in vivo* adult skeletal muscle niche is still necessary. More importantly perhaps, the effects of aged or pathological environments on skeletal muscle engraftment has yet to be fully characterized. Furthermore, debate still remains over whether or not all satellite cells (considered to be heterogeneous in genetic markers and functional properties) are in fact stem cells, and what implications this could have on *in vitro* regeneration strategies[72].

Autologous muscle transplants result in donor site morbidity and often lack proper functionality at the site of engraftment[73]. We have already suggested that biomaterials may be uniquely suited to addressing some of the issues with adult skeletal muscle regeneration due to various myopathies or to the effects of aging. In this section we will outline three different areas of application of biomaterials to the muscle stem cell niche. First we will discuss the advancement of biomaterial scaffolds for the *in vitro* growth of muscle and how these could be further developed to combat muscle dystrophies or aging. Next we will look at biomaterial methods to specifically remedy the inhibitory effects of TGF-β1 in the aged niche, starting with gene and drug delivery methods, followed by some novel molecular targeting strategies. Finally, we will discuss a novel biomaterial method to better define satellite cell heterogeneity and optimize selection of muscle stem cells to be used in tissue-regenerative therapies.

3.4.1 Engineering an *in Vitro* Niche for Robust Skeletal Muscle Regeneration

Effectively mimicking *in vivo* niches for *in vitro* tissue engineering is an important research tool to create possible regenerative therapies. Much *in vitro* work is done in two dimensions however and thus does not adequately reflect the *in vivo* environment of the skeletal muscle niche. Subsequently, culture systems that utilize *in vitro* 3-dimensional niches for proliferation, differentiation, and fusion of muscle fiber progenitor cells are more likely to generate more suitable tissues for *in vivo* muscle repair therapies[74-76].

Indeed, it is clearly not an easy thing to mimic the native satellite cell niche *ex vivo*. First of all, the satellite cell is intimately associated with a muscle fiber which allows for better regeneration if implanted with intact satellite cells[8,77]. *In vitro* satellite cell culture leads to a loss in proliferative activity of satellite cells as well, in addition to loss of self-renewal, as they rapidly differentiate into myoblasts; this loss in regenerative capacity is likely due to the removal of satellite cells from their *in vivo* niche[78]. The satellite cell niche supplies mechanical (adhesion/stiffness), structural, and chemical (small molecules) signals to the satellite cells[78,79]. The basement membrane, below which satellite cells reside, is composed of entactin-linked networks of laminin and collagen type IV with a high number of integrin and proteoglycan binding sites[77,78] and provides a physiological elasticity of around 21 kPa[80]. Changes in mechanical or chemical cues due to pathology or aging can significantly affect the regeneration potential of satellite cells[79]; for example young, healthy skeletal muscle tissue has been reported to have a stiffness of around 12 kPa[80,81] that increases to over 18 kPa in some disease[81,82] or aged states[83,84]. Altered signaling through focal adhesion complexes can then lead to changes in cell fate[85,86]. For example, polyacrylamide gels that are softer or stiffer than the optimal *in vitro* C2C12 stiffness or *in vivo* primary myoblast niche stiffness have been shown to impair cell proliferation[77,81].

Biomaterial scaffolds have long been used to create 3-dimensional niches for tissue regeneration *ex vivo*[87,88]. For skeletal muscle regeneration, the scaffold should allow muscle progenitor adherence, growth, and proliferation, followed by fusion of myoblasts into multinucleated muscle fibers. Not only that, muscle fibers that are large, strong, aligned, and properly oxygenated and nourished will be more likely to be viable after engraftment. Generating functional, contracting muscle is one of the most important goals of regenerative medicine[73].

Choice of the appropriate cell type to use also has to be determined, but is often limited to myoblasts, since satellite cells cannot be maintained in culture[89-91]. However, myoblasts themselves may not be adequate for human transplantation as they have shown poor migration abilities after engraftment into non-human primates[73,92]. A recent review provides a comprehensive list of cell lines (muscle-derived or other) used in skeletal muscle tissue engineering[93]. Once adequately tested, functional *in vitro* regeneration systems may then be applied to *in vivo* models of genetic myopathies (e.g., Duchenne's Muscular Dystrophy, (DMD)) where muscle repair is inefficient due to the functional exhaustion of resident satellite cells[94-96]. The success of *in vivo* muscle regeneration systems to date has been low, due to cell death and immune rejection of the transplanted cell types (most often myoblasts)[97-99] and is a topic of intense research.

The first biomaterial scaffolds for *in vitro* skeletal muscle regeneration aimed only to create functional myotubes from seeded myoblasts; over time, numerous substrates, both artificial (biodegradable or non-biodegradable) and natural (or combinations of both) have been used to test muscle regeneration[99-111]: polymers such as poly(glycolic acid) (PGA)[112], poly(lactic acid) (PLA)[105], the PLGA co-polymer of the two[113,114], poly(dimethylsiloxane) (PDMS)[115], poly(ethylene glycol) (PEG)[116], self-assembling peptide nanofibers[117], and many

more[107,109,118,119]. Biological substrates made up of various tissue extracellular matrix proteins such as collagen, hyaluronic acid[101,102,120-124], or other biologically-active molecules[125,126], and micropatterned surfaces including various ECM proteins or signaling molecules[127-132] have also garnered significant interest. However, many of these scaffold systems had drawbacks such as difficulty of fabrication[115] or high elastic modulus which did not adequately mimic the *in vivo* muscle niche[107] (Figure 4).
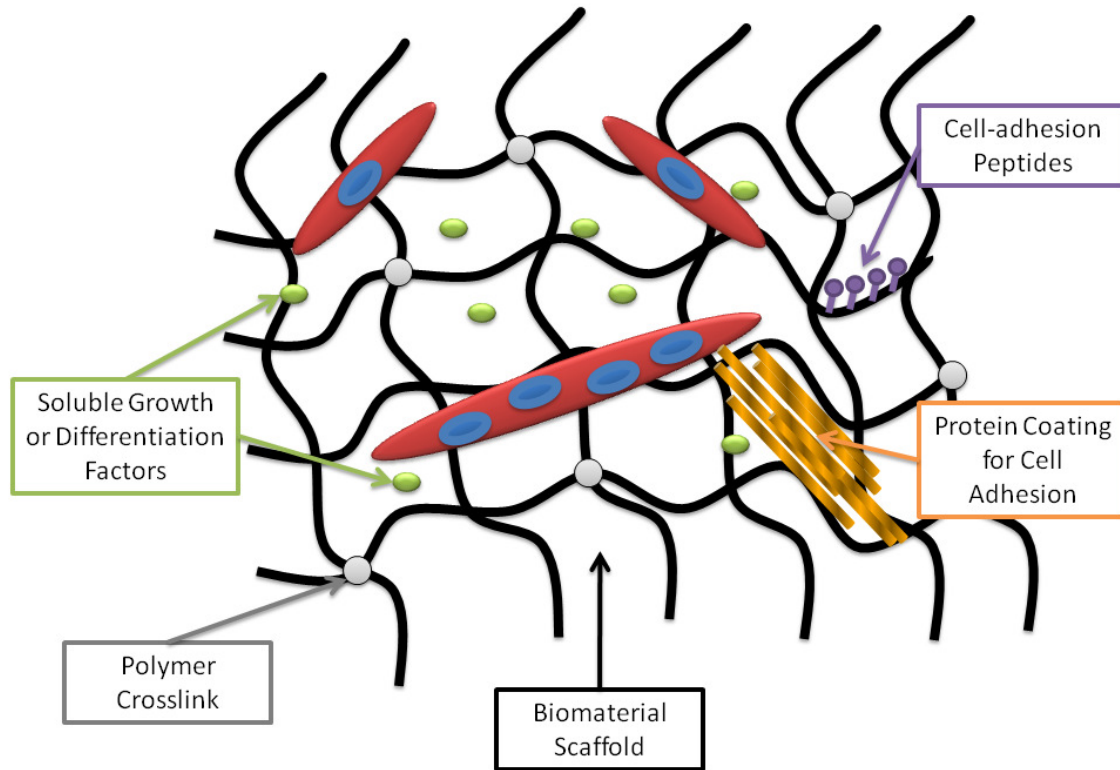
Figure 3.4 Biomaterial Scaffolds for Skeletal Muscle Tissue Engineering. Engineered bio-materials aim to recreate the skeletal muscle niche *in vitro*. Substrate stiffness can be varied to promote adhesion, spreading, proliferation, or differentiation (e.g. varying polymer scaffold crosslinking). Natural extracellular matrix protein coatings (e.g., collagen, elastin) or peptides can be displayed to promote cell adhesion and signaling. Soluble growth and differentiation factors can also be incorporated to affect cell fate

Therefore, to more efficiently and accurately tissue engineer skeletal muscle *in vitro*, the focus has shifted to more closely mimicking the *in vivo* niche in biomaterial scaffolds. Specifically, researchers have moved towards simpler scaffolding systems with controllable stiffnesses that are able to promote generation of aligned myofibers into densely packed parallel bundles and mechanically and electrically stimulate myofiber contraction[133,134]. We will look at some of the more recent work done to optimize these scaffolds and then focus on some of the most advanced systems to date and suggest what the future may hold.

3.4.2 Alignment of *in Vitro* Skeletal Muscle Fibers

Randomly-oriented fibers generated *in vitro* would not be useful for *in vivo* muscle transplantation therapies as aligned fibers are required for proper force generation[73]. Therefore, the initial work done in *in vitro* skeletal muscle regeneration which focused only on myofiber formation is now focused on scaffolds to generate parallel arrays of aligned fibers that could then be easily engrafted.

Previous work has looked at arranged muscle fibers *in vitro* from rat satellite cells grown on an aligned collagen gel system[111,135] which could then be transplanted *in vivo*. Collagen sponges consisting of collagen-I with parallel pores were also successfully used to culture and fuse C2C12 myoblasts[101]. A more recent study has proposed the use of a cell/hydrogel system cast inside polydimethylsiloxane (PDMS) molds decorated with elongated posts that were able to organize the regeneration of both mouse and rat skeletal muscle tissue in such a fashion[133]. Their method, in which the post size and dimensions could be varied, allowed control of muscle fiber size, thickness, alignment, and porosity (which is important for oxygen transport). Another group using PDMS created laminin-coated microtopographically-patterned, wavy PDMS substrates[128]. This allows one to first align the growing myotubes on the substrate, and then organize them spatially in 3-dimensions by transferring them to a degradable hydrogel. This method circumvents the issue of using rigid scaffolds alone, which promote myofiber alignment, but inhibit mechanical function of the generated fiber.

3.4.3 Effects of Synthetic Niche Stiffness on Skeletal Muscle Regeneration

Alignment of tissue-engineered myofibers is essential to generating functional skeletal muscle for subsequent engraftment. However as noted previously, rigid scaffolds may be used to promote alignment, but also inhibit myofiber contractility. The stiffness of the biomaterial scaffold is thus intricately related to the allowable contractility of the nascent myofibers. Substrate stiffness has been known to influence cell survival, adhesion, spreading, growth, proliferation, and differentiation[77,136,137]. For skeletal muscle, substrate stiffness affects myogenic precursor proliferation, while differentiation is controlled by both stiffness and adhesion site type and number[77]. In one study, an optimal stiffness of 21 kPa was determined for proliferation which not surprisingly corresponds to the *in vivo* elasticity of skeletal muscle[77,80]. A more recent study measured elasticity of muscle at 12 kPa and showed that muscle stem cells could be made to self-renew *in vitro* and help regenerate muscle when injected *in vivo*[138]. Other studies have shown that increasing substrate stiffness leads to increased proliferation of myoblasts[137] though the time-course of experiments must be taken into account[77]. Additionally important in skeletal muscle regeneration is allowing myotubes to spontaneously contract. On laminin- and poly-D-lysine-coated substrates, spontaneous contraction of myotubes was often observed, but not on collagen type IV-, Matrigel-, or entactin-collagen-laminin-coated substrates[77]. As such, 2- and 3-dimensional peptide-modified alginate scaffolds[103,137] demonstrated that mouse myoblasts in non-degradable, stiff gels proliferated more, but fused less than cells seeded onto degradable gels[139]. This work is important in determining the characteristics of future scaffolds to be used for *in vivo* muscle regeneration.

3.4.4 Electrical Stimulation of Tissue-Engineered Skeletal Muscle

While mechanical stimulation of myotubes can allow for contraction, external electrical stimulation has also been looked into as a means of inducing myotube contraction. Skele-

tal myoblasts cultured on aligned electrospun polyurethane fibers and subjected to external electric stimuli formed more aligned, contractile myotubes than those cultured on unaligned fibers without stimulation[140] (Figure 5). A quantitative study of the effects of electrical pulse frequency on myotube formation was recently completed and determined the proper frequency for synchronous contractility of myotubes[141]. Another study showed that it is possible to also locally stimulate myoblasts using a microporous alumina membrane on a PDMS substrate[142]. Finally, a recent study has shown that electrical stimulation can even encourage myofiber alignment[143]. Previous studies had shown that myoblasts could be coaxed to fuse into aligned myofibers based on the growth substrate itself, such as elastic membranes or micropatterned scaffolds[144,145], or if subjected to external mechanical stimuli such as stretching[146]. The latter method recapitulates the *in vivo* passive stretching of muscle[147] and is a reminder that closely mimicking *in vivo* regenerative processes *in vitro* by manipulating synthetic biomaterial systems can lead to effective myofiber synthesis methods for therapeutic purposes[148].
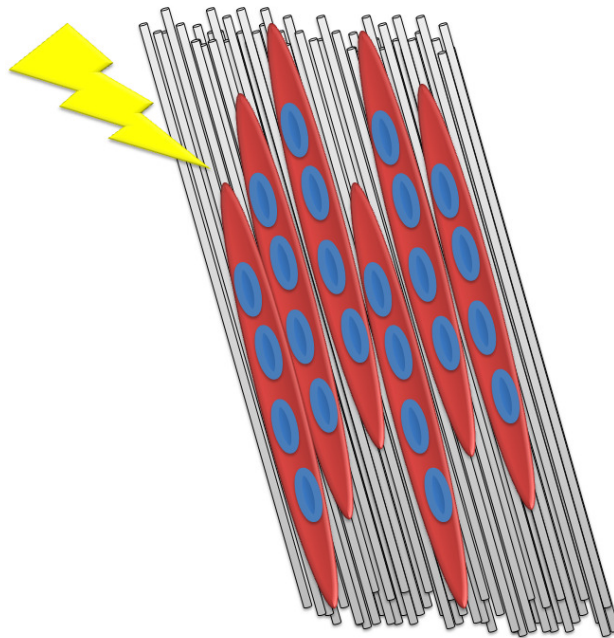
Figure 3.5 Electrospun Nanofibers for Generation of Aligned Myotubes. Parallel bundles of electrospun polymeric nanofibers can generate groups of aligned myotubes. Conductive polymers can be used to generate contracting fibers through electrical stimulation.

Some of the most advanced biomaterial niches seek to optimize substrate stiffness, myofiber alignment, and electrical stimulation all at once. Electrospinning of poly(caprolactone)/collagen nanofibers was recently used to create a scaffold for generating human skeletal muscle *in vitro* with controlled orientation[149]. Unlike randomly-oriented nanofibers, parallel electrospun nanofibers were able to induce aligned myotube formation and generated longer, more native-like myofibers. A subsequent, more pointed study[150] electrospun fibers of poly(L-lactide-co-3-caprolactone) blended with conductive polyaniline[151] in order to generate myotubes through electrical stimulation of C2C12 myoblasts.

3.4.5 Vascularization of Tissue-Engineered Skeletal Muscle

Tissue-engineered constructs require proper oxygenation and nutrient delivery to survive and integrate with the host tissue upon engraftment. In order for that to be possible, no tissue can be located at more than approximately 150 µm from supply sources[144]. This issue has been considered as well for tissue-engineered skeletal muscle. The foreign body reaction that occurs upon transplantation of tissue leads to some viable vascularization[13,152-154]. Other methods involve prevascularizing the tissue engineering construct[106,155] before implantation; the method by Levenberg et al. co-cultures endothelial cells and embryonic fibroblasts with the myoblasts leading to improved integration with the host vasculature upon transplantation. However, few vascularization methods have been developed to date and none was applied in humans.

To conclude this section on synthetic biomaterial niches, we have seen that they are highly modifiable, adaptable systems and are currently being optimized to more effectively mimic the *in vivo* skeletal muscle niche. The initial steps of generating myofibers, aligning them, and stimulating their contraction electromechanically are fairly well understood and developed. However, the issue of providing proper vascularization once engrafted has yet to be fully addressed, especially for human transplantation. A summary of the *in vitro* biomaterial strategies for skeletal muscle regeneration can be found in Table 1. In addition, issues of biocompatibility and immune response to foreign constructs and the likelihood of inflammation upon engrafting still remain. In attempts to circumvent some of these issues, attention for skeletal muscle tissue engineering has been shifting to *in vitro* niches that are more biologically natural in composition, and are the subject of our next section.

Strategy	Method	Materials	References
Myofiber Alignment	Aligned collagen gel	Collagen	104, 127
	Collagen sponge	Collagen	94
	Hydrogel/mold with elongated posts	PDMS	125
	Micropatterned surface	Laminin on wavy PDMS substrate	120
	Micropatterned hydrogel	Micro-contact printing of ECM proteins	150
	Electrospinning of parallel fibers	Poly(caprolactone)/collagen or poly(caprolactone)/polyaniline	141, 143
	Electrical Stimulation	Micropatterned poly-(L-lactic acid) membranes	134
Substrate Stiffness	Selection of appropriate stiffness substrate that allows myofiber contraction and mimics *in vivo* stiffness	Laminin	77
		Poly-D-lysine	77
		2- and 3-D peptide-modified alginate scaffolds	96, 129-130
Electrical Stimulation	External electric stimuli	Electrospun polyurethane fibers	131-132
		Microporous alumina membrane on PDMS substrate	133
		ECM-coated conductive polypyrrole substrate	923
Vascularization	Prevascularization of tissue engineering construct	Co-culture system within highly porous, biodegradable polymer scaffold	99, 147

Table 3.1 Biomaterial Strategies for Skeletal Muscle Regeneration

3.4.6 Natural Skeletal Muscle Niches: Mimicking the in *Vivo* Environment

While synthetic materials used for 3-dimensional skeletal muscle scaffolds may be very versatile and tunable, they may not recapitulate the *in vivo* muscle niche as well as natu-

ral biomaterials already present in the niche. Specifically the extracellular matrix, composed of collagen, laminin, fibronectin, among other components[156], provides both 3-dimensional structure and cell-adhesion sites for organizing muscle precursors into functional tissue. Natural biomaterials, including such ECM proteins, are also being heavily researched for *in vitro* muscle regeneration. A recent study used collagen in combination with Matrigel, an ECM extract from an Engelbreth Holm-Swarm murine sarcoma, to form rat skeletal muscle fibers from myoblasts *in vitro* before injecting the gel-like cell/matrix structure *in vivo*[157]. Other work with 3D collagen matrices used a co-culture system of human myoblasts and fibroblasts to determine that the non-myogenic cells were essential for differentiation, matrix remodeling, and force generation[74]. This study also confirms that the *in vivo* niche provides not only adhesion and organization of cells into 3-D tissues, but also provides soluble factors to the cells that influence growth, proliferation, and differentiation. Another group studied the proliferation and fusion of myogenic precursors from wild type and MDX mice (a model for DMD) on hydrogels micro-contact-printed with various ECM proteins for selective adhesion of satellite cells[158]. Using their micropatterning technique to mimic ECM adhesion sites, they generated nicely aligned muscle fibers from seeded satellite cells. A more recent study went further by using both a conductive polymer substrate in combination with the coating of ECM proteins (in this case hyaluronic acid and chondroitin sulfate) for adhesion, proliferation, and differentiation of both murine C2C12's and mouse primary myoblasts[100].

In a very interesting study ECM was extracted from rats and used as an *in vitro* substrate for skeletal muscle growth and differentiation[159]. This novel substrate allowed greater proliferation and differentiation of myoblasts than uncoated surfaces or collagen-coated surfaces. Importantly, this study also showed that collagen is the major component of the *in vivo* skeletal muscle niche, and that the extracted ECM must also contain additional components, as treatment with collagenase did not obviate adhesion and proliferation of myogenic cells. This study thus provided an important step in deconstructing the *in vivo* skeletal muscle niche in order to create enhanced *in vitro* niches.

The Conboy lab has also done work in this area of natural 3-dimensional matrices for skeletal muscle regeneration, specifically focusing on reconstructing an *in vitro* skeletal muscle niche that highly mimics the *in vivo* niche[127]. In a first series of experiments, myogenic cell fate was intricately controlled using a combination of known myogenic growth and differentiation factors embedded in Matrigel[9,71,160-162]. A related delivery mechanism has just been developed that is used to pattern nanoliter amounts of reagents (e.g., growth/differentiation factors) that will stay in a defined space, even in the presence of a second aqueous phase (e.g., cell culture medium)[163]. In the system developed by de Juan-Pardo et al., delivery of the factors was manipulated spatially so as to locally promote growth or differentiation of myoblasts even in the presence of differentiation or growth medium, respectively. By having the power to control cell fate regardless of the external medium, this artificial niche could be a great tool in promoting muscle regeneration in various myopathic conditions caused by changes in the *in vivo* niche. This was enabled by the unique method of incorporating growth and differentiation factors into the ECM gel, and allowing both proliferation and differentiation to occur simultaneously in the same dish. As expected, cells in growth medium alone proliferated, while cells in differentiation medium alone fused into myotubes. However cells in growth medium exposed to embedded differentiation factors preferentially differentiated, while cells in differentiation medium exposed to growth factors preferentially proliferated. In addition, cells cultured in neutral medium (which promotes neither proliferation nor differentiation) could be spatially directed to proliferate or differentiate if locally exposed to growth or differentiation factors respectively.

In the future, a completely reverse-engineering *in vivo* skeletal muscle niche, reconstructed from defined components and factors may provide an optimal solution as an *in vitro* skeletal muscle regeneration platform.

Section 3.4.1 looked at the current state of biomaterial niches for generating functional muscle *in vitro* for *in vivo* transplantation. The use of biomaterials has rapidly advanced the work by moving to recapitulate the *in vivo* skeletal muscle niche *ex vivo* (e.g., conductive polymers for electrical stimulation or the use of extracellular matrix components for adhesion). In addition, biomaterials have provided the tools to generate large, aligned, and strong muscle fibers which are more suitable for transplantation. And although synthetic biomaterials are highly modular and modifiable, the move now seems to be towards simpler niches, which more greatly mimic the *in vivo* niche through use of extracellular matrix components and signaling factors. Natural niches (e.g., collagen, Matrigel) provide more numerous and higher affinity binding sites for skeletal muscle and better mimic the *in vivo* niche.

What comes next? While there are therefore countless possible scaffolds and methods for preparation of muscle progenitors or myotubes *ex vivo*, which could then be used for muscle regeneration or replacement for various myopathies or dystrophies, no one has yet to address the task of muscle regeneration where the *in vivo* niche inhibits or prevents regeneration. Specifically, skeletal muscle regeneration in an aged niche is inhibited by increased TGF-β1 signaling and may therefore impede proper functioning of any of these systems upon implantation. Future work in this area may look at the incorporation of TGF-β1 inhibitors into such scaffolds or of the Notch ligand Delta to promote proliferation of implanted cells. However, as we have seen previously, satellite cells in an aged niche are still very capable of regeneration, and "rejuvenating" the niche itself may be the only necessity to restoring youthful muscle regeneration. The next section will analyze the use of biomaterial methods to address this issue of regeneration of skeletal muscle in aging.

3.5 Biomaterial Strategies to Combat Aging of the Muscle Stem Cell Niche

3.5.1   Gene and Drug Delivery Methods to Promote Skeletal Muscle Regeneration

Biomaterials have long been used in drug and gene delivery methods in order to protect cargo, target specific cells or tissues, and provide controlled, sustained release for treatment[164]. Gene delivery methods to skeletal muscle could provide possible treatment for degenerative myopathies such as Duchenne's Muscular Dystrophy, in which the protein dystrophin, which is essential in maintaining interactions between the extracellular matrix and the muscle fiber cytoskeleton, is not expressed[165]. Typical gene delivery methods include naked plasmid DNA, plasmid DNA delivered in polymeric particles[166], or through viruses[167]. However, naked DNA transfection is very inefficient and viral transfection, although very efficient, raises several concerns about oncogenicity, immune response, and safety[167]. Polymeric vehicles which release DNA based on diffusion and polymer degradation[166], allow long-term controlled and sustained release of DNA[168]. Therefore, in past years research focused on optimizing polymeric delivery vehicles in order to enhance gene delivery without the viral side effects. Various polymeric vehicles have been developed[169-172] and 'smart' polymers that are pH or temperature-sensitive have become popular[173-178]. Temperature-sensitive polymers, which are liquid at room temperature, but gel in the body at 37° C provide ease of use and injectability, in addition to the controlled, sustained release of a drug or gene payload[179]. Recent work has been done to enhance these methods of delivery to skeletal muscle cells[180] and is thus promising for possible therapies. Specifically, *in vitro* and *in vivo* delivery of plasmid DNA was mediated via multi-block copolymers (MBCPs) of pluronic® and di-(ethylene gly-

col) divinyl ether[181]. Importantly, the MBCPs were much more effective at *in vivo* (although not *in vitro*) transfection than both naked DNA or polymeric/DNA complexes that incorporated poly(ethylenimine), a standard cationic polymer used in drug delivery applications that had been previously shown ineffective as a gene delivery vehicle in muscle[182,183].

As explained above, gene delivery systems could be useful in delivering plasmid DNA to skeletal muscle cells. This could obviously apply in cases of genetic disorders, many of which lead to muscular dystrophies such as DMD, Facioscapulohumeral Dystrophy, Limb-Girdle Muscular Dystrophy, etc. where replacing deleted or mutated genes with healthy ones could be used to restore proper muscle physiology. In terms of promoting muscle regeneration in the aged niche, gene delivery of the Notch ligand Delta or the TGF-β1 receptor kinase inhibitor could be considered as possible therapeutics for restoring 'youthful' skeletal muscle regeneration, either through activation of the Notch pathway or through inhibition of TGF-β1 signaling, respectively. The next section will discuss novel biomaterial applications to the regulation of TGF-β1 signaling in the aged niche.

3.5.2 Novel Targeting Strategies for TGF-β1 Inhibition

<u>A biomaterial platform for regulating TGF-β1 levels to 'young' levels in the aged niche</u>

As described previously[11], attenuation of TGF-β1 signaling in the aged muscle niche promotes restoration of skeletal muscle regeneration. However, inhibition of TGF-β1 signaling required twice-a-day injection of TGF-β1 receptor I kinase inhibitor or Notch, or lentiviral transfection of shRNA against pSmad3, a downstream effector of TGF-β1 signaling. Complete silencing of signaling using viral transfection would be harmful as TGF-β1 is involved in many other signaling pathways[42], and non-viral transfection methods, which are less efficient than viral methods, would need to be optimized. In addition, were these strategies to be considered for clinical use, fewer injections, and a more efficient delivery system would be desired.

As such, novel biomaterial constructs may pave the way for some solutions. Future work will generate a wide array of biodegradable, biocompatible, nanoparticulate platform technologies that allow the display of a wide array of peptides or proteins at the particle surface through site-selective conjugation. These particles can be engineered to both encapsulate drugs or proteins of interest, and target specifically based on what molecule is used to decorate them. Unlike most drug delivery particles however, the site-specific conjugation technique provides controlled and consistent orientation of the displayed molecule of choice. This allows the display of the desired portion of surface molecule (i.e. actively targeting portion), and a significant increase in efficiency, as none of the displayed molecules will be randomly oriented. Such particles could be used in a variety of ways to combat the effects of aging in the muscle niche. Specifically, activation of Notch signaling through long-term sustained delivery of Delta[49] encapsulated in nanoparticles may promote youthful muscle regeneration and effectively reduce the amount of injections. Tailoring protein release rate, particle degradation rate, and amount of protein loaded will all be important in determining the efficacy of such a treatment. In addition, determining which possible targeting molecules to use or generating targeting peptides will have to be done. However, a systemic delivery of Delta may not be the most efficient. Nanoparticles will not exit blood vessels into tissues and may be rapidly cleared from circulation[184], (although the delivery time would greatly exceed that of Delta alone). Delta is also involved in many other signaling pathways so a non-localized delivery of Delta could generate unwanted effects. Nevertheless, a localized, controlled, and sustained release of Delta would be beneficial in enhancing muscle repair, but intramuscular

injections would be difficult and injections would need to be timed to moments of injury (or before going to exercise). A more precise targeting strategy would therefore need to be established in order to consider this a viable therapy.

Similarly to these targeted Delta delivery strategies, delivery of TGF-β1 receptor kinase inhibitor, which was also effectively used to regulate TGF-β1 signaling in the aged muscle niche could be used[11,12]. In this case, however, as aged mice treated with systemically-injected TGF-β1 receptor kinase inhibitor showed a marked improvement in muscle regeneration, a circulating particle loaded with TGF-β1 receptor kinase inhibitor may be suitable[12].

As a parallel strategy, the same nanoparticulate platforms could be used to directly inhibit the action of TGF-β1. Specifically, the nanoparticles could be decorated with TGF-β1-binding molecules such as antibodies, antibody fragments, etc. Unlike in the Delta or TGF-β1 receptor kinase inhibitor cases, the decorated nanoparticles will not be delivering a payload, but will instead serve as TGF-β1 scavengers that will bind and inhibit the action of TGF-β1 in the aged niche. These multivalent TGF-β1 'sponges' could collect hundreds of TGF-β1 molecules each and will greatly improve efficiency of TGF-β1 inhibition (over free antibody injections). Regulating 'aged' TGF-β1 levels to the precise 'young' levels will require manipulation of the number of TGF-β1-binding sites on the particles and the number of particles to be used; too few particles will have little or no effect on the TGF-β1 inhibition of muscle regeneration; too many particles will also have deleterious effects, as a certain level of TGF-β1 signaling must be maintained[12,42]. As in the previous case with delivery of Delta, the immune clearance of nanoparticles will occur. However, in this case, this removal of TGF-β1-decorated particles by immune cells will be beneficial as it will decrease active TGF-β1 signaling levels, thus lowering the block on muscle regeneration. The remaining issue is that of TGF-β1 localization. It is known that TGF-β1 can be internal to circulating platelets or secreted by various cell types[12,42], (though some TGF-β1 has been observed systemically in diseased states[185]); upon platelet activation, TGF-β1 is released, crosses into tissue, and becomes active in the local extracellular matrix[12,42]. Therefore the issue of targeting TGF-β1 locally (in the muscle niche) arises, and consequently the same concerns as in the Delta delivery situation. In any case, this multivalent nanoparticulate platform can provide greater local regulation of TGF-β1 levels than a simple free antibody-driven system and may at least be very useful as a model for *in vitro* studies, where niche targeting is not an issue.

3.6 Satellite Cells and Muscle Stem Cells: Biomaterials to Help Determine Who is Who

Skeletal muscle satellite cells make up a small portion of the cells on muscle fibers [186]. Correctly identifying adult muscle stem cells in order to generate new muscle is therefore essential for therapeutic purposes. However, whether or not satellite cells are the only myogenic precursor cells, and whether all satellite cells are in fact muscle stem cells is still a topic of debate[7,38,79]. Several other cell lines, including hematopoeitic cells[187-190], mesoangioblasts[191], and pericytes[192] have shown myogenic potential[79]. Satellite cells may even differ between muscle types[1,193]. In fact disagreement still remains over which markers define satellite cells and which characterize actual muscle stem cells[7,72]. Finally there is the disputed place of reserve cells which arise during myoblast differentiation *in vitro* and may contribute to replenishing the satellite cell pool[38,48,194-196]. These problems are exacerbated by the fact that there are so few satellite cells per fiber, which makes identifying surface markers with conventional methods such as flow cytometry or immunostaining less reliable. Novel uses of biomaterials may provide the answers to some of these questions and after discussing the current satellite cell classification, we will suggest one such method.

Originally, satellite cells were identified solely based on their biological location beneath the basal lamina of skeletal muscle fibers[2]. The most often cited current satellite cell marker (and muscle stem cell marker) is the paired box transcription factor Pax7[1,7,38,40,48,57,91,194,196,197]. However, a recent publication suggests that this Pax7 may not be a unique identifier and that it is only a subpopulation of the Pax7-positive satellite cell population (i.e., satellite cells that are Pax7$^+$/Myf5$^+$) that actually contributes to muscle regeneration. The Pax7$^+$/Myf5$^-$ population was found to serve as a muscle stem cell reservoir to replenish satellite cells after a cycle of regeneration[7].

Current satellite cell isolation and sorting strategies are mostly limited to FACSs sorting based on specific markers[7]. One such example defines CD34$^+$, α7-integrin$^+$, CD31$^-$, CD45$^-$, CD11b$^-$, Sca1$^-$ as satellite cells[7] (>95% satellite cells) while another includes CD45$^-$, Sca-1$^-$, Mac-1$^-$, CXCR4$^+$, β1-integrin$^+$ as part of the satellite cell pool[198]. Overall, surface markers that have been considered as identifying of quiescent satellite cells include: CXCR4$^+$ (fusin), CD34$^+$ (not specific, but useful for sorting from heterogeneous populations of cells)[1,38,57,193,199], α7-integrin$^+$, CD31$^-$ (PECAM-1), CD45$^-$ (PTPRC), CD11b$^-$ (Integrin αM, Mac-1,CR3A), Sca1$^-$ (ATX1, D6S504E), Syndecan-3$^+$ [38,200], Syndecan-4$^+$ [7,38,48,57,193,197,199-202], cMet$^+$ (hepatocyte growth factor receptor (HGFR))[38,203,204], caveolin1$^+$ [204], Fzd7$^+$ [7], M-cadherin (CDH15)[38,57,203,205], β1 integrin (CD29)[57,206], VCAM-1$^+$ [38,207], NCAM$^+$ (CD56, leu-19) [38,208,209], ABGC2[79,210], and the antigen for the SM/C-2.6 monoclonal antibody[79,211], while internal markers include: MyoD[48,201], Myf5[38,57,67,193,197,199,201] (though this is now debated by Le Grand's work), MNF (myocyte nuclear factor)[38,212], myostatin (growth differentiation factor 8)[38,200,213,214], IRF-2, (interferon regulatory factor-2)[38,207], Msx1 (hox7, hyd1)[38,200].

However there is still a lack of agreement on which markers completely define satellite cells, but maybe more importantly, which define the muscle stem cell population. In order to work on isolating these markers from such minute populations of cells, novel biomaterial-based microfluidic devices could be used to effectively sort small numbers of cells based on their surface markers (based on past work[215]). A recent paper from the Sohn and Conboy labs describes a novel microfluidic device that highlights the heterogeneity of the satellite cell population[72]. This microfluidic channel, equipped with a small antibody-functionalized pore, analyzes surface marker expression of single satellite cells using a technique called resistive-pulse sensing[217,218]. Briefly, a 4-point electrode measurement monitors current across the pore; as a cell transits the pore, resistance increases, leading to a drop (downward pulse) in current. The transit time of the cell through the pore is also monitored. Longer transit times indicate interaction between the cell and the antibody-functionalized pore and expression of specific cell surface receptors. This publication demonstrated that even within the satellite cell population there is significant heterogeneity in expression of markers that have previously been identified as satellite cell markers. Further work in the Sohn lab aims to analyze multiple markers on a single cell using a single microfluidic device[219].

Incorporation of other microfluidic technologies such as single-cell protein analysis techniques could push this work further by allowing determination of gene expression at the single cell level[216]. This will allow detection of differences between these small populations of cells and identification of subpopulations of cells within the satellite cell niche. Together, this work has promise in shedding light on the characteristics of skeletal muscle satellite cells, and the determination of the subpopulation of muscle stem cells.

3.7 Use of Biomaterials in Tissue Engineering Applications

As we have seen, biomaterials have many applications in tissue regenerative therapies for adult skeletal muscle. However, the possible negative impact of biomaterials must still be

kept in mind. Biocompatibility of materials, the effects of biomaterial degradation and degradation products on the niche, the host response to non-degrading implants or materials, and the inflammatory and immune response will all need to be considered once biomaterial platforms are optimized and ready for clinical trials. Nevertheless, the potential to treat myopathic conditions or the effects of aging on the adult skeletal muscle niche with biomaterials is real and perhaps not that distant.

Conclusion

Adult skeletal muscle regeneration is orchestrated by a complex network of signaling molecules that are still being uncovered. The onset of aging impedes the regenerative potential of muscle stem cells and much work is being done to reverse these effects. However, there are still some doubts as to whether all satellite cells are muscle stem cells and how to most efficiently enhance muscle regeneration in the old and in individuals afflicted by genetic muscle wasting. The use of biomaterials as 3-D muscle satellite cell niches, delivery vehicles for genes, drugs, or pro-regenerative factors, and for further definition of the heterogeneous skeletal muscle stem cell pool will likely lead to efficient, robust, and clinically-feasible enhancements to muscle regeneration strategies.

Acknowledgments

Chapter 4

Attenuation of TGF-β Signaling

via Incorporation

of a Dominant-negative TGF-β Type II Receptor

Improves Differentiation of Murine Skeletal

Myoblasts

Introduction

As discussed in Chapter 3, aging affects skeletal muscle repair by impairing regeneration of muscle fibers. Notably, increased systemic and local levels of transforming growth factor β1 (TGF-β1) lead to decreased activation of satellite cells upon injury and therefore contribute to decreased repaired myofibers and increased scar tissue formation. In order to study the effects of TGF-β signaling on muscle repair, I transfected skeletal muscle myoblasts with a dominant-negative TGF-β Type II receptor (dnTGFβRII) and studied the effects of TGF-β1 signaling on myoblast differentiation. Incorporation of a dnTGFβRII into myoblasts led to decrease TGF-β1 signaling and improved differentiation as evidenced by western blotting of downstream signaling molecules from the TGF-β signaling pathway and quantification of myotube size and myogenic index in established differentiation experiments.

4.1 Expansion, Purification, and Confirmation of a dnTGFβRII plasmid

The plasmid containing the dnTGFβRII (Plasmid 12640: LNCX TbetaRII DN[1] (Figure 4.1) was purchased through Addgene (Cambridge, MA) .
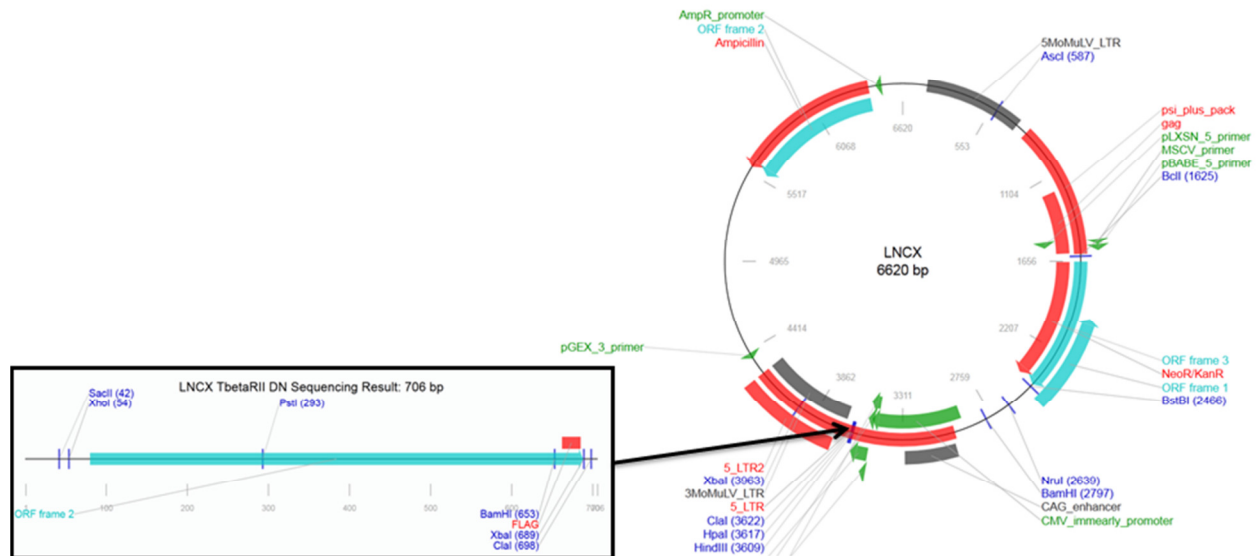
Figure 4.1 LNCX TbetaRIIDN plasmid 12640 from Addgene. The plasmid contains a FLAG-tagged dnTGFβRII receptor cloned into the HpaI (3617) site.

Luria Broth (LB) agar plates with 100 µg/mL ampicillin were streaked with bacteria containing plasmid 12640 and selected colonies were expanded in 3-5 mL LB medium with 100 µg/mL ampicillin for 8 hours at 37°C, before a larger, overnight expansion in 200 mL of LB with 100 µg/mL ampicillin on a shaker in a warm room (37°C). The dnTGFβRII plasmid was purified using a Qiagen Maxi Prep (Qiagen Düsseldorf, Germany) and plasmid DNA concentration was determined via NanoDrop (Thermo Scientific, Wilmington, DE). The DNA sequence of the

dnTGFβRII plasmid was verified and confirmed both by digestion and agarose gel electrophoresis (Figure 4.2), and by submitting samples and primers to the UC Berkeley DNA Sequencing Facility (2 µg of DNA and 3.2 pmol of LNCX CMV Primer - AGCTCGTTTAGTGAACCGTCAGATC Human CMV promoter, forward primer, Life Technologies) (Figure 4.3).
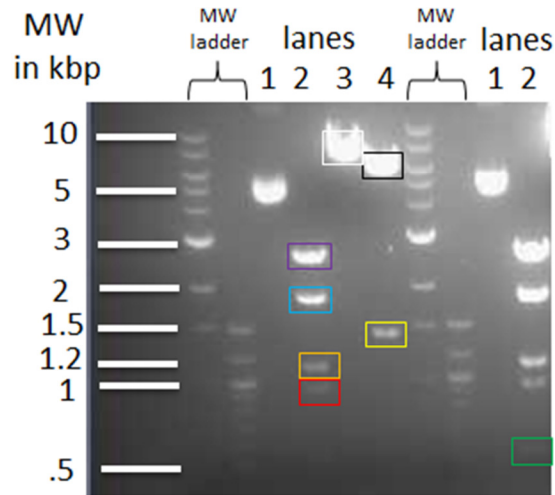
Figure 4.2 Agarose gel of plasmid 12640. Bands represent fragments cut with various restriction enzymes. Lane 1 – uncut plasmid; lane 2 – cut with PstI, generating fragments at 8bp, 176 bp, - **522bp**, **923bp**, **1150bp**, **1878bp**, **2669bp**; lane 3 – cut with XbaI, generating fragments at 363bp (visible only upon overexposure of gel) and 6963bp (white); lane 4 – cut with BamHI, generating fragments at **1473bp** and **5853 bp**.

4.2 Transfection and selection of skeletal muscle myoblasts with dnTGFβRII

Skeletal muscle myoblasts derived from satellite cells of C57/Bl-6 mice were maintained in Ham's F-10 media (GIBCO, Life Technologies, Grand Island, NY) supplemented with 20% bovine growth serum (Hyclone, Thermo Scientific, Logan, UT), 1% Penicillin/Streptomycin (Life Technologies), and 6 ng/mL fibroblast growth factor on 1:250-diluted Matrigel-coated (BD Biosciences, San Jose, CA) 10 cm dishes. Myoblasts plated into Matrigel-coated 6-well dishes were transfected with the dnTGFβRII plasmid using Lipofectamine 2000 (Life Technologies) following the manufacturer's protocol. 4 samples containing 2.5 µg of plasmid DNA were combined with 6, 9, 12, and 15 µL of Lipofectamine 2000, incubated at room temperature for five minutes and then added to myoblasts at 50-70% confluency. The plasmid was incubated with the myoblasts overnight before fresh growth media was added. The myoblasts were cultured and passed as usual for 2 days before selecting for transfected cells.
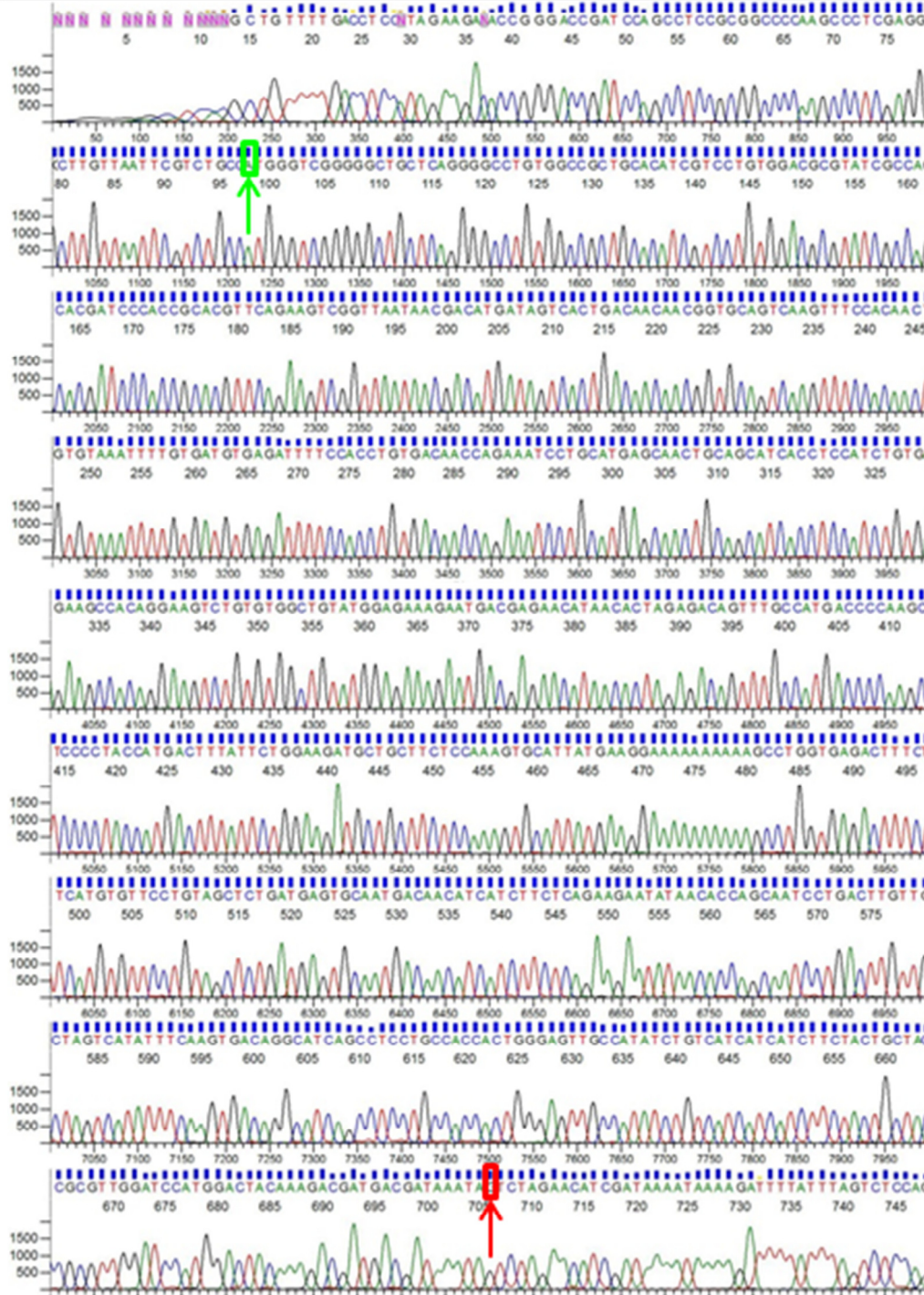
Figure 4.3 Plasmid 12640 sequencing data. The green and red arrows indicate the start and end sites coding for the dnTGFβRII.

The 12640 plasmid also confers resistance to the antibiotic geneticin (G418). Selection of transfected cells was done after determining a suitable concentration of G418 to kill un-transfected myoblasts in 3-4 days (Figure 4.4). The 400 µg/mL concentration was selected, and transfected cells were
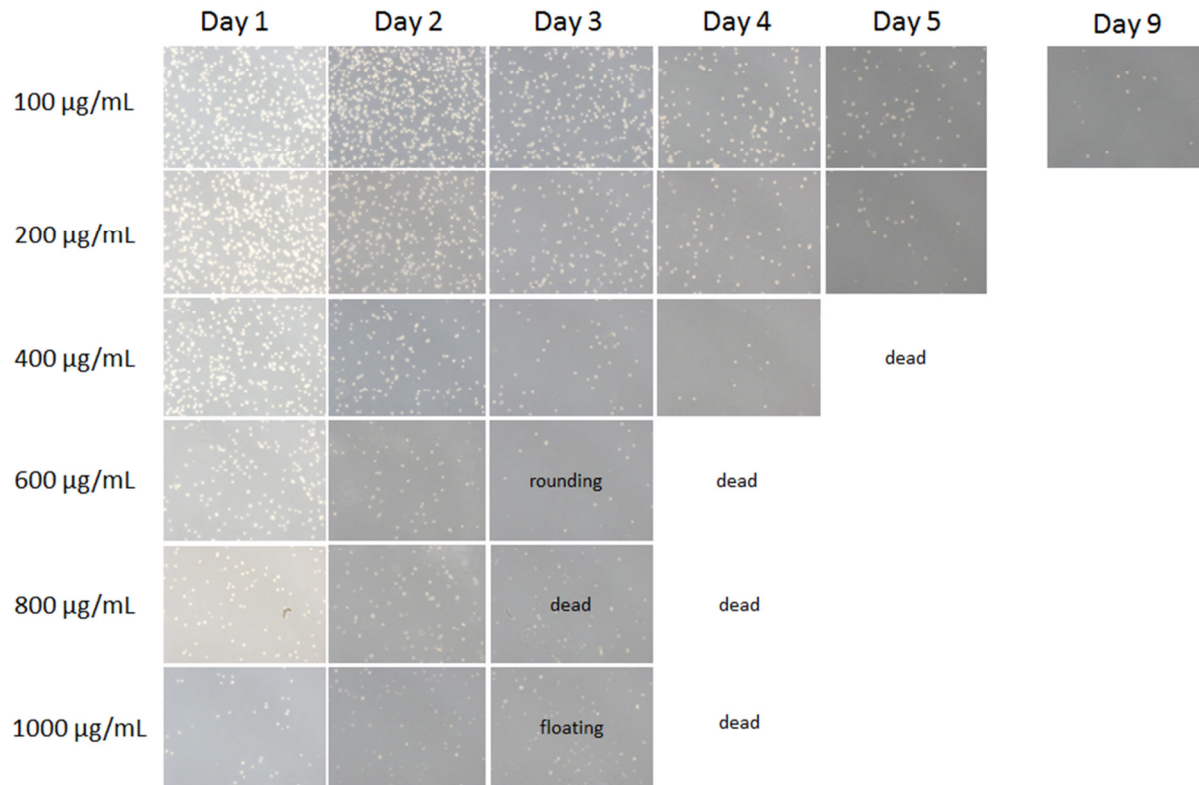
Figure 4.4 Determination of killing concentration of G418 antibiotic on un-transfected myoblasts. Myoblasts plated in 6-well culture dishes were maintained in growth media containing increasing concentrations of G418 (0-1 mg/mL). Cell growth was monitored daily and the concentration that killed cells in 3-4 days (400 µg/mL) was chosen to select transfected cells.

cultured subsequently in growth media containing 400 µg/mL G418. Whereas myoblasts cultured with 400 µg/mL G418 died within 3-4 days, transfected cells cultured with 400 µg/mL G418 survived and proliferated, indicating incorporation of the plasmid DNA and expression of the resistance to G418.

4.3 Expression of dnTGFβRII in skeletal muscle myoblasts

While resistance to G418 confirms that the dnTGFβRII plasmid has been integrated into the cells, it does not imply with all certainty that the dnTGFβRII is in fact expressed in the

transfected cells. In order to confirm expression of the dnTGFβRII in our cells, I prepared skeletal muscle myoblasts lysates from both un-transfected and dnTGFβRII-transfected cells. Cells were washed twice with PBS, scraped on ice in RIPA buffer, sonicated briefly, centrifuged to pellet cell membrane and debris, and the cell supernatants were collected and quantified for protein concentration. Cell protein lysates were separated by molecular weight by SDS-PAGE and probed for dnTGFβRII expression with anti-FLAG antibodies (Figure 4.5). β–actin expression was determined as a loading control.
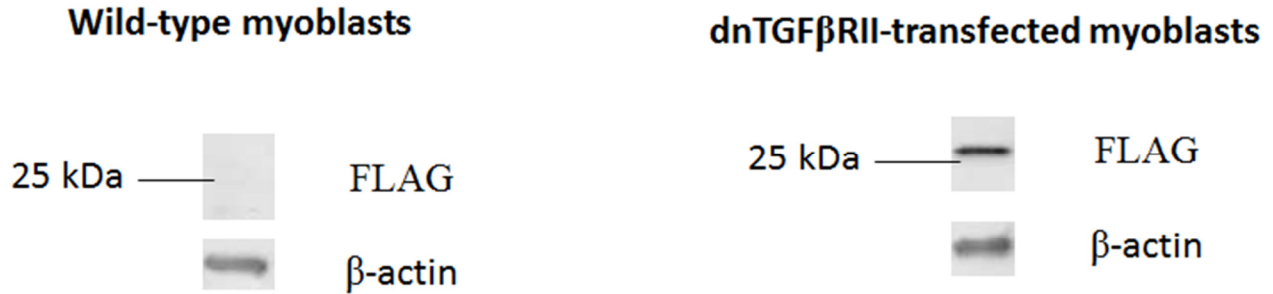
Figure 4.5 Western blot for FLAG-tagged dnTGFβRII. Un-transfected myoblasts show no expression of dnTGFβRII whereas transfected and selected myoblasts show a clear band indicating dnTGFβRII expression.

4.4 Expression of dnTGFβRII attenuates TGFβ-1 signaling

As described in Chapter 3, TGFβ-1 initially binds to a TGFβ type II receptor, which then phosphorylates a TGFβ type I receptor, before downstream signaling occurs. The dominant-negative TGFβ type II receptor is truncated cytoplasmically and is therefore not able to phosphorylate the type I receptor and induce downstream signaling. Therefore the dnTGFβRII will compete with wild-type TGFβ type II receptors to bind the TGFβ-1 ligand, but will not induce TGFβ signaling, potentially attenuating the effects of TGFβ signaling. To confirm that the transfected dnTGFβRII is having a functional effect, I prepared cell lysates from un-transfected and transfected cells with the addition of TGFβ-1. In order to eliminate the uncertainty of TGFβ-1 in bovine growth serum (present in growth media), cells were passaged into serum-free defined OPTI-MEM media (GIBCO) (containing 1 % Penstrep, and 6 ng/mL fibroblast growth factor (FGF)), adhered to Matrigel-coated dishes overnight, and then pulsed with 10 ng/mL TGFβ-1 in OPTI-MEM + FGF for 1 hour. Cell lysates were then prepared as previously described. Protein lysates were probed for the downstream effector pSmad3 (Smad3 is phosphorylated to pSmad3 by the TGFβ type I receptor), total Smad2/3, and the β-actin control (Figure 4.6a). As shown in Figure 4.6a, expression of the dnTGFβRII leads to a significant ~1.6-fold decrease in TGFβ-1 signaling, as evidenced by a decreased expression of pSmad3. Total Smad2/3 levels were not significantly changed (Figure 4.7). Cell lysates were prepared from control-plasmid-transfected myoblasts (SABiosciences, Valencia, CA), cultured with or without TGFβ-1, and probed for

pSmad2, pSmad3, Smad2/3, and β-actin (Figure 4.6b). As expected, cells that were exposed to 10 ng/mL TGFβ-1 in OPTI-MEM + FGF for 1 hour expressed pSmad2 and pSmad3, while cells without exposure showed no downstream TGFβ-1 signaling.

4.5 Expression of dnTGFβRII enhances skeletal muscle myoblast differentiation

In order to assess the effects of incorporating a dnTGFβRII on skeletal muscle myoblast differentiation, I plated un-transfected and dnTGFβRII-transfected myoblasts at 30,000 cells/well in Matrigel-coated 8-well Lab-Tek II Chamber Slides (Thermo Scientific) for 22 hours in
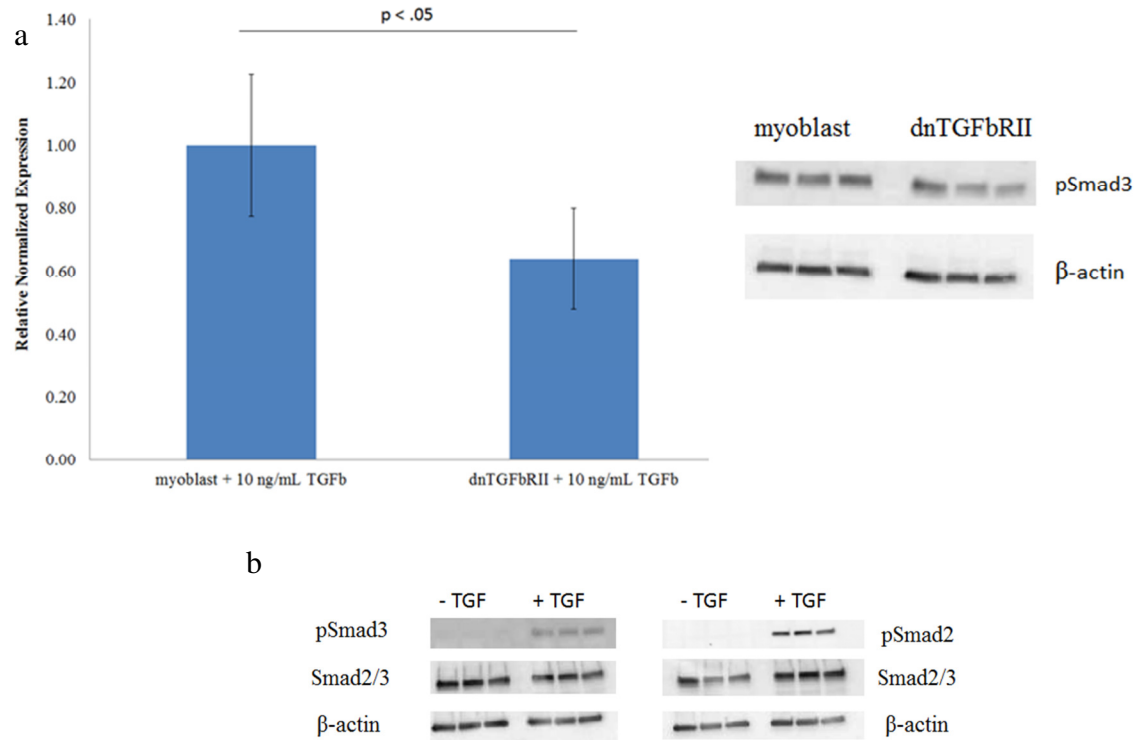
Figure 4.6 a) Expression of dnTGFβRII attenuates TGFβ-1 signaling via 1.6-fold decrease in pSmad3 expression. Un-transfected and transfected (dnTGFbRII) samples were analyzed by western blot for the expression of the downstream TGFβ-1 effector pSmad3 and β-actin control. Expression in three samples for both un-transfected and transfected cells was averaged and normalized values were compared relative to myoblasts culture with 10 ng/mL TGFβ-1 for one hour at 37°C in OPTI-MEM + FGF. b) Control-plasmid-transfected myoblasts cultured with or without 10 ng/mL TGFβ-1 in OPTI-MEM + FGF for 1 hour were analyzed by western blot for the expression of the downstream TGFβ-1 effectors, pSmad2 and pSmad3, total Smad2/3, and β-actin control. As expected, pSmad2 and pSmad3 expression is upregulated only in samples exposed to TGFβ-1.

51
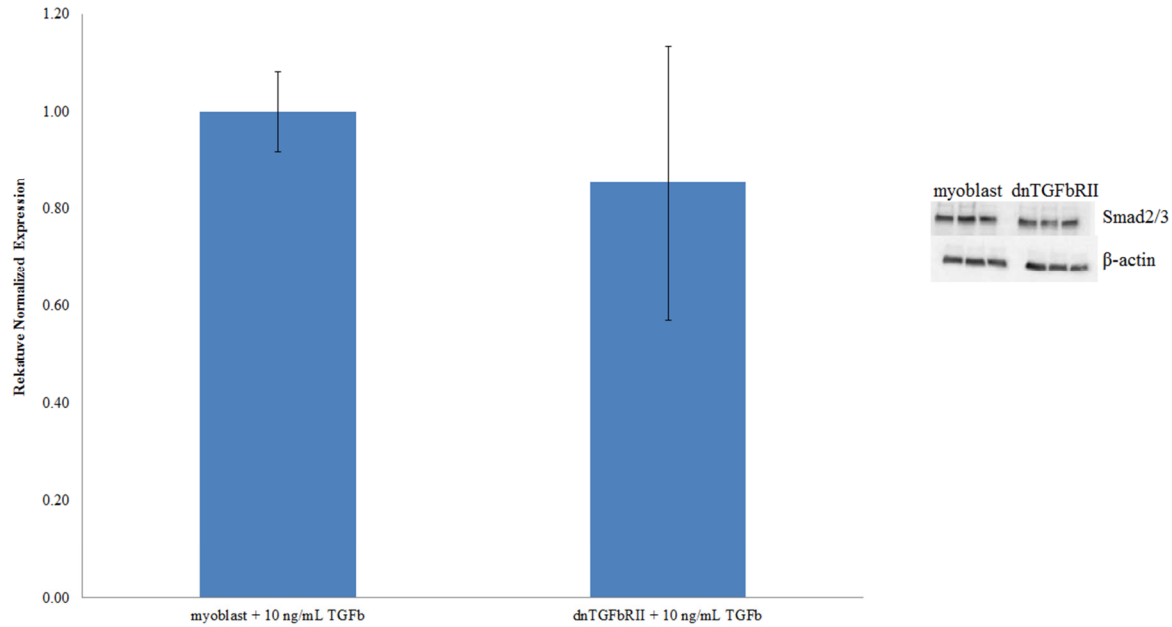
Figure 4.7 Expression of dnTGFβRII does not significantly affect total Smad2/3 levels. Untransfected and transfected (dnTGFbRII) samples were analyzed by western blot for the expression of total Smad2/3 and β-actin control. Expression in three samples for both untransfected and transfected cells was averaged and normalized values were compared relative to myoblasts culture with 10 ng/mL TGFβ-1 for one hour at 37°C in OPTI-MEM + FGF.

OPTI+FGF media +/- 10 ng/mL TGFβ1. Cells were then washed once with differentiation media (DM: DMEM + 2% horse serum + 1 % penicillin/streptomycin) and incubated for 48 hours in fresh DM to induce differentiation into myotubes. Plated cells were then washed once with cold PBS, fixed in cold 70% ethanol for at least 30 minutes, washed 2x 5 minutes with PBS, 1x 5 minutes with staining buffer (SB: 1x PBS with 1 % bovine growth serum, 0.1% sodium azide), permeabilized with 0.25% Triton-X 100 in SB for 15 minutes at room temperature, washed 3x5 minutes with SB and incubated overnight at 4°C with primary antibodies (anti-eMyHC at 1:10 from DHSP, University of Iowa, or the corresponding mouse IgG control 1-5 µg/mL, Thermo Scientific). Primary-labeled cells were washed 3x 5 minutes with SB then labeled with fluorophore-tagged secondary antibodies (Thermo Scientific) at 1 µg/mL and Hoechst at 2 µM for 1 hour at room temperature. Cells were washed finally 3x 5 minutes with SB, mounted with Fluoromount Aqueous Mounting Medium and imaged at 10X with an ImageXpress Micro Widefield High Content Screening System. Figure 4.8 shows the effect of incorporating the dnTGFβRII into myoblasts with or without the addition of exogenous TGFβ-1. In parallel, control-plasmid-transfected myoblasts were also differentiated (as above) and compared to wild-type myoblasts differentiation, with or without the presence of TGF-β1 (Figure 4.8).

a)

b)

Average Myogenic Index (Percentage of nuclei in myotubes (2+ nuclei) / total number of nuclei)

c)
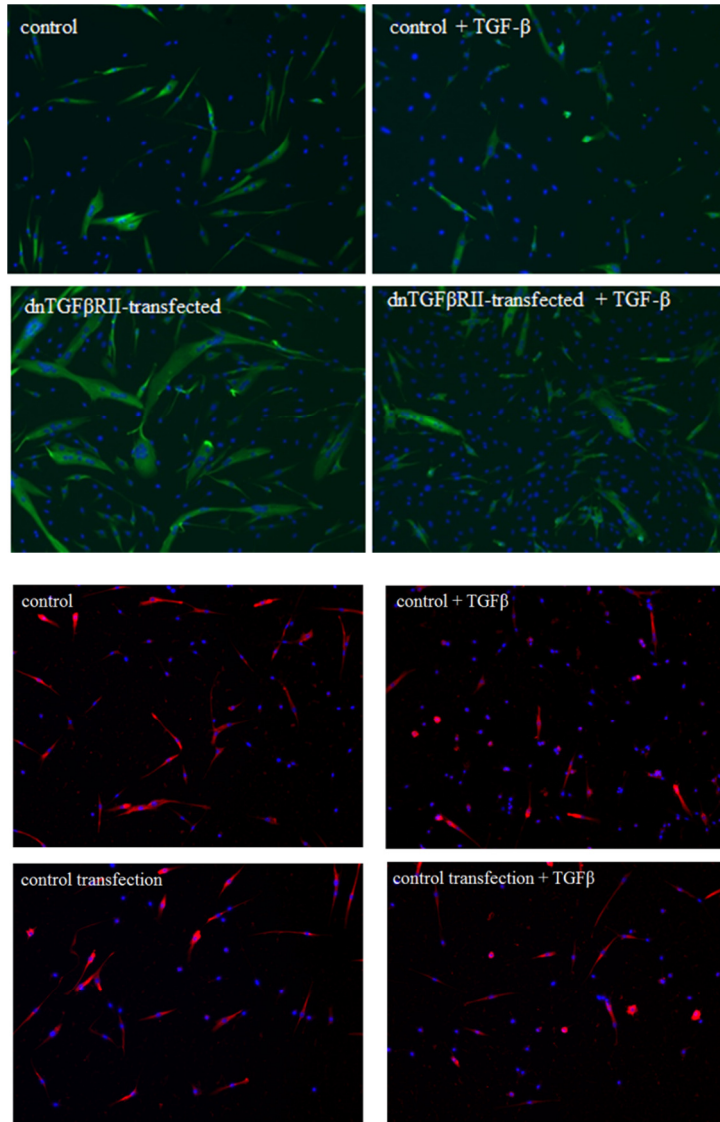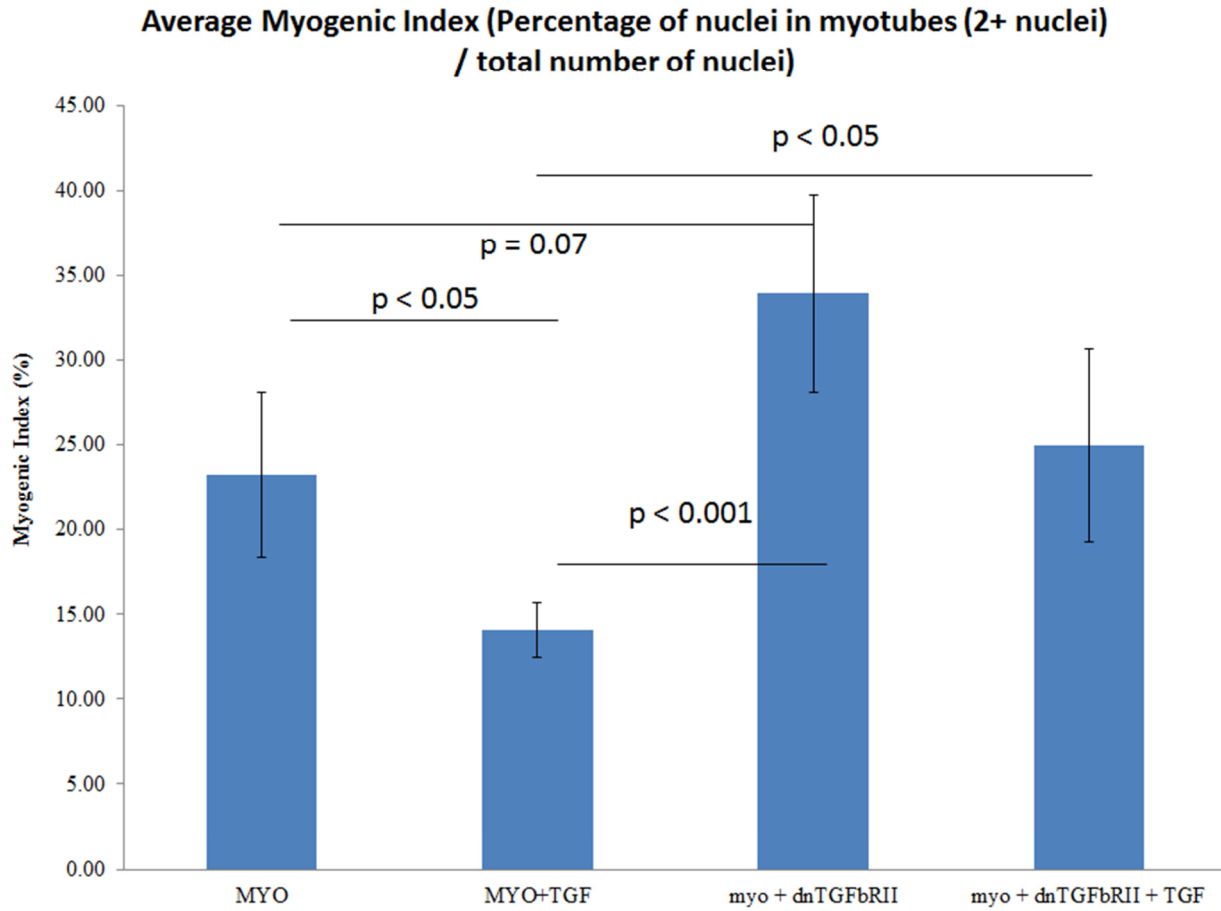
Average Myogenic Index (Percentage of nuclei in myotubes (3+ nuclei) / total number of nuclei)
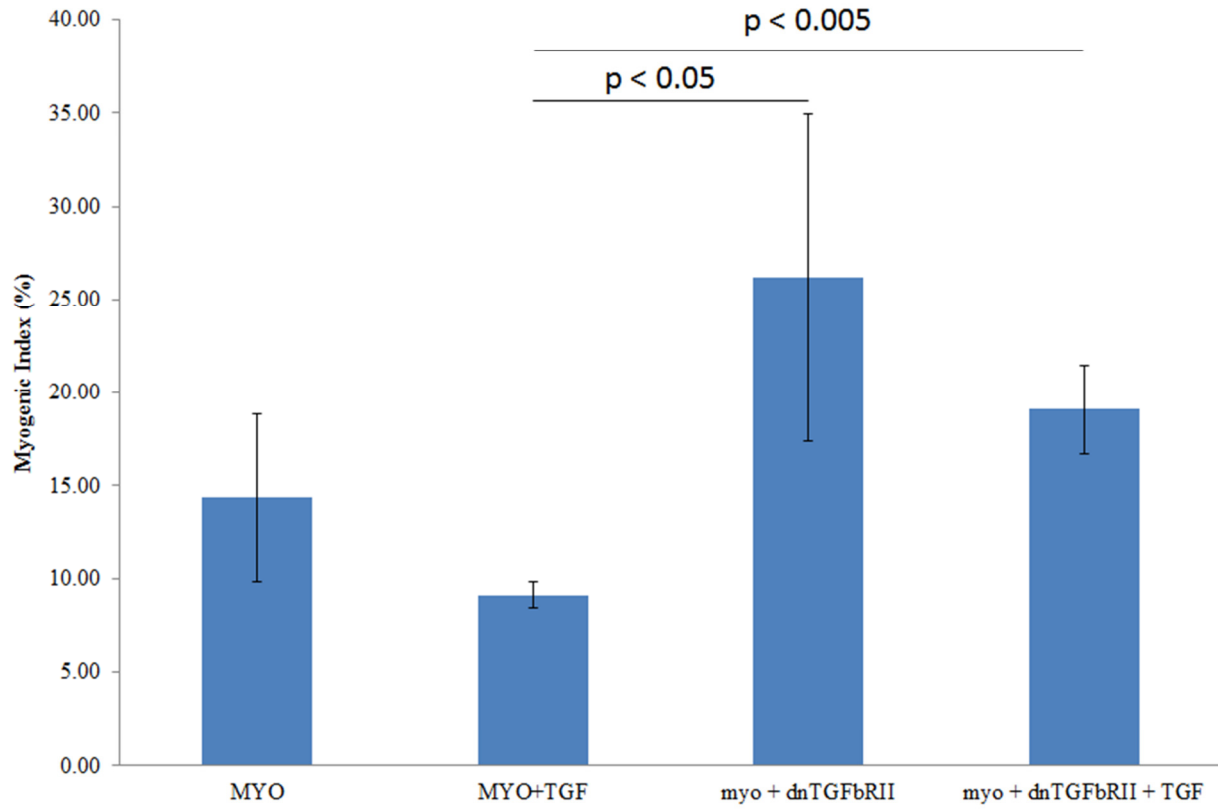
d)
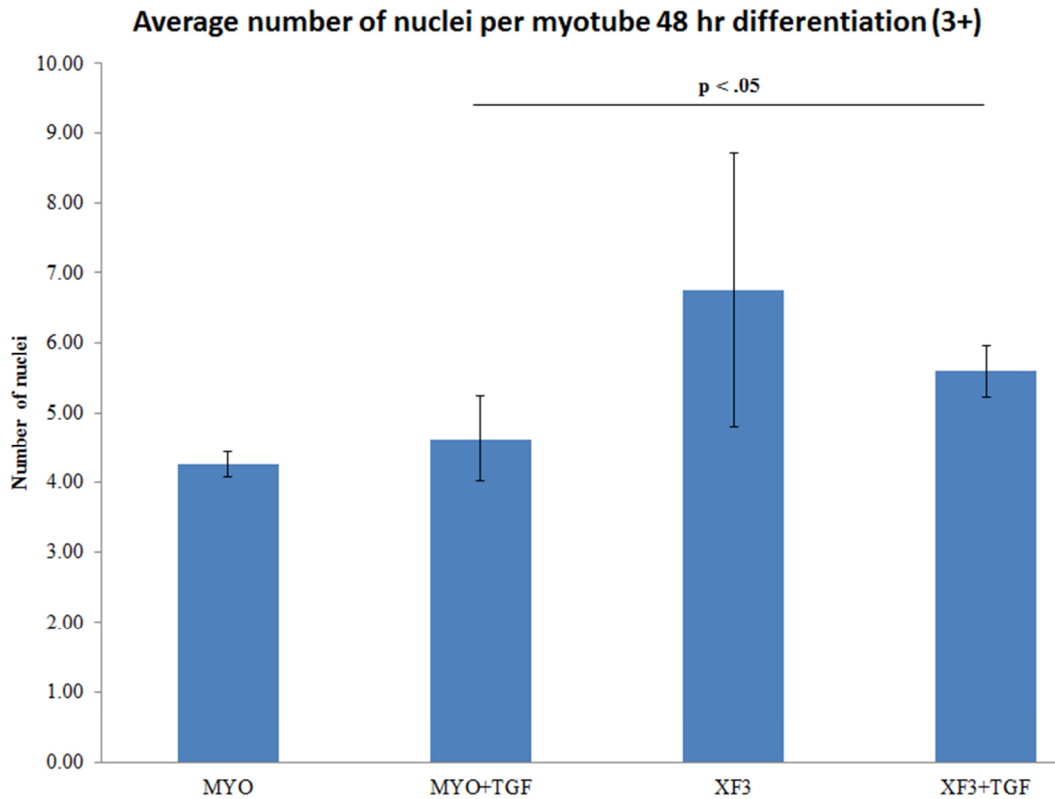
Figure 4.8 a) Representative images of differentiated un-transfected or transfected myoblasts with or without the addition of TGFβ1 followed by representative images of differentiated myoblasts and differentiated myoblasts transfected with control plasmid with or without the addition of TGFβ1. b,c) Average myogenic index = number of nuclei in newly-formed myofibers/total number of nuclei (defining a myotube as a cell with 2+ nuclei = b or 3+ nuclei = c). Average values and standard deviation from n = 3 independent experiments. p values computed using t-test. d) Average number of nuclei per myotube after 48 hours of differentiation in DM.

In order to quantify the effects of incorporating a dnTGFβRII on skeletal muscle myoblast differentiation, I calculated the myogenic index which is determined as follows:

$$Myogenic\ index = \frac{number\ of\ nuclei\ in\ newly-formed\ myotubes}{total\ number\ of\ nuclei} * 100$$

I quantified the myogenic index defining myotubes as either containing 2 or more or 3 or more nuclei (as this is still up for debate). As expected, exposure of myoblasts to TGFβ1 led to a significant ~1.6-fold decrease in the myogenic index of differentiating un-transfected cells. Incorporation of the dnTGFβRII receptor, however, led to a significant ~2-fold increase in the myogenic index of differentiating cells exposed to TGF-β1 as compared to their un-transfected counterparts, indicating that the transfected dnTGFβRII improves muscle differentiation. Furthermore, analysis of the average number of nuclei per myotube (Figure 4.8d) indicated that dnTGFβRII-transfected cells created larger myotubes, thus having a more robust regenerative capacity to form myotubes/myofibers. Although the control fusion experiment did not work well, there was no significant difference in differentiation between the control-plasmid-transfected myoblasts and the wild-type myoblasts. While the fusion is too low and the experiment should be repeated, the possibility remains that the incorporation of the dnTGFβRII enhances the fusion of myoblasts into myotubes.

4.6 Discussion

As discussed in Chapter 3, TGF-β signaling has a negative impact on skeletal muscle regeneration; in this chapter, I focused on the effects of TGF-β signaling on skeletal muscle myoblast differentiation. However, the effects of TGF-β on skeletal muscle cell proliferation have also been extensively studied[2–5]. It has long been known that Notch signaling is needed for satellite cells to break quiescence[6–10]. However, recent work from the Conboy lab has shown that there is in fact a balancing game between Notch and TGF-β signaling that contributes to activation of skeletal muscle satellite cells[3]. TGF-β signaling through TGF-β type I and type II receptors, leads to phosphorylation of Smads 2 and 3, formation of Smad2 and Smad3 complexes with Smad4, and translocation to the nucleus, ultimately leading to the activation of cell-cycle inhibitors p15, p16, p21, and p27. Thus, in the aged skeletal muscle niche, where TGF-β levels are increased, the satellite cell-cycle progression is inhibited, contributing to poorer muscle regeneration. Knock-down of Smad3 signaling using shRNA enhanced muscle regeneration in old muscle[3]. The effects of TGF-β signaling on cell proliferation observed in mouse models were also seen in human muscle samples[2]. Similarly, skeletal muscle niche levels of TGF-β were elevated in the aged as were nuclear pSmad3 levels in human satellite cells.

Methods to knock-down TGF-β signaling may therefore provide a significant advantage in enhancing muscle repair. To this end, we incorporated a dnTGFβRII into skeletal muscle myoblasts and studied the effects with or without the presence of TGF-β.

We began by purifying plasmid DNA containing our FLAG-tagged dnTGFβRII and confirmed the plasmid by DNA sequencing and Southern blot. Incorporation of the dnTGFβRII into skeletal muscle myoblasts in culture was confirmed by the cells' resistance to antibiotic treatment and detection of the FLAG-tagged dnTGFβRII by western blot. Functional effects of

the dnTGFβRII translated into a decrease in downstream signaling upon addition of TGFβ-1 and an increase in myogenic index and myotube size when differentiating myoblasts into myotubes.

The use of OPTI-MEM in the study was important as the presence of TGFβ and other factors in growth medium sera could confound the results. Specifically, initial western blot experiments were conducted in growth media (containing 20% BGS) and pSmad3 levels were markedly higher than if samples had been cultured in OPTI-MEM (data not shown).

This work suggests that downregulation of TGFβ signaling via incorporation of a dnTGFβRII could boost muscle regeneration. These findings could be especially important in the context of aged muscle, where it is known that TGFβ levels are elevated. Further work in our laboratory is focused on investigating the effects of expressing this dnTGFβRII in vivo in both young and old mice and observing the effects on muscle regeneration. Additionally, we hope to more deeply study the crosstalk between the TGFβ signaling pathway and other pathways such as the MAPK/ERK pathway. It is well known that fibroblast growth factor 2, a MAPK agonist induces Delta and active Notch[2]. Forced activation of the MAPK pathway promotes regeneration of both young and old satellite cells and inhibition of the MAPK pathway (through MEK inhibitor) significantly decreases Delta and active Notch levels, impeding muscle regeneration. There are several known crosstalk points with between the MAPK and TGFβ pathways[5]. Some of the crosstalk elements lead to increased TGFβ signaling. For example, the transcriptional corepressor Grouch/transducin-like enhancer of split is phosphorylated by active ERK/MAPK, leading to knockdown of TGFβ inhibition caused by the repressor Brinker[11]. Additionally, TGFβ signaling can be increased by JNK which enhances Smad2/3-Smad4 interactions[12]. On the other hand, TGFβ signaling can be inhibited by ERK/MAPK via phosphorylation of Smad2/3 in their linker regions, preventing nuclear accumulation of these transcription factors and subsequent activation of CDK inhibitors[12]. Future work will explore this crosstalk in greater detail.

REFERENCES

Chapter 1 – Microfluidic Devices for Cell Sorting

1.   Gao, Y., Li, W. & Pappas, D. Recent advances in microfluidic cell separations. *Analyst* 138, 4714–21 (2013).

2.   Chapman, M. R. *et al.* Sorting single satellite cells from individual myofibers reveals heterogeneity in cell-surface markers and myogenic capacity. *Integr. Biol. (Camb).* 5, 692–702 (2013).

3.   Fong, C.-Y., Gauthaman, K. & Bongso, A. Teratomas from pluripotent stem cells: A clinical hurdle. *J. Cell. Biochem.* 111, 769–81 (2010).

4.   Didar, T. F. & Tabrizian, M. Adhesion based detection, sorting and enrichment of cells in microfluidic Lab-on-Chip devices. *Lab Chip* 10, 3043–53 (2010).

5.   Jabart, E. B., Balakrishnan, K. R. & Sohn, L. L. in *Stem Cells Tissue Eng. 2nd version* (World Scientific Publishing, Inc.).

6.   Toh, Y.-C. & Voldman, J. Fluid shear stress primes mouse embryonic stem cells for differentiation in a self-renewing environment via heparan sulfate proteoglycans transduction. *FASEB J. Off. Publ. Fed. Am. Soc. Exp. Biol.* 25, 1208–1217 (2011).

7.   Li, P., Stratton, Z. S., Dao, M., Ritz, J. & Huang, T. J. Probing circulating tumor cells in microfluidics. *Lab Chip* 13, 602–9 (2013).

8.   Yu, M., Stott, S., Toner, M., Maheswaran, S. & Haber, D. a. Circulating tumor cells: approaches to isolation and characterization. *J. Cell Biol.* 192, 373–82 (2011).

9.   Wachtel, S., Shulman, L. & Sammons, D. Fetal cells in maternal blood. *Clin. Genet.* 59, 74–79 (2001).

10.   Wu, H.-W., Lin, C.-C. & Lee, G.-B. Stem cells in microfluidics. *Biomicrofluidics* 5, 13401 (2011).

11.   Wu, T.-H. *et al.* Pulsed laser triggered high speed microfluidic fluorescence activated cell sorter. *Lab Chip* 12, 1378–83 (2012).

12.   Plouffe, B. D., Mahalanabis, M., Lewis, L. H., Klapperich, C. M. & Murthy, S. K. Clinically relevant microfluidic magnetophoretic isolation of rare-cell populations for diagnostic and therapeutic monitoring applications. *Anal. Chem.* 84, 1336–44 (2012).

13.   Cho, S. H., Chen, C. H., Tsai, F. S., Godin, J. M. & Lo, Y.-H. Human mammalian cell sorting using a highly integrated micro-fabricated fluorescence-activated cell sorter (microFACS). *Lab Chip* 10, 1567–73 (2010).

59

14. Hur, S. C., Brinckerhoff, T. Z., Walthers, C. M., Dunn, J. C. Y. & Di Carlo, D. Label-free enrichment of adrenal cortical progenitor cells using inertial microfluidics. *PLoS One* 7, e46550 (2012).

15. Lieu, V. H., House, T. a & Schwartz, D. T. Hydrodynamic tweezers: impact of design geometry on flow and microparticle trapping. *Anal. Chem.* 84, 1963–8 (2012).

16. Sun, J. *et al.* Simultaneous on-chip DC dielectrophoretic cell separation and quantitative separation performance characterization. *Anal. Chem.* 84, 2017–24 (2012).

17. Ling, S. H., Lam, Y. C. & Chian, K. S. Continuous cell separation using dielectrophoresis through asymmetric and periodic microelectrode array. *Anal. Chem.* 84, 6463–70 (2012).

18. Yang, A. H. J. & Soh, H. T. Acoustophoretic Sorting of Viable Mammalian Cells in a Micro fl uidic Device. (2012).

19. Chapman, M. R. *et al.* Sorting single satellite cells from individual myofibers reveals heterogeneity in cell-surface markers and myogenic capacity. *Integr. Biol. Quant. Biosci. from nano to macro* 692–702 (2013). doi:10.1039/c3ib20290a

20. Mittal, S., Wong, I. Y., Deen, W. M. & Toner, M. Antibody-functionalized fluid-permeable surfaces for rolling cell capture at high flow rates. *Biophys. J.* 102, 721–30 (2012).

21. Carbonaro, A., Mohanty, S. K., Huang, H., Godley, L. A. & Sohn, L. L. Cell characterization using a protein-functionalized pore. *Lab Chip* 8, 1478–1485 (2008).

22. Carbonaro, A. & Sohn, L. L. A resistive-pulse sensor chip for multianalyte immunoassays. *Lab Chip* 5, 1155–1160 (2005).

23. Wang, S. *et al.* Efficient on-chip isolation of HIV subtypes. *Lab Chip* 12, 1508–15 (2012).

24. Nagrath, S. *et al.* Isolation of rare circulating tumour cells in cancer patients by microchip technology. *Nature* 450, 1235–1239 (2007).

25. Sheng, W. *et al.* Aptamer-Enabled E ffi cient Isolation of Cancer Cells from Whole Blood Using a Micro fl uidic Device. (2012).

26. Stott, S. L. *et al.* Isolation of circulating tumor cells using a microvortex-generating herringbone-chip. *Proc. Natl. Acad. Sci.* 107, 18392–18397 (2010).

27. Chen, Y., Wu, T.-H., Kung, Y.-C., Teitell, M. a & Chiou, P.-Y. 3D pulsed laser-triggered high-speed microfluidic fluorescence-activated cell sorter. *Analyst* 138, 7308–15 (2013).

28. Ibrahim, S. F. & van den Engh, G. Flow cytometry and cell sorting. *Adv Biochem Eng Biotechnol* 106, 19–39 (2007).

29. Ibrahim, S. F. & van den Engh, G. High-speed cell sorting: fundamentals and recent advances. *Curr. Opin. Biotechnol.* 14, 5–12 (2003).

30. Leary, J. F. Ultra high-speed sorting. *Cytometry. A* 67, 76–85 (2005).

31. Hammer, D. a & Tirrell, M. Biological Adhesion at Interfaces. *Annu. Rev. Mater. Sci.* 26, 651–691 (1996).

32. Myung, J. H., Launiere, C. a, Eddington, D. T. & Hong, S. Enhanced tumor cell isolation by a biomimetic combination of E-selectin and anti-EpCAM: implications for the effective separation of circulating tumor cells (CTCs). *Langmuir* 26, 8589–96 (2010).

33. Guo, K.-T. *et al.* A new technique for the isolation and surface immobilization of mesenchymal stem cells from whole bone marrow using high-specific DNA aptamers. *Stem Cells* 24, 2220–2231 (2006).

34. Elliot, S. Cell Damage due to Hydrodynamic Stress in Fluorescence Activated Cell Sorters. 42 (2009).

35. Kubitschek, H. Electronic Counting and Sizing of Bacteria. *Nature* 182, 234–235 (1958).

36. DeBlois, R. W. Counting and Sizing of Submicron Particles by the Resistive Pulse Technique. *Rev. Sci. Instrum.* 41, 909 (1970).

37. Saleh, O. a & Sohn, L. L. Direct detection of antibody-antigen binding using an on-chip artificial pore. *Proc. Natl. Acad. Sci. U. S. A.* 100, 820–4 (2003).

38. Schmalbruch, H. THE SATELLITE CELL OF SKELETAL MUSCLE FIBRES. 23, 159–172 (2006).

39. Balakrishnan, K. R. *et al.* Node-pore sensing: a robust, high-dynamic range method for detecting biological species. *Lab Chip* 1302–1307 (2013). doi:10.1039/c3lc41286e

40. Thomson, J. a. Embryonic Stem Cell Lines Derived from Human Blastocysts. *Science (80-.).* 282, 1145–1147 (1998).

41. Chen, Q. *et al.* Microfluidic isolation of highly pure embryonic stem cells using feeder-separated co-culture system. *Sci. Rep.* 3, 2433 (2013).

42. Brignier, A. C. & Gewirtz, A. M. Embryonic and adult stem cell therapy. *J. Allergy Clin. Immunol.* 125, S336–44 (2010).

43. Takahashi, K. *et al.* Induction of pluripotent stem cells from adult human fibroblasts by defined factors. *Cell* 131, 861–72 (2007).

44. Takahashi, K. & Yamanaka, S. Induction of pluripotent stem cells from mouse embryonic and adult fibroblast cultures by defined factors. *Cell* 126, 663–76 (2006).

45. Cao, F. *et al.* Spatial and temporal kinetics of teratoma formation from murine embryonic stem cell transplantation. *Stem Cells Dev.* 16, 883–891 (2007).

46. Yamanaka, S. Strategies and new developments in the generation of patient-specific pluripotent stem cells. *Cell Stem Cell* 1, 39–49 (2007).

47. Wang, X. *et al.* Enhanced cell sorting and manipulation with combined optical tweezer and microfluidic chip technologies. *Lab Chip* 11, 3656–62 (2011).

48. Schriebl, K. *et al.* Selective Removal of Undifferentiated Human Embryonic Stem Cells Using Magnetic Activated Cell Sorting Followed by a Cytotoxic Antibody. 18, (2012).

49. Singh, A. *et al.* Adhesion strength-based, label-free isolation of human pluripotent stem cells. *Nat. Methods* 10, 438–44 (2013).

50. Ohgushi, M. *et al.* Molecular pathway and cell state responsible for dissociation-induced apoptosis in human pluripotent stem cells. *Cell Stem Cell* 7, 225–39 (2010).

Chapter 2 – A Microfluidic Method for the Selection of Undifferentiated Human Embryonic Stem Cells and *in Situ* Analysis

1.   Chapman, M. R. *et al.* Sorting single satellite cells from individual myofibers reveals heterogeneity in cell-surface markers and myogenic capacity. *Integr. Biol. Quant. Biosci. from nano to macro* 692–702 (2013). doi:10.1039/c3ib20290a

2.   Fong, C.-Y., Gauthaman, K. & Bongso, A. Teratomas from pluripotent stem cells: A clinical hurdle. *J. Cell. Biochem.* 111, 769–81 (2010).

3.   Didar, T. F. & Tabrizian, M. Adhesion based detection, sorting and enrichment of cells in microfluidic Lab-on-Chip devices. *Lab Chip* 10, 3043–53 (2010).

4.   Toh, Y.-C. & Voldman, J. Fluid shear stress primes mouse embryonic stem cells for differentiation in a self-renewing environment via heparan sulfate proteoglycans transduction. *FASEB J. Off. Publ. Fed. Am. Soc. Exp. Biol.* 25, 1208–1217 (2011).

5.   Jabart, E. B., Balakrishnan, K. R. & Sohn, L. L. in *Stem Cells Tissue Eng. 2nd version* (World Scientific Publishing, Inc.).

6.   Lindström, S. & Andersson-Svahn, H. Overview of single-cell analyses: microdevices and applications. *Lab Chip* 10, 3363–3372 (2010).

7.   Tárnok, A., Ulrich, H. & Bocsi, J. Phenotypes of stem cells from diverse origin. *Cytom. Part A J. Int. Soc. Anal. Cytol.* 77, 6–10 (2010).

8.   Singh, A. *et al.* Adhesion strength-based, label-free isolation of human pluripotent stem cells. *Nat. Methods* 10, 438–44 (2013).

9.   Fong, C. Y., Peh, G. S. L., Gauthaman, K. & Bongso, A. Separation of SSEA-4 and TRA-1-60 labelled undifferentiated human embryonic stem cells from a heterogeneous cell population using magnetic-activated cell sorting (MACS) and fluorescence-activated cell sorting (FACS). *Stem Cell Rev.* 5, 72–80 (2009).

10.   Hewitt, Z. *et al.* Fluorescence-activated single cell sorting of human embryonic stem cells. *Cloning Stem Cells* 8, 225–34 (2006).

11.   Eiges, R. *et al.* Establishment of human embryonic stem cell-transfected clones carrying a marker for undifferentiated cells. *Curr. Biol.* 11, 514–8 (2001).

12.   Sidhu, K. S. & Tuch, B. E. Cell Lines by FACS Sorting and Their Characterization. 69, 61–69 (2006).

13.   Schriebl, K. *et al.* Selective Removal of Undifferentiated Human Embryonic Stem Cells Using Magnetic Activated Cell Sorting Followed by a Cytotoxic Antibody. 18, (2012).

14. Wang, X. *et al.* Enhanced cell sorting and manipulation with combined optical tweezer and microfluidic chip technologies. *Lab Chip* 11, 3656–62 (2011).

15. Carbonaro, A., Mohanty, S. K., Huang, H., Godley, L. A. & Sohn, L. L. Cell characterization using a protein-functionalized pore. *Lab Chip* 8, 1478–1485 (2008).

16. Abcam. Indirect flow cytometry (FACS) protocol. at <http://www.abcam.com/index.html?pageconfig=resource&rid=11381>

17. Emre, N. *et al.* The ROCK inhibitor Y-27632 improves recovery of human embryonic stem cells after fluorescence-activated cell sorting with multiple cell surface markers. *PLoS One* 5, e12148 (2010).

18. Holm, F. in *Hum. Embryonic Induc. Pluripotent Stem Cells* (Ye, K. & Jin, S.) 85–90 (Humana Press, 2012). doi:10.1007/978-1-61779-267-0

19. Quinlan, L. R. in *Methods Mol. Biol. Embryonic Stem Cell Protoc.* 329, 127–149 (2006).

20. Abruzzese, R. V & Fekete, R. A. in *Pluripotent Stem Cells* 997, 217–224 (2013).

21. Liu, Y., Judd, K. & Lakshmipathy, U. in *Pluripotent Stem Cells* (Lakshmipathy, U. & Vemuri, M. C.) 997, 263–272 (Humana Press, 2013).

22. Hwang, N. S., Varghese, S. & Elisseeff, J. in *Stem Cell Assays* 407, 351–373 (2007).

23. Liu, Y. *et al.* in *Hum. Embryonic Stem Cell Protoc.* (Turksen, K.) 584, 229–268 (Humana Press, 2010).

24. McCarty, O. J. T., Jadhav, S., Burdick, M. M., Bell, W. R. & Konstantopoulos, K. Fluid shear regulates the kinetics and molecular mechanisms of activation-dependent platelet binding to colon carcinoma cells. *Biophys. J.* 83, 836–848 (2002).

25. Draper, J. S., Pigott, C., Thomson, J. a & Andrews, P. W. Surface antigens of human embryonic stem cells: changes upon differentiation in culture. *J. Anat.* 200, 249–58 (2002).

26. Zhao, W., Ji, X., Zhang, F., Li, L. & Ma, L. Embryonic stem cell markers. *Molecules* 17, 6196–236 (2012).

27. Qiu, D. *et al.* Profiling TRA-1-81 antigen distribution on a human embryonic stem cell. *Biochem. Biophys. Res. Commun.* 369, 735–40 (2008).

28. Cozens-Roberts, C., Quinn, J. A. & Lauffenberger, D. A. Receptor-mediated adhesion phenomena. Model studies with the Radical-Flow Detachment Assay. *Biophys. J.* 58, 107–125 (1990).

29. Clausen, J. *Laboratory Techniques in Biochemistry and Molecular Biology, Vol. 1.* (North-Holland Publishing Co., New York, 1981).

30. Armstrong, J. K., Wenby, R. B., Meiselman, H. J. & Fisher, T. C. The hydrodynamic radii of macromolecules and their effect on red blood cell aggregation. *Biophys. J.* 87, 4259–70 (2004).

31. Stewart, M. H. *et al.* Clonal isolation of hESCs reveals heterogeneity within the pluripotent stem cell compartment. *Nat. …* 3, (2006).

32. Gu, B. *et al.* Global expression of cell surface proteins in embryonic stem cells. *PLoS One* 5, e15795 (2010).

33. Mantel, C. *et al.* Checkpoint-apoptosis uncoupling in human and mouse embryonic stem cells: a source of karyotpic instability. *Blood* 109, 4518–27 (2007).

34. Mittal, S., Wong, I. Y., Deen, W. M. & Toner, M. Antibody-functionalized fluid-permeable surfaces for rolling cell capture at high flow rates. *Biophys. J.* 102, 721–30 (2012).

35. Alix-Panabières, C. & Pantel, K. Technologies for detection of circulating tumor cells: facts and vision. *Lab Chip* (2014). doi:10.1039/c3lc50644d

36. Nagrath, S. *et al.* Isolation of rare circulating tumour cells in cancer patients by microchip technology. *Nature* 450, 1235–1239 (2007).

37. Pratt, E. D., Huang, C., Hawkins, B. G., Gleghorn, J. P. & Kirby, B. J. Rare Cell Capture in Microfluidic Devices. *Chem. Eng. Sci.* 66, 1508–1522 (2011).

38. Sekine, K., Revzin, A., Tompkins, R. G. & Toner, M. Panning of multiple subsets of leukocytes on antibody-decorated poly(ethylene) glycol-coated glass slides. *J. Immunol. Methods* 313, 96–109 (2006).

39. Murthy, S. K., Sin, A., Tompkins, R. G. & Toner, M. Effect of flow and surface conditions on human lymphocyte isolation using microfluidic chambers. *Langmuir Acs J. Surfaces Colloids* 20, 11649–11655 (2004).

40. Plouffe, B. D., Kniazeva, T., Mayer, J. E., Murthy, S. K. & Sales, V. L. Development of microfluidics as endothelial progenitor cell capture technology for cardiovascular tissue engineering and diagnostic medicine. *FASEB J. Off. Publ. Fed. Am. Soc. Exp. Biol.* 23, 3309–3314 (2009).

41. Cheng, X. *et al.* A microfluidic device for practical label-free CD4(+) T cell counting of HIV-infected subjects. *Lab Chip* 7, 170–178 (2007).

42. Stott, S. L. *et al.* Isolation of circulating tumor cells using a microvortex-generating herringbone-chip. *Proc. Natl. Acad. Sci.* 107, 18392–18397 (2010).

43. Wang, S. *et al.* Highly efficient capture of circulating tumor cells by using nanostructured silicon substrates with integrated chaotic micromixers. *Angew. Chemie Int. Ed.* 50, 3084–3088 (2011).

44. Wang, S. *et al.* Three-dimensional nanostructured substrates toward efficient capture of circulating tumor cells. *Angew. Chemie Int. Ed.* 48, 8970–8973 (2009).

45. Gleghorn, J. P. *et al.* Capture of circulating tumor cells from whole blood of prostate cancer patients using geometrically enhanced differential immunocapture (GEDI) and a prostate-specific antibody. *Lab Chip* 10, 27–29 (2010).

46. Cheung, L. S.-L. *et al.* Adhesion dynamics of circulating tumor cells under shear flow in a bio-functionalized microchannel. *J. Micromechanics Microengineering* 21, 054033 (2011).

47. Zheng, X., Cheung, L. S.-L., Schroeder, J. a, Jiang, L. & Zohar, Y. Cell receptor and surface ligand density effects on dynamic states of adhering circulating tumor cells. *Lab Chip* 11, 3431–9 (2011).

48. Myung, J. H., Launiere, C. a, Eddington, D. T. & Hong, S. Enhanced tumor cell isolation by a biomimetic combination of E-selectin and anti-EpCAM: implications for the effective separation of circulating tumor cells (CTCs). *Langmuir* 26, 8589–96 (2010).

Chapter 3 - Introduction to Skeletal Muscle Regeneration, Aging, and Repair Mechanisms

1.   Zammit PS, Partridge TA & Yablonka-Reuveni Z (2006) The skeletal muscle satellite cell: the stem cell that came in from the cold. *J Histochem Cytochem* 54, 1177-1191.

2.   Mauro A (1961) Satellite cell of skeletal muscle fibers. *The Journal of biophysical and biochemical cytology* 9, 493-495.

3.   Moss FP & Leblond CP (1971) Satellite cells as the source of nuclei in muscles of growing rats. *The Anatomical record* 170, 421-435.

4.   Bischoff R (1975) Regeneration of single skeletal muscle fibers in vitro. *The Anatomical record* 182, 215-235.

5.   Bischoff R (1986) Proliferation of muscle satellite cells on intact myofibers in culture. *Developmental biology* 115, 129-139.

6.   Konigsberg UR, Lipton BH & Konigsberg IR (1975) The regenerative response of single mature muscle fibers isolated in vitro. *Developmental biology* 45, 260-275.

7.   Le Grand F, Jones AE, Seale V, Scime A & Rudnicki MA (2009) Wnt7a activates the planar cell polarity pathway to drive the symmetric expansion of satellite stem cells. *Cell stem cell* 4, 535-547.

8.   Collins CA, Olsen I, Zammit PS, Heslop L, Petrie A, Partridge TA & Morgan JE (2005) Stem cell function, self-renewal, and behavioral heterogeneity of cells from the adult muscle satellite cell niche. *Cell* 122, 289-301.

9.   Conboy IM & Rando TA (2002) The regulation of Notch signaling controls satellite cell activation and cell fate determination in postnatal myogenesis. *Developmental cell* 3, 397-409.

10.   Brack AS, Conboy IM, Conboy MJ, Shen J & Rando TA (2008) A temporal switch from notch to Wnt signaling in muscle stem cells is necessary for normal adult myogenesis. *Cell stem cell* 2, 50-59.

11.   Carlson ME, Hsu M & Conboy IM (2008) Imbalance between pSmad3 and Notch induces CDK inhibitors in old muscle stem cells. *Nature* 454, 528-532.

12.   Carlson ME, Conboy MJ, Hsu M, Barchas L, Jeong J, Agrawal A, Mikels AJ, Agrawal S, Schaffer DV & Conboy IM (2009) Relative roles of TGF-beta1 and Wnt in the systemic regulation and aging of satellite cell responses. *Aging cell*.

13.   Zhao P & Hoffman EP (2004) Embryonic myogenesis pathways in muscle regeneration. *Dev Dyn* 229, 380-392.

14.   Carlson ME & Conboy IM (2007) Regulating the Notch pathway in embryonic, adult and old stem cells. *Current opinion in pharmacology* 7, 303-309.

15.   Artavanis-Tsakonas S, Rand MD & Lake RJ (1999) Notch signaling: cell fate control and signal integration in development. *Science (New York, NY* 284, 770-776.

16.   Bray SJ (2006) Notch signalling: a simple pathway becomes complex. *Nature reviews* 7, 678-689.

17.   Kadesch T (2004) Notch signaling: the demise of elegant simplicity. *Current opinion in genetics & development* 14, 506-512.

18.   Cheng P, Nefedova Y, Miele L, Osborne BA & Gabrilovich D (2003) Notch signaling is necessary but not sufficient for differentiation of dendritic cells. *Blood* 102, 3980-3988.

19.   Schroeder T, Kohlhof H, Rieber N & Just U (2003) Notch signaling induces multilineage myeloid differentiation and up-regulates PU.1 expression. *J Immunol* 170, 5538-5548.

20.   Schroeder T, Meier-Stiegen F, Schwanbeck R, Eilken H, Nishikawa S, Hasler R, Schreiber S, Bornkamm GW, Nishikawa S & Just U (2006) Activated Notch1 alters differentiation of embryonic stem cells into mesodermal cell lineages at multiple stages of development. *Mechanisms of development* 123, 570-579.

21.   Nofziger D, Miyamoto A, Lyons KM & Weinmaster G (1999) Notch signaling imposes two distinct blocks in the differentiation of C2C12 myoblasts. *Development (Cambridge, England)* 126, 1689-1702.

22.   Rosenblatt JD, Lunt AI, Parry DJ & Partridge TA (1995) Culturing satellite cells from living single muscle fiber explants. *In vitro cellular & developmental biology* 31, 773-779.

23.   Kamakura S, Oishi K, Yoshimatsu T, Nakafuku M, Masuyama N & Gotoh Y (2004) Hes binding to STAT3 mediates crosstalk between Notch and JAK-STAT signalling. *Nature cell biology* 6, 547-554.

24.   Molofsky AV, Pardal R & Morrison SJ (2004) Diverse mechanisms regulate stem cell self-renewal. *Current opinion in cell biology* 16, 700-707.

25.   Sundaram MV (2005) The love-hate relationship between Ras and Notch. *Genes & development* 19, 1825-1839.

26.   Carlson ME, Silva HS & Conboy IM (2008) Aging of signal transduction pathways, and pathology. *Experimental cell research* 314, 1951-1961.

27. Cossu G & Borello U (1999) Wnt signaling and the activation of myogenesis in mammals. *The EMBO journal* 18, 6867-6872.

28. Anakwe K, Robson L, Hadley J, Buxton P, Church V, Allen S, Hartmann C, Harfe B, Nohno T, Brown AM, Evans DJ & Francis-West P (2003) Wnt signalling regulates myogenic differentiation in the developing avian wing. *Development (Cambridge, England)* 130, 3503-3514.

29. Petropoulos H & Skerjanc IS (2002) Beta-catenin is essential and sufficient for skeletal myogenesis in P19 cells. *The Journal of biological chemistry* 277, 15393-15399.

30. Brack AS, Conboy MJ, Roy S, Lee M, Kuo CJ, Keller C & Rando TA (2007) Increased Wnt signaling during aging alters muscle stem cell fate and increases fibrosis. *Science (New York, NY* 317, 807-810.

31. DasGupta R & Fuchs E (1999) Multiple roles for activated LEF/TCF transcription complexes during hair follicle development and differentiation. *Development (Cambridge, England)* 126, 4557-4568.

32. Hagen T, Di Daniel E, Culbert AA & Reith AD (2002) Expression and characterization of GSK-3 mutants and their effect on beta-catenin phosphorylation in intact cells. *The Journal of biological chemistry* 277, 23330-23335.

33. Yuan H, Mao J, Li L & Wu D (1999) Suppression of glycogen synthase kinase activity is not sufficient for leukemia enhancer factor-1 activation. *The Journal of biological chemistry* 274, 30419-30423.

34. Schmalbruch H & Hellhammer U (1977) The number of nuclei in adult rat muscles with special reference to satellite cells. *The Anatomical record* 189, 169-175.

35. Gibson MC & Schultz E (1983) Age-related differences in absolute numbers of skeletal muscle satellite cells. *Muscle & nerve* 6, 574-580.

36. Charlton CA, Mohler WA, Radice GL, Hynes RO & Blau HM (1997) Fusion competence of myoblasts rendered genetically null for N-cadherin in culture. *The Journal of cell biology* 138, 331-336.

37. Bockhold KJ, Rosenblatt JD & Partridge TA (1998) Aging normal and dystrophic mouse muscle: analysis of myogenicity in cultures of living single fibers. *Muscle & nerve* 21, 173-183.

38. Charge SB & Rudnicki MA (2004) Cellular and molecular regulation of muscle regeneration. *Physiological reviews* 84, 209-238.

39.   Snow MH (1983) A quantitative ultrastructural analysis of satellite cells in denervated fast and slow muscles of the mouse. *The Anatomical record* 207, 593-604.

40.   Carlson ME & Conboy IM (2007) Loss of stem cell regenerative capacity within aged niches. *Aging cell* 6, 371-382.

41.   Schultz E & Lipton BH (1982) Skeletal muscle satellite cells: changes in proliferation potential as a function of age. *Mechanisms of ageing and development* 20, 377-383.

42.   Derynck R & Zhang YE (2003) Smad-dependent and Smad-independent pathways in TGF-beta family signalling. *Nature* 425, 577-584.

43.   Massague J (1998) TGF-beta signal transduction. *Annual review of biochemistry* 67, 753-791.

44.   Massague J & Chen YG (2000) Controlling TGF-beta signaling. *Genes & development* 14, 627-644.

45.   Studitsky AN (1964) Free Auto- and Homografts of Muscle Tissue in Experiments on Animals. *Annals of the New York Academy of Sciences* 120, 789-801.

46.   Sadeh M, Czyewski K & Stern LZ (1985) Chronic myopathy induced by repeated bupivacaine injections. *Journal of the neurological sciences* 67, 229-238.

47.   Luz MA, Marques MJ & Santo Neto H (2002) Impaired regeneration of dystrophin-deficient muscle fibers is caused by exhaustion of myogenic cells. *Brazilian journal of medical and biological research = Revista brasiliera de pesquisas medicas e biologicas / Sociedade Brasileira de Biofisica [et al* 35, 691-695.

48.   Shefer G, Van de Mark DP, Richardson JB & Yablonka-Reuveni Z (2006) Satellite-cell pool size does matter: defining the myogenic potency of aging skeletal muscle. *Developmental biology* 294, 50-66.

49.   Conboy IM, Conboy MJ, Smythe GM & Rando TA (2003) Notch-mediated restoration of regenerative potential to aged muscle. *Science (New York, NY* 302, 1575-1577.

50.   Gibson A & Yu O (1983) Biphasic non-adrenergic, non-cholinergic relaxations of the mouse anococcygeus muscle. *British journal of pharmacology* 79, 611-615.

51.   Nnodim JO (2000) Satellite cell numbers in senile rat levator ani muscle. *Mechanisms of ageing and development* 112, 99-111.

52.   Roth SM, Martel GF, Ivey FM, Lemmer JT, Metter EJ, Hurley BF & Rogers MA (2000) Skeletal muscle satellite cell populations in healthy young and older men and women. *The Anatomical record* 260, 351-358.

53. Carlson M SC, Conboy MJ, Aagaard P, Mackey A, Kjaer M, Conboy IM (2009) Molecular aging and rejuvenation of human muscle stem cells. *EMBO Molecular Medicine*.

54. Conboy IM, Conboy MJ, Wagers AJ, Girma ER, Weissman IL & Rando TA (2005) Rejuvenation of aged progenitor cells by exposure to a young systemic environment. *Nature* 433, 760-764.

55. Carlson BM, Dedkov EI, Borisov AB & Faulkner JA (2001) Skeletal muscle regeneration in very old rats. *The journals of gerontology* 56, B224-233.

56. McCay CM, Pope F, Lunsford W, Sperling G & Sambhavaphol P (1957) Parabiosis between old and young rats. *Gerontologia* 1, 7-17.

57. Conboy IM & Rando TA (2005) Aging, stem cells and tissue regeneration: lessons from muscle. *Cell cycle (Georgetown, Tex* 4, 407-410.

58. Assoian RK, Komoriya A, Meyers CA, Miller DM & Sporn MB (1983) Transforming growth factor-beta in human platelets. Identification of a major storage site, purification, and characterization. *The Journal of biological chemistry* 258, 7155-7160.

59. Massague J (1987) The TGF-beta family of growth and differentiation factors. *Cell* 49, 437-438.

60. Tang P, Jasser SA, Sung JC, Shi Y, Steck PA & Yung WK (1999) Transforming growth factor-alpha antisense vectors can inhibit glioma cell growth. *Journal of neuro-oncology* 43, 127-135.

61. Yu JH & Schaffer DV (2006) High-throughput, library-based selection of a murine leukemia virus variant to infect nondividing cells. *Journal of virology* 80, 8981-8988.

62. Gellibert F, Woolven J, Fouchet MH, Mathews N, Goodland H, Lovegrove V, Laroze A, Nguyen VL, Sautet S, Wang R, Janson C, Smith W, Krysa G, Boullay V, De Gouville AC, Huet S & Hartley D (2004) Identification of 1,5-naphthyridine derivatives as a novel series of potent and selective TGF-beta type I receptor inhibitors. *Journal of medicinal chemistry* 47, 4494-4506.

63. Singh J, Chuaqui CE, Boriack-Sjodin PA, Lee WC, Pontz T, Corbley MJ, Cheung HK, Arduini RM, Mead JN, Newman MN, Papadatos JL, Bowes S, Josiah S & Ling LE (2003) Successful shape-based virtual screening: the discovery of a potent inhibitor of the type I TGFbeta receptor kinase (TbetaRI). *Bioorganic & medicinal chemistry letters* 13, 4355-4359.

64. Yeom SY, Jeoung D, Ha KS & Kim PH (2004) Small interfering RNA (siRNA) targetted to Smad3 inhibits transforming growth factor-beta signaling. *Biotechnology letters* 26, 699-703.

65. Zacks SI & Sheff MF (1982) Age-related impeded regeneration of mouse minced anterior tibial muscle. *Muscle & nerve* 5, 152-161.

66. Carlson BM & Faulkner JA (1989) Muscle transplantation between young and old rats: age of host determines recovery. *The American journal of physiology* 256, C1262-1266.

67. Alliston T, Ko TC, Cao Y, Liang YY, Feng XH, Chang C & Derynck R (2005) Repression of bone morphogenetic protein and activin-inducible transcription by Evi-1. *The Journal of biological chemistry* 280, 24227-24237.

68. Annes JP, Munger JS & Rifkin DB (2003) Making sense of latent TGFbeta activation. *Journal of cell science* 116, 217-224.

69. Hyytiainen M, Penttinen C & Keski-Oja J (2004) Latent TGF-beta binding proteins: extracellular matrix association and roles in TGF-beta activation. *Critical reviews in clinical laboratory sciences* 41, 233-264.

70. Husmann I, Soulet L, Gautron J, Martelly I & Barritault D (1996) Growth factors in skeletal muscle regeneration. *Cytokine & growth factor reviews* 7, 249-258.

71. Barcellos-Hoff MH (1996) Latency and activation in the control of TGF-beta. *Journal of mammary gland biology and neoplasia* 1, 353-363.

72. Chapman, M. R. et al. Sorting single satellite cells from individual myofibers reveals heterogeneity in cell-surface markers and myogenic capacity. *Integr. Biol.* (Camb). 5, 692–702 (2013).

73. Scime A, Caron AZ & Grenier G (2009) Advances in myogenic cell transplantation and skeletal muscle tissue engineering. *Front Biosci* 14, 3012-3023.

74. Brady MA, Lewis MP & Mudera V (2008) Synergy between myogenic and non-myogenic cells in a 3D tissue-engineered craniofacial skeletal muscle construct. *Journal of tissue engineering and regenerative medicine* 2, 408-417.

75. Cheema U, Yang SY, Mudera V, Goldspink GG & Brown RA (2003) 3-D in vitro model of early skeletal muscle development. *Cell motility and the cytoskeleton* 54, 226-236.

76. Kosnik PE DR, Vandenburgh HH (2003) Tissue engineering skeletal muscle. In *In Functional Tissue Engineering* (Guilak F BD, Goldstein SA et al., ed^eds), pp. 377-392. Springer, New York.

77.   Boonen KJ, Rosaria-Chak KY, Baaijens FP, van der Schaft DW & Post MJ (2009) Essential environmental cues from the satellite cell niche: optimizing proliferation and differentiation. *American journal of physiology* 296, C1338-1345.

78.   Boonen KJ & Post MJ (2008) The muscle stem cell niche: regulation of satellite cells during regeneration. *Tissue Eng Part B Rev* 14, 419-431.

79.   Cosgrove BD, Sacco A, Gilbert PM & Blau HM (2009) A home away from home: challenges and opportunities in engineering in vitro muscle satellite cell niches. *Differentiation; research in biological diversity* 78, 185-194.

80.   Collinsworth AM, Zhang S, Kraus WE & Truskey GA (2002) Apparent elastic modulus and hysteresis of skeletal muscle cells throughout differentiation. *American journal of physiology* 283, C1219-1227.

81.   Engler AJ, Griffin MA, Sen S, Bonnemann CG, Sweeney HL & Discher DE (2004) Myotubes differentiate optimally on substrates with tissue-like stiffness: pathological implications for soft or stiff microenvironments. *The Journal of cell biology* 166, 877-887.

82.   Stedman HH, Sweeney HL, Shrager JB, Maguire HC, Panettieri RA, Petrof B, Narusawa M, Leferovich JM, Sladky JT & Kelly AM (1991) The mdx mouse diaphragm reproduces the degenerative changes of Duchenne muscular dystrophy. *Nature* 352, 536-539.

83.   Gao Y, Kostrominova TY, Faulkner JA & Wineman AS (2008) Age-related changes in the mechanical properties of the epimysium in skeletal muscles of rats. *Journal of biomechanics* 41, 465-469.

84.   Rosant C, Nagel MD & Perot C (2007) Aging affects passive stiffness and spindle function of the rat soleus muscle. *Experimental gerontology* 42, 301-308.

85.   Geiger B, Spatz JP & Bershadsky AD (2009) Environmental sensing through focal adhesions. *Nature reviews* 10, 21-33.

86.   Lopez JI, Mouw JK & Weaver VM (2008) Biomechanical regulation of cell orientation and fate. *Oncogene* 27, 6981-6993.

87.   Langer R & Vacanti JP (1993) Tissue engineering. *Science (New York, NY* 260, 920-926.

88.   Mooney DJ, Organ G, Vacanti JP & Langer R (1994) Design and fabrication of biodegradable polymer devices to engineer tubular tissues. *Cell transplantation* 3, 203-210.

89.   Partridge TA, Grounds M & Sloper JC (1978) Evidence of fusion between host and donor myoblasts in skeletal muscle grafts. *Nature* 273, 306-308.

90.   Peault B, Rudnicki M, Torrente Y, Cossu G, Tremblay JP, Partridge T, Gussoni E, Kunkel LM & Huard J (2007) Stem and progenitor cells in skeletal muscle development, maintenance, and therapy. *Mol Ther* 15, 867-877.

91.   O'Connor MS, Carlson ME & Conboy IM (2009) Differentiation rather than aging of muscle stem cells abolishes their telomerase activity. *Biotechnology progress* 25, 1130-1137.

92.   Skuk D, Goulet M, Roy B & Tremblay JP (2002) Efficacy of myoblast transplantation in nonhuman primates following simple intramuscular cell injections: toward defining strategies applicable to humans. *Experimental neurology* 175, 112-126.

93.   Koning M, Harmsen MC, van Luyn MJ & Werker PM (2009) Current opportunities and challenges in skeletal muscle tissue engineering. *Journal of tissue engineering and regenerative medicine* 3, 407-415.

94.   Chakkalakal JV, Thompson J, Parks RJ & Jasmin BJ (2005) Molecular, cellular, and pharmacological therapies for Duchenne/Becker muscular dystrophies. *Faseb J* 19, 880-891.

95.   Negroni E, Butler-Browne GS & Mouly V (2006) Myogenic stem cells: regeneration and cell therapy in human skeletal muscle. *Pathologie-biologie* 54, 100-108.

96.   Partridge T (2002) Myoblast transplantation. *Neuromuscul Disord* 12 Suppl 1, S3-6.

97.   Mouly V, Aamiri A, Perie S, Mamchaoui K, Barani A, Bigot A, Bouazza B, Francois V, Furling D, Jacquemin V, Negroni E, Riederer I, Vignaud A, St Guily JL & Butler-Browne GS (2005) Myoblast transfer therapy: is there any light at the end of the tunnel? *Acta Myol* 24, 128-133.

98.   Das M, Rumsey JW, Bhargava N, Stancescu M & Hickman JJ (2009) Skeletal muscle tissue engineering: a maturation model promoting long-term survival of myotubes, structural development of the excitation-contraction coupling apparatus and neonatal myosin heavy chain expression. *Biomaterials* 30, 5392-5402.

99.   Saxena AK, Marler J, Benvenuto M, Willital GH & Vacanti JP (1999) Skeletal muscle tissue engineering using isolated myoblasts on synthetic biodegradable polymers: preliminary studies. *Tissue engineering* 5, 525-532.

100. Gilmore KJ, Kita M, Han Y, Gelmi A, Higgins MJ, Moulton SE, Clark GM, Kapsa R & Wallace GG (2009) Skeletal muscle cell proliferation and differentiation on polypyrrole substrates doped with extracellular matrix components. *Biomaterials* 30, 5292-5304.

101. Kroehne V, Heschel I, Schugner F, Lasrich D, Bartsch JW & Jockusch H (2008) Use of a novel collagen matrix with oriented pore structure for muscle cell differentiation in cell culture and in grafts. *Journal of cellular and molecular medicine* 12, 1640-1648.

102. Bardouille C, Lehmann J, Heimann P & Jockusch H (2001) Growth and differentiation of permanent and secondary mouse myogenic cell lines on microcarriers. *Applied microbiology and biotechnology* 55, 556-562.

103. Rowley JA, Madlambayan G & Mooney DJ (1999) Alginate hydrogels as synthetic extracellular matrix materials. *Biomaterials* 20, 45-53.

104. Huang YC, Dennis RG, Larkin L & Baar K (2005) Rapid formation of functional muscle in vitro using fibrin gels. *J Appl Physiol* 98, 706-713.

105. Cronin EM, Thurmond FA, Bassel-Duby R, Williams RS, Wright WE, Nelson KD & Garner HR (2004) Protein-coated poly(L-lactic acid) fibers provide a substrate for differentiation of human skeletal muscle cells. *Journal of biomedical materials research* 69, 373-381.

106. Levenberg S, Rouwkema J, Macdonald M, Garfein ES, Kohane DS, Darland DC, Marini R, van Blitterswijk CA, Mulligan RC, D'Amore PA & Langer R (2005) Engineering vascularized skeletal muscle tissue. *Nature biotechnology* 23, 879-884.

107. Neumann T, Hauschka SD & Sanders JE (2003) Tissue engineering of skeletal muscle using polymer fiber arrays. *Tissue engineering* 9, 995-1003.

108. Shen JY, Chan-Park MB, Feng ZQ, Chan V & Feng ZW (2006) UV-embossed microchannel in biocompatible polymeric film: application to control of cell shape and orientation of muscle cells. *J Biomed Mater Res B Appl Biomater* 77, 423-430.

109. Riboldi SA, Sampaolesi M, Neuenschwander P, Cossu G & Mantero S (2005) Electrospun degradable polyesterurethane membranes: potential scaffolds for skeletal muscle tissue engineering. *Biomaterials* 26, 4606-4615.

110. Vandenburgh HH, Karlisch P & Farr L (1988) Maintenance of highly contractile tissue-cultured avian skeletal myotubes in collagen gel. *In Vitro Cell Dev Biol* 24, 166-174.

111. Okano T, Satoh S, Oka T & Matsuda T (1997) Tissue engineering of skeletal muscle. Highly dense, highly oriented hybrid muscular tissues biomimicking native tissues. *Asaio J* 43, M749-753.

112. Saxena AK, Willital GH & Vacanti JP (2001) Vascularized three-dimensional skeletal muscle tissue-engineering. *Bio-medical materials and engineering* 11, 275-281.

113. Levy-Mishali M, Zoldan J & Levenberg S (2009) Effect of scaffold stiffness on myoblast differentiation. *Tissue Eng Part A* 15, 935-944.

114. Boldrin L, Malerba A, Vitiello L, Cimetta E, Piccoli M, Messina C, Gamba PG, Elvassore N & De Coppi P (2008) Efficient delivery of human single fiber-derived muscle precursor cells via biocompatible scaffold. *Cell transplantation* 17, 577-584.

115. Lam MT, Sim S, Zhu X & Takayama S (2006) The effect of continuous wavy micropatterns on silicone substrates on the alignment of skeletal muscle myoblasts and myotubes. *Biomaterials* 27, 4340-4347.

116. Lutolf MP & Hubbell JA (2005) Synthetic biomaterials as instructive extracellular microenvironments for morphogenesis in tissue engineering. *Nature biotechnology* 23, 47-55.

117. Dubois G, Segers VF, Bellamy V, Sabbah L, Peyrard S, Bruneval P, Hagege AA, Lee RT & Menasche P (2008) Self-assembling peptide nanofibers and skeletal myoblast transplantation in infarcted myocardium. *Journal of biomedical materials research* 87, 222-228.

118. Mulder MM, Hitchcock RW & Tresco PA (1998) Skeletal myogenesis on elastomeric substrates: implications for tissue engineering. *Journal of biomaterials science* 9, 731-748.

119. Ren K, Crouzier T, Roy C & Picart C (2008) Polyelectrolyte multilayer films of controlled stiffness modulate myoblast cells differentiation. *Advanced functional materials* 18, 1378-1389.

120. Wang W, Fan M, Zhang L, Liu SH, Sun L & Wang CY (2009) Compatibility of hyaluronic acid hydrogel and skeletal muscle myoblasts. *Biomedical materials (Bristol, England)* 4, 25011.

121. Loken S, Jakobsen RB, Aroen A, Heir S, Shahdadfar A, Brinchmann JE, Engebretsen L & Reinholt FP (2008) Bone marrow mesenchymal stem cells in a hyaluronan scaffold for treatment of an osteochondral defect in a rabbit model. *Knee Surg Sports Traumatol Arthrosc* 16, 896-903.

122. David-Raoudi M, Tranchepain F, Deschrevel B, Vincent JC, Bogdanowicz P, Boumediene K & Pujol JP (2008) Differential effects of hyaluronan and its fragments on fibroblasts: relation to wound healing. *Wound Repair Regen* 16, 274-287.

123. Cui FZ, Tian WM, Hou SP, Xu QY & Lee IS (2006) Hyaluronic acid hydrogel immobilized with RGD peptides for brain tissue engineering. *Journal of materials science* 17, 1393-1401.

124. Han F, Ishiguro N, Ito T, Sakai T & Iwata H (1999) Effects of sodium hyaluronate on experimental osteoarthritis in rabbit knee joints. *Nagoya journal of medical science* 62, 115-126.

125. Gupta P, Vermani K & Garg S (2002) Hydrogels: from controlled release to pH-responsive drug delivery. *Drug discovery today* 7, 569-579.

126. Beier JP, Kneser U, Stern-Strater J, Stark GB & Bach AD (2004) Y chromosome detection of three-dimensional tissue-engineered skeletal muscle constructs in a syngeneic rat animal model. *Cell transplantation* 13, 45-53.

127. de Juan-Pardo EM, Hoang MB & Conboy IM (2006) Geometric control of myogenic cell fate. *International journal of nanomedicine* 1, 203-212.

128. Lam MT, Huang YC, Birla RK & Takayama S (2009) Microfeature guided skeletal muscle tissue engineering for highly organized 3-dimensional free-standing constructs. *Biomaterials* 30, 1150-1155.

129. Riboldi SA, Sadr N, Pigini L, Neuenschwander P, Simonet M, Mognol P, Sampaolesi M, Cossu G & Mantero S (2008) Skeletal myogenesis on highly orientated microfibrous polyesterurethane scaffolds. *Journal of biomedical materials research* 84, 1094-1101.

130. Rockwood DN, Woodhouse KA, Fromstein JD, Chase DB & Rabolt JF (2007) Characterization of biodegradable polyurethane microfibers for tissue engineering. *Journal of biomaterials science* 18, 743-758.

131. Evans DJ, Britland S & Wigmore PM (1999) Differential response of fetal and neonatal myoblasts to topographical guidance cues in vitro. *Development genes and evolution* 209, 438-442.

132. Clark P, Dunn GA, Knibbs A & Peckham M (2002) Alignment of myoblasts on ultrafine gratings inhibits fusion in vitro. *The international journal of biochemistry & cell biology* 34, 816-825.

133. Bian W & Bursac N (2009) Engineered skeletal muscle tissue networks with controllable architecture. *Biomaterials* 30, 1401-1412.

134. Davis BH, Schroeder T, Yarmolenko PS, Guilak F, Dewhirst MW & Taylor DA (2007) An in vitro system to evaluate the effects of ischemia on survival of cells used for cell therapy. *Annals of biomedical engineering* 35, 1414-1424.

135. Simpson DG, Terracio L, Terracio M, Price RL, Turner DC & Borg TK (1994) Modulation of cardiac myocyte phenotype in vitro by the composition and orientation of the extracellular matrix. *Journal of cellular physiology* 161, 89-105.

136. Engler AJ, Sen S, Sweeney HL & Discher DE (2006) Matrix elasticity directs stem cell lineage specification. *Cell* 126, 677-689.

137. Boontheekul T, Hill EE, Kong HJ & Mooney DJ (2007) Regulating myoblast phenotype through controlled gel stiffness and degradation. *Tissue engineering* 13, 1431-1442.

138. Gilbert PM, Havenstrite KL, Magnusson KEG, Sacco A, Leonardi NA, Kraft P, Nguyen NK, Thrun S, Lutolf MP, Blau HM (2010) Substrate elasticity regulates skeletal muscle stem cell self-renewal in culture. *Science* (*New York, NY*, 329, 1078-1081.

139. Dhoot NO, Tobias CA, Fischer I & Wheatley MA (2004) Peptide-modified alginate surfaces as a growth permissive substrate for neurite outgrowth. *Journal of biomedical materials research* 71, 191-200.

140. Liao IC, Liu JB, Bursac N & Leong KW (2008) Effect of Electromechanical Stimulation on the Maturation of Myotubes on Aligned Electrospun Fibers. *Cellular and molecular bioengineering* 1, 133-145.

141. Yamasaki K, Hayashi H, Nishiyama K, Kobayashi H, Uto S, Kondo H, Hashimoto S & Fujisato T (2009) Control of myotube contraction using electrical pulse stimulation for bio-actuator. *J Artif Organs* 12, 131-137.

142. Ishibashi T, Hoshino Y, Kaji H, Kanzaki M, Sato M & Nishizawa M (2009) Localized electrical stimulation to C2C12 myotubes cultured on a porous membrane-based substrate. *Biomedical microdevices* 11, 413-419.

143. Flaibani M, Boldrin L, Cimetta E, Piccoli M, De Coppi P & Elvassore N (2009) Muscle differentiation and myotubes alignment is influenced by micropatterned surfaces and exogenous electrical stimulation. *Tissue Eng Part A* 15, 2447-2457.

144. Dennis RG & Kosnik PE, 2nd (2000) Excitability and isometric contractile properties of mammalian skeletal muscle constructs engineered in vitro. *In vitro cellular & developmental biology* 36, 327-335.

145. Vandenburgh HH, Swasdison S & Karlisch P (1991) Computer-aided mechanogenesis of skeletal muscle organs from single cells in vitro. *Faseb J* 5, 2860-2867.

146. Tatsumi R, Hattori A, Ikeuchi Y, Anderson JE & Allen RE (2002) Release of hepatocyte growth factor from mechanically stretched skeletal muscle satellite cells and role of pH and nitric oxide. *Molecular biology of the cell* 13, 2909-2918.

147. Tatsumi R, Liu X, Pulido A, Morales M, Sakata T, Dial S, Hattori A, Ikeuchi Y & Allen RE (2006) Satellite cell activation in stretched skeletal muscle and the role of nitric oxide and hepatocyte growth factor. *Am J Physiol Cell Physiol* 290, C1487-1494.

148. Desai TA (2000) Micro- and nanoscale structures for tissue engineering constructs. *Medical engineering & physics* 22, 595-606.

149. Choi JS, Lee SJ, Christ GJ, Atala A & Yoo JJ (2008) The influence of electrospun aligned poly(epsilon-caprolactone)/collagen nanofiber meshes on the formation of self-aligned skeletal muscle myotubes. *Biomaterials* 29, 2899-2906.

150. Jun I, Jeong S & Shin H (2009) The stimulation of myoblast differentiation by electrically conductive sub-micron fibers. *Biomaterials* 30, 2038-2047.

151. Jeong SI, Jun ID, Choi MJ, Nho YC, Lee YM & Shin H (2008) Development of electroactive and elastic nanofibers that contain polyaniline and poly(L-lactide-co-epsilon-caprolactone) for the control of cell adhesion. *Macromolecular bioscience* 8, 627-637.

152. Tanaka Y, Tsutsumi A, Crowe DM, Tajima S & Morrison WA (2000) Generation of an autologous tissue (matrix) flap by combining an arteriovenous shunt loop with artificial skin in rats: preliminary report. *British journal of plastic surgery* 53, 51-57.

153. Mian R, Morrison WA, Hurley JV, Penington AJ, Romeo R, Tanaka Y & Knight KR (2000) Formation of new tissue from an arteriovenous loop in the absence of added extracellular matrix. *Tissue Eng* 6, 595-603.

154. Beier JP, Stern-Straeter J, Foerster VT, Kneser U, Stark GB & Bach AD (2006) Tissue engineering of injectable muscle: three-dimensional myoblast-fibrin injection in the syngeneic rat animal model. *Plastic and reconstructive surgery* 118, 1113-1121; discussion 1122-1114.

155. Bach AD, Stem-Straeter J, Beier JP, Bannasch H & Stark GB (2003) Engineering of muscle tissue. *Clinics in plastic surgery* 30, 589-599.

156. Lodish B, Zipursky, Matsudaira, Baltimore, Darnell (2000) *Molecular Cell Biology, Fourth Edition*, New York.

157. Giraud MN, Ayuni E, Cook S, Siepe M, Carrel TP & Tevaearai HT (2008) Hydrogel-based engineered skeletal muscle grafts normalize heart function early after myocardial infarction. *Artificial organs* 32, 692-700.

158. Cimetta E, Pizzato S, Bollini S, Serena E, De Coppi P & Elvassore N (2009) Production of arrays of cardiac and skeletal muscle myofibers by micropatterning techniques on a soft substrate. *Biomedical microdevices* 11, 389-400.

159. Stern MM, Myers RL, Hammam N, Stern KA, Eberli D, Kritchevsky SB, Soker S & Van Dyke M (2009) The influence of extracellular matrix derived from skeletal muscle tissue on the proliferation and differentiation of myogenic progenitor cells ex vivo. *Biomaterials* 30, 2393-2399.

160. Pola R, Ling LE, Aprahamian TR, Barban E, Bosch-Marce M, Curry C, Corbley M, Kearney M, Isner JM & Losordo DW (2003) Postnatal recapitulation of embryonic hedgehog pathway in response to skeletal muscle ischemia. *Circulation* 108, 479-485.

161. Tidball JG (2005) Inflammatory processes in muscle injury and repair. *Am J Physiol Regul Integr Comp Physiol* 288, R345-353.

162. Wagers AJ & Conboy IM (2005) Cellular and molecular signatures of muscle regeneration: current concepts and controversies in adult myogenesis. *Cell* 122, 659-667.

163. Tavana H, Jovic A, Mosadegh B, Lee QY, Liu X, Luker KE, Luker GD, Weiss SJ & Takayama S (2009) Nanolitre liquid patterning in aqueous environments for spatially defined reagent delivery to mammalian cells. *Nature materials* 8, 736-741.

164. Ratner H, Schoen, Lemons (2004) *Biomaterials Science, Second Edition An Introduction to Materials in Medicine*.

165. Bushby A (2001) *Muscular Dystrophy, Methods and Protocols* Humana Press, New York.

166. Pannier AK & Shea LD (2004) Controlled release systems for DNA delivery. *Mol Ther* 10, 19-26.

167. Lodish B, Zipursky, Matsudaira, Baltimore, Darnell (2000) *Molecular Cell Biology, Fourth Edition*, New York.

168. Masotti A & Ortaggi G (2009) Chitosan micro- and nanospheres: fabrication and applications for drug and DNA delivery. *Mini reviews in medicinal chemistry* 9, 463-469.

169. Ziauddin J & Sabatini DM (2001) Microarrays of cells expressing defined cDNAs. *Nature* 411, 107-110.

170. Jewell CM, Zhang J, Fredin NJ & Lynn DM (2005) Multilayered polyelectrolyte films promote the direct and localized delivery of DNA to cells. *J Control Release* 106, 214-223.

171. Segura T, Chung PH & Shea LD (2005) DNA delivery from hyaluronic acid-collagen hydrogels via a substrate-mediated approach. *Biomaterials* 26, 1575-1584.

172. Segura T & Shea LD (2002) Surface-tethered DNA complexes for enhanced gene delivery. *Bioconjugate chemistry* 13, 621-629.

173. Jeong B, Bae YH, Lee DS & Kim SW (1997) Biodegradable block copolymers as injectable drug-delivery systems. *Nature* 388, 860-862.

174. Booth C, Attwood D & Price C (2006) Self-association of block copoly(oxyalkylene)s in aqueous solution. Effects of composition, block length and block architecture. *Phys Chem Chem Phys* 8, 3612-3622.

175. Bhardwaj R & Blanchard J (1996) Controlled-release delivery system for the alpha-MSH analog melanotan-I using poloxamer 407. *Journal of pharmaceutical sciences* 85, 915-919.

176. Wenzel JG, Balaji KS, Koushik K, Navarre C, Duran SH, Rahe CH & Kompella UB (2002) Pluronic F127 gel formulations of deslorelin and GnRH reduce drug degradation and sustain drug release and effect in cattle. *J Control Release* 85, 51-59.

177. Hinrichs WL, Schuurmans-Nieuwenbroek NM, van de Wetering P & Hennink WE (1999) Thermosensitive polymers as carriers for DNA delivery. *J Control Release* 60, 249-259.

178. Li Z, Ning W, Wang J, Choi A, Lee PY, Tyagi P & Huang L (2003) Controlled gene delivery system based on thermosensitive biodegradable hydrogel. *Pharmaceutical research* 20, 884-888.

179. Zentner GM, Rathi R, Shih C, McRea JC, Seo MH, Oh H, Rhee BG, Mestecky J, Moldoveanu Z, Morgan M & Weitman S (2001) Biodegradable block copolymers for delivery of proteins and water-insoluble drugs. *J Control Release* 72, 203-215.

180. Namgung R, Nam S, Kim SK, Son S, Singha K, Kwon JS, Ahn Y, Jeong MH, Park IK, Garripelli VK, Jo S & Kim WJ (2009) An acid-labile temperature-responsive sol-gel reversible polymer for enhanced gene delivery to the myocardium and skeletal muscle cells. *Biomaterials* 30, 5225-5233.

181. Garripelli VK, Kim JK, Namgung R, Kim WJ, Repka MA & Jo S (2009) A novel thermosensitive polymer with pH-dependent degradation for drug delivery. *Acta biomaterialia*.

182. Chang CW, Choi D, Kim WJ, Yockman JW, Christensen LV, Kim YH & Kim SW (2007) Non-ionic amphiphilic biodegradable PEG-PLGA-PEG copolymer enhances gene delivery efficiency in rat skeletal muscle. *J Control Release* 118, 245-253.

183. Anderson DG, Peng W, Akinc A, Hossain N, Kohn A, Padera R, Langer R & Sawicki JA (2004) A polymer library approach to suicide gene therapy for cancer. *Proceedings of the National Academy of Sciences of the United States of America* 101, 16028-16033.

184. Dobrovolskaia MA, Aggarwal P, Hall JB & McNeil SE (2008) Preclinical studies to understand nanoparticle interaction with the immune system and its potential effects on nanoparticle biodistribution. *Molecular pharmaceutics* 5, 487-495.

185. Matt P, Schoenhoff F, Habashi J, Holm T, Van Erp C, Loch D, Carlson OD, Griswold BF, Fu Q, De Backer J, Loeys B, Huso DL, McDonnell NB, Van Eyk JE & Dietz HC (2009) Circulating transforming growth factor-beta in Marfan syndrome. *Circulation* 120, 526-532.

186. Morgan JE & Partridge TA (2003) Muscle satellite cells. *The international journal of biochemistry & cell biology* 35, 1151-1156.

187. Camargo FD, Green R, Capetanaki Y, Jackson KA & Goodell MA (2003) Single hematopoietic stem cells generate skeletal muscle through myeloid intermediates. *Nature medicine* 9, 1520-1527.

188. Corbel SY, Lee A, Yi L, Duenas J, Brazelton TR, Blau HM & Rossi FM (2003) Contribution of hematopoietic stem cells to skeletal muscle. *Nature medicine* 9, 1528-1532.

189. Doyonnas R, LaBarge MA, Sacco A, Charlton C & Blau HM (2004) Hematopoietic contribution to skeletal muscle regeneration by myelomonocytic precursors. *Proceedings of the National Academy of Sciences of the United States of America* 101, 13507-13512.

190. Sacco A, Doyonnas R, LaBarge MA, Hammer MM, Kraft P & Blau HM (2005) IGF-I increases bone marrow contribution to adult skeletal muscle and enhances the fusion of myelomonocytic precursors. *The Journal of cell biology* 171, 483-492.

191. Sampaolesi M, Blot S, D'Antona G, Granger N, Tonlorenzi R, Innocenzi A, Mognol P, Thibaud JL, Galvez BG, Barthelemy I, Perani L, Mantero S, Guttinger M, Pansarasa O, Rinaldi C, Cusella De Angelis MG, Torrente Y, Bordignon C, Bottinelli R & Cossu G (2006) Mesoangioblast stem cells ameliorate muscle function in dystrophic dogs. *Nature* 444, 574-579.

192. Dellavalle A, Sampaolesi M, Tonlorenzi R, Tagliafico E, Sacchetti B, Perani L, Innocenzi A, Galvez BG, Messina G, Morosetti R, Li S, Belicchi M, Peretti G,

Chamberlain JS, Wright WE, Torrente Y, Ferrari S, Bianco P & Cossu G (2007) Pericytes of human skeletal muscle are myogenic precursors distinct from satellite cells. *Nature cell biology* 9, 255-267.

193. Beauchamp JR, Heslop L, Yu DS, Tajbakhsh S, Kelly RG, Wernig A, Buckingham ME, Partridge TA & Zammit PS (2000) Expression of CD34 and Myf5 defines the majority of quiescent adult skeletal muscle satellite cells. *The Journal of cell biology* 151, 1221-1234.

194. Halevy O, Piestun Y, Allouh MZ, Rosser BW, Rinkevich Y, Reshef R, Rozenboim I, Wleklinski-Lee M & Yablonka-Reuveni Z (2004) Pattern of Pax7 expression during myogenesis in the posthatch chicken establishes a model for satellite cell differentiation and renewal. *Dev Dyn* 231, 489-502.

195. Schultz E (1996) Satellite cell proliferative compartments in growing skeletal muscles. *Developmental biology* 175, 84-94.

196. Zammit PS, Golding JP, Nagata Y, Hudon V, Partridge TA & Beauchamp JR (2004) Muscle satellite cells adopt divergent fates: a mechanism for self-renewal? *The Journal of cell biology* 166, 347-357.

197. Seale P, Sabourin LA, Girgis-Gabardo A, Mansouri A, Gruss P & Rudnicki MA (2000) Pax7 is required for the specification of myogenic satellite cells. *Cell* 102, 777-786.

198. Cerletti M, Jurga S, Witczak CA, Hirshman MF, Shadrach JL, Goodyear LJ & Wagers AJ (2008) Highly efficient, functional engraftment of skeletal muscle stem cells in dystrophic muscles. *Cell* 134, 37-47.

199. Cornelison DD, Filla MS, Stanley HM, Rapraeger AC & Olwin BB (2001) Syndecan-3 and syndecan-4 specifically mark skeletal muscle satellite cells and are implicated in satellite cell maintenance and muscle regeneration. *Developmental biology* 239, 79-94.

200. Cornelison DD, Olwin BB, Rudnicki MA & Wold BJ (2000) MyoD(-/-) satellite cells in single-fiber culture are differentiation defective and MRF4 deficient. *Developmental biology* 224, 122-137.

201. Brack AS, Bildsoe H & Hughes SM (2005) Evidence that satellite cell decrement contributes to preferential decline in nuclear number from large fibres during murine age-related muscle atrophy. *Journal of cell science* 118, 4813-4821.

202. Cornelison DD, Wilcox-Adelman SA, Goetinck PF, Rauvala H, Rapraeger AC & Olwin BB (2004) Essential and separable roles for Syndecan-3 and Syndecan-4 in skeletal muscle development and regeneration. *Genes & development* 18, 2231-2236.

203. Cornelison DD & Wold BJ (1997) Single-cell analysis of regulatory gene expression in quiescent and activated mouse skeletal muscle satellite cells. *Developmental biology* 191, 270-283.

204. Volonte D, Liu Y & Galbiati F (2005) The modulation of caveolin-1 expression controls satellite cell activation during muscle repair. *Faseb J* 19, 237-239.

205. Irintchev A, Zeschnigk M, Starzinski-Powitz A & Wernig A (1994) Expression pattern of M-cadherin in normal, denervated, and regenerating mouse muscles. *Dev Dyn* 199, 326-337.

206. Sherwood RI, Christensen JL, Conboy IM, Conboy MJ, Rando TA, Weissman IL & Wagers AJ (2004) Isolation of adult mouse myogenic progenitors: functional heterogeneity of cells within and engrafting skeletal muscle. *Cell* 119, 543-554.

207. Jesse TL, LaChance R, Iademarco MF & Dean DC (1998) Interferon regulatory factor-2 is a transcriptional activator in muscle where It regulates expression of vascular cell adhesion molecule-1. *The Journal of cell biology* 140, 1265-1276.

208. Illa I, Leon-Monzon M & Dalakas MC (1992) Regenerating and denervated human muscle fibers and satellite cells express neural cell adhesion molecule recognized by monoclonal antibodies to natural killer cells. *Annals of neurology* 31, 46-52.

209. Schubert W, Zimmermann K, Cramer M & Starzinski-Powitz A (1989) Lymphocyte antigen Leu-19 as a molecular marker of regeneration in human skeletal muscle. *Proceedings of the National Academy of Sciences of the United States of America* 86, 307-311.

210. Tanaka KK, Hall JK, Troy AA, Cornelison DD, Majka SM & Olwin BB (2009) Syndecan-4-expressing muscle progenitor cells in the SP engraft as satellite cells during muscle regeneration. *Cell stem cell* 4, 217-225.

211. Fukada S, Higuchi S, Segawa M, Koda K, Yamamoto Y, Tsujikawa K, Kohama Y, Uezumi A, Imamura M, Miyagoe-Suzuki Y, Takeda S & Yamamoto H (2004) Purification and cell-surface marker characterization of quiescent satellite cells from murine skeletal muscle by a novel monoclonal antibody. *Experimental cell research* 296, 245-255.

212. Garry DJ, Yang Q, Bassel-Duby R & Williams RS (1997) Persistent expression of MNF identifies myogenic stem cells in postnatal muscles. *Developmental biology* 188, 280-294.

213. Kirk S, Oldham J, Kambadur R, Sharma M, Dobbie P & Bass J (2000) Myostatin regulation during skeletal muscle regeneration. *Journal of cellular physiology* 184, 356-363.

214. Mendler L, Zador E, Ver Heyen M, Dux L & Wuytack F (2000) Myostatin levels in regenerating rat muscles and in myogenic cell cultures. *Journal of muscle research and cell motility* 21, 551-563.

215. Saleh OA & Sohn LL (2003) Direct detection of antibody-antigen binding using an on-chip artificial pore. *Proceedings of the National Academy of Sciences of the United States of America* 100, 820-824.

216. He M & Herr AE (2009) Microfluidic polyacrylamide gel electrophoresis with in situ immunoblotting for native protein analysis. *Analytical chemistry* 81, 8177-8184.

217. Carbonaro A, Sohn LL (2005) A resistive-pulse sensor chip for multianalyte immunoassys. *Lab on a Chip* 5, 1155-1160.

218. Carbonaro A, Mohanty SK, Huang H, Godley LA, Sohn LL (2008) Cell characterization using a protein-functionalized pore. *Lab Chip* 9, 1478-85.

219. Balarishnan KR, Anwar G, Chapman MR, Nguyen T, Kesavaraju A, Sohn LL (2013) Node-pore sensing: a robust, high dynamic-range method for detecting biological species. *Lab Chip* 7, 1302-7.

Chapter 4 - Attenuation of TGF-β Signaling via Incorporation of a Dominant-negative TGF-β Type II Receptor Improves Differentiation of Murine Skeletal Myoblasts

1.   Choy, L., Skillington, J. & Derynck, R. Roles of Autocrine TGF-β Receptor and Smad Signaling in Adipocyte Differentiation. *J. Cell Biol.* **149,** 667–682 (2000).

2.   Carlson, M. E. *et al.* Molecular aging and rejuvenation of human muscle stem cells. *EMBO Mol. Med.* **1,** 381–91 (2009).

3.   Carlson, M. E., Hsu, M. & Conboy, I. M. Imbalance between pSmad3 and Notch induces CDK inhibitors in old muscle stem cells. *Nature* **454,** 528–32 (2008).

4.   Carlson, M. E. *et al.* Relative roles of TGF-beta1 and Wnt in the systemic regulation and aging of satellite cell responses. *Aging Cell* **8,** 676–89 (2009).

5.   Carlson, M. E., Silva, H. S. & Conboy, I. M. Aging of signal transduction pathways, and pathology. *Exp. Cell Res.* **314,** 1951–61 (2008).

6.   Conboy, I. M., Conboy, M. J., Smythe, G. M. & Rando, T. a. Notch-mediated restoration of regenerative potential to aged muscle. *Science* **302,** 1575–7 (2003).

7.   Wagers, A. J. & Conboy, I. M. Cellular and molecular signatures of muscle regeneration: current concepts and controversies in adult myogenesis. *Cell* **122,** 659–67 (2005).

8.   Collins, C. A. & Partridge, T. A. Self-Renewal of the Adult Skeletal Muscle Satellite Cell Extra View ND ES ACKNOWLEDGEMENTS SC RIB. **4,** 1338–1341 (2005).

9.   Morgan, J. E. *et al.* Myogenic cell proliferation and generation of a reversible tumorigenic phenotype are triggered by preirradiation of the recipient site. *J. Cell Biol.* **157,** 693–702 (2002).

10.   Schultz, E. & Lipton, B. H. Skeletal muscle satellite cells: changes in proliferation potential as a function of age. **20,** 377–383 (1982).

11.   Hasson, P. & Paroush, Z. Crosstalk between the EGFR and other signalling pathways at the level of the global transcriptional corepressor Groucho/TLE. *Br. J. Cancer* **94,** 771–5 (2006).

12.   Zhang, Y. & Derynck, R. Regulation of Smad signalling by protein associations and signalling crosstalk. *Trends Cell Biol.* **9,** 274–9 (1999).

Appendix – Site-Directed Conjugation of Antibody Fragments to Poly(lactic-co-glycolic) Acid Microparticles

1.   Kamaly, N., Xiao, Z., Valencia, P. M., Radovic-Moreno, A. F. & Farokhzad, O. C. Targeted polymeric therapeutic nanoparticles: design, development and clinical translation. *Chem. Soc. Rev.* **41,** 2971–3010 (2012).

2.   Brigger, I., Dubernet, C. & Couvreur, P. Nanoparticles in cancer therapy and diagnosis. *Adv. Drug Deliv. Rev.* **54,** 631–51 (2002).

3.   Sapra, P. & Shor, B. Monoclonal antibody-based therapies in cancer: advances and challenges. *Pharmacol. Ther.* **138,** 452–69 (2013).

4.   Parolo, C. *et al.* Design, Preparation, and Evaluation of a Fixed-Orientation Antibody/Gold-Nanoparticle Conjugate as an Immunosensing Label. *ACS Appl. Mater. Interfaces* (2013). doi:10.1021/am4029153

5.   Benita, S. *Microencapsulation: Methods and Industrial Applications*. (Taylor and Francis, 2005).

6.   Kumar, S., Aaron, J. & Sokolov, K. Directional conjugation of antibodies to nanoparticles for synthesis of multiplexed optical contrast agents with both delivery and targeting moieties. *Nat. Protoc.* **3,** 314–20 (2008).

7.   Jain, S., O'Hagan, D. T. & Singh, M. The long-term potential of biodegradable poly(lactideco-glycolide) microparticles as the next-generation vaccine adjuvant. *Expert Rev. Vaccines* **10,** 1731–1742 (2011).

8.   Semete, B. *et al.* In vivo evaluation of the biodistribution and safety of PLGA nanoparticles as drug delivery systems. *Nanomedicine* **6,** 662–71 (2010).

9.   Gref, R. *et al.* Long-Circulating Biodegradable Nanospheres Polymeric Yoshiharu. **263,** 1600–1603 (2010).

10.   Mundargi, R. C., Babu, V. R., Rangaswamy, V., Patel, P. & Aminabhavi, T. M. Nano/micro technologies for delivering macromolecular therapeutics using poly(D,L-lactide-co-glycolide) and its derivatives. *J. Control. Release* **125,** 193–209 (2008).

11.   Astete, C. E. & Sabliov, C. M. Synthesis and characterization of PLGA nanoparticles. *J. Biomater. Sci. Polym. Ed.* **17,** 247–89 (2006).

12.   Mohamed, F. & Christopher, F. Engineering Biodegradable Polyester Particles With Specific Drug Targeting and Drug Release Properties. **97,** 71–87 (2008).

13.   McAteer, M. a & Choudhury, R. P. *Chapter 4 - Applications of nanotechnology in molecular imaging of the brain. Prog. Brain Res.* **180,** 72–96 (Elsevier, 2009).

14.   Wang, S. *et al.* Highly efficient capture of circulating tumor cells by using nanostructured silicon substrates with integrated chaotic micromixers. *Angew. Chemie Int. Ed.* **50,** 3084–3088 (2011).

15.   Arruebo, M., Valladares, M. & González-Fernández, Á. Antibody-Conjugated Nanoparticles for Biomedical Applications. *J. Nanomater.* **2009,** 1–24 (2009).

16.   Pourcelle, V., Devouge, S., Garinot, M., Préat, V. & Marchand-Brynaert, J. PCL-PEG-based nanoparticles grafted with GRGDS peptide: preparation and surface analysis by XPS. *Biomacromolecules* **8,** 3977–83 (2007).

17.   Beaudette, T. T. *et al.* NIH Public Access. **131,** 10360–10361 (2010).

18.   Paramonov, S. E. *et al.* Fully acid-degradable biocompatible polyacetal microparticles for drug delivery. *Bioconjug. Chem.* **19,** 911–9 (2008).

19.   Schlick, T. L., Ding, Z., Kovacs, E. W. & Francis, M. B. Dual-surface modification of the tobacco mosaic virus. *J. Am. Chem. Soc.* **127,** 3718–23 (2005).

20.   Gaertner, H. F. & Offord, R. E. Site-specific attachment of functionalized poly(ethylene glycol) to the amino terminus of proteins. *Bioconjug. Chem.* **7,** 38–44 (1996).

21.   Scheck, R. a & Francis, M. B. Regioselective labeling of antibodies through N-terminal transamination. *ACS Chem. Biol.* **2,** 247–51 (2007).

22.   Gilmore, J. M., Scheck, R. a, Esser-Kahn, A. P., Joshi, N. S. & Francis, M. B. N-terminal protein modification through a biomimetic transamination reaction. *Angew. Chem. Int. Ed. Engl.* **45,** 5307–11 (2006).

23.   Scheck, R. a, Dedeo, M. T., Iavarone, A. T. & Francis, M. B. Optimization of a biomimetic transamination reaction. *J. Am. Chem. Soc.* **130,** 11762–70 (2008).

24.   Moghimi, S. M., Hunter, a C. & Murray, J. C. Long-circulating and target-specific nanoparticles: theory to practice. *Pharmacol. Rev.* **53,** 283–318 (2001).

25.   Pacheco, P., White, D. & Sulchek, T. Effects of microparticle size and Fc density on macrophage phagocytosis. *PLoS One* **8,** e60989 (2013).

26.   Sheng, Y. *et al.* Long-circulating polymeric nanoparticles bearing a combinatorial coating of PEG and water-soluble chitosan. *Biomaterials* **30,** 2340–8 (2009).

27.   Park, J. *et al.* PEGylated PLGA nanoparticles for the improved delivery of doxorubicin. *Nanomedicine* **5,** 410–8 (2009).

Appendix

<u>Site-Directed Conjugation of Antibody Fragments to Poly(lactic-co-glycolic) Acid Microparticles</u>

This appendix describes work I completed between 2008 and 2010 while working in the Conboy and Sohn Labs and with the help of Dr. Brett Helms, Principal Investigator at the Lawrence Berkeley National Laboratory.

Introduction

Selectively directing polymeric micro- or nanoparticles loaded with bioactive cargo to targets in the body is critical to the biomedical sciences[1,2]. Antibodies (and fragments thereof) typically afford such discrimination in heterogeneous environments like the body due to their high affinity and specificity for cell-surface receptors, etc.[3] It has been difficult, however, to conjugate these to polymers while retaining the orientation and correctly-folded conformation required for optimal binding[4–6]. Here, we present a strategy whereby these important targeting groups are immobilized onto the widely implemented platform, poly(lactic-*co*-glycolic) acid (PLGA) microparticles[7–12]. Antibody fragments produced by papain digest of intact antibodies are modified at their N-terminus with a glyoxyl group using pyridoxal 5'-phosphate. These glyoxyl-modified antibody fragments readily conjugate to PLGA microparticles modified with complementary alkoxyamine moieties at their surface. Chemoselective immobilization dramatically increases the fraction of covalent fragments appended to the polymer. This platform technology provides consistent biomolecule orientation and the possibility to site-specifically conjugate a wide-range of bioactive molecules including proteins and peptides.

Display of bioactive molecules, such as antibodies, on the surface of polymeric microparticles has applications in fields such as drug delivery and imaging[1,13–16]. However, maintaining bioactivity through consistent, proper orientation of such molecules is not altogether trivial. Passive adsorption of bioactive species, while simple, can lead to an improper orientation of active groups, misfolding, etc. and therefore concomitant reduced functionality[17]. On the other hand, many covalent conjugation techniques are non-specific (e.g., via reaction with any number of primary amines or carboxylates on the biomolecule of interest) and may lead to improper orientation or even inactivation of bioactive moieties[15,17]. To address the issue of orientation control for preservation of bioactivity, we have recently applied a site-specific conjugation strategy to couple bioactive molecules to the surface of PLGA microparticles. In this work, we describe the conjugation of IgG1 antibody Fab fragments to PLGA microparticles as a proof of principle.

Materials and Methods

Generation of PLGA-ONH$_2$ polymer chains

PLGA (75:25, MW 20k, Polysciences, Warrington, PA) polymer chains were modified with alkoxyamines through reaction with a Boc-protected aminooxyacetic acid followed by subsequent Boc deprotection using TFA. Briefly, 1 g of PLGA was dissolved in dichloromethane (DCM) with 10 molar equivalents of Boc-aminooxyacetic acid, 10 molar equivalents of dicyclohexylcarbodiimide (DCC), and 1 molar equivalent of pyridinium p-Toluenesulfonate (PPTS) (Figure A1a). The condensation reaction was carried out overnight and the resultant PLGA-Boc polymer chains were purified from the excess small molecules through precipitation in cold methanol and subsequent filtration. PLGA-Boc was then redissolved in DCM and treated with trifluoroacetic acid (TFA) overnight to generate PLGA-ONH$_2$ (Figure A2a). Generation of PLGA-Boc and PLGA-ONH$_2$ were verified by ^{1}H NMR (Figures A1b and A2b).
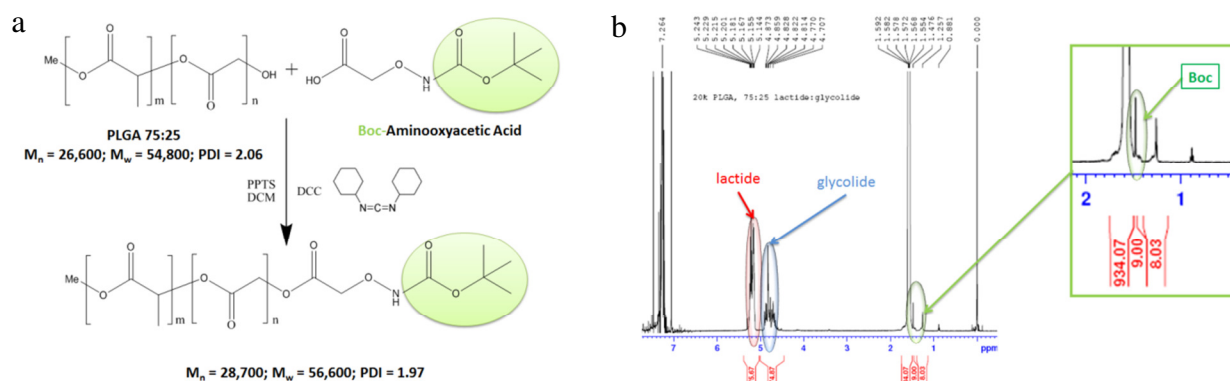

Figure A1. a) Functionalization of PLGA with Boc-protected aminooxyacetic acid. b) Characteristic NMR peaks for lactide (red) and glycolide (blue) components of PGLA as well as addition of Boc protecting group (green).
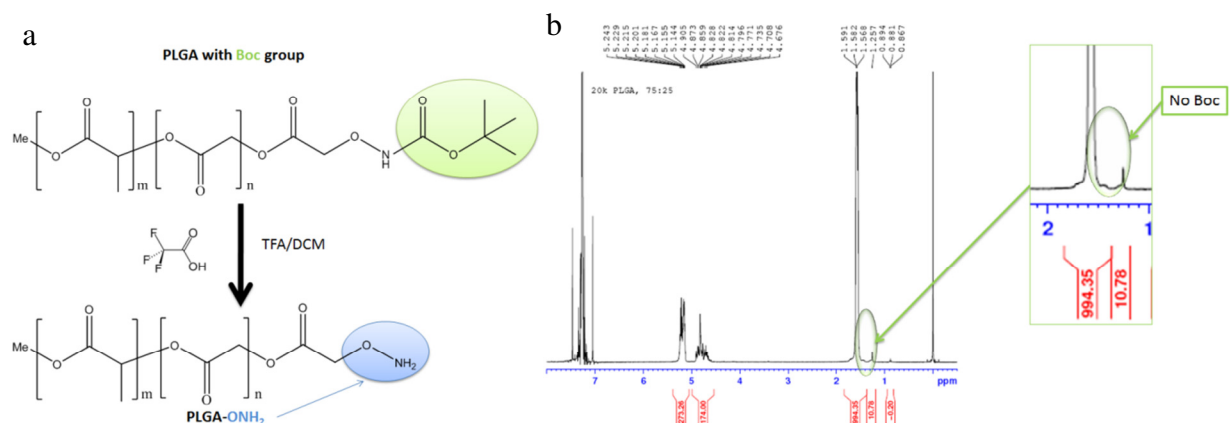

Figure A2. a) De-proctection of Boc group with TFA to generate PLGA-ONH$_2$. b) NMR verification of removal of Boc peak.

Microparticle Synthesis

PLGA and PLGA-ONH$_2$ particles were synthesized using a w/o/w double emulsion process as previously described[18]. Briefly, 100 mg of PLGA-ONH$_2$ polymer was dissolved in 1 mL of DCM. 100 μL of 3 % polyvinyl alcohol (PVA) in water was added and the primary water in oil emulsion was sonicated on ice using a Branson Sonifier 450 (Branson, Danbury, CT) Microtip for 30 seconds at duty cycle 10, output 6. After the addition of 2 mL of 3 % PVA, sonication was repeated and the double emulsion was then added to 10 mL of 0.3 % PVA spinning at 700 rpm for four hours to evaporate off the DCM. Microparticles were then tangentially flow filtered (Spectrum Labs, Rancho Dominguez, CA) with ultrapure water in order to remove any residual dichloromethane or surfactant. Microparticle size was measured using dynamic light scattering on a Malvern Zetasizer NS (Malvern, UK) and then the microparticles were freeze-dried and lyophilized (1-2 days).

Antibody Fragment Preparation through N-terminal Transamination

Whole mouse IgG (Rockland Immunochemical, Gilbertsville, PA) antibody was digested for 6 hours using a Pierce Fab Preparation Kit (Thermo Fisher Scientific, Rockford, IL) containing papain, and the resulting Fab fragments were separated and purified from the Fc fragments using Protein A. A portion of the purified Fab fragments were spin dialyzed to 25 mM pH 6.5 phosphate buffer and the amount of Fab was determined by measuring absorption at 280 nm using a Biorad SmartSpec Plus Spectrophotometer (Biorad, Hercules, CA) blanked with phosphate buffer and using the following equation:

$$[Fab] = \frac{Abs_{280\,nm}}{\varepsilon_{Fab}} * dilution\ factor$$

where the Fab fragment extinction coefficient ε_{Fab} = 1.4 and [Fab] is in mg/mL. The buffer-exchanged Fab fragments were then incubated 18-20 hours with 600 molar equivalents of 20 mM pyridoxal 5'-phosphate (PLP) in 25 mM pH 6.5 phosphate buffer at 50°C to generate an N-terminal glyoxyl. Confirmation of N-terminal transamination was achieved by conjugation of either a 5 kDa PEG-ONH$_2$ (synthesized as previously described[19,20]) or of an alkoxyamine-modified Alexa 488 (Invitrogen, Carlsbad, CA), followed by subsequent gel electrophoresis and image analysis using ImageJ software.

Conjugation of Fab Fragments to Microparticles

PLP-modified Fab fragments were conjugated to PLGA or PLGA-ONH$_2$ microparticles overnight in 25 mM pH 6.5 Phosphate Buffer. Unconjugated fragments were separated from microparticle–fragment conjugates via tangential flow filtration. Antibody fragments, previously

labeled with a non-specific amine-reactive Alexa 488, were used to measure conjugation efficiency using UV-Vis Spectrophotometry or fluorescence.

Results

PLGA-ONH$_2$ Synthesis and Microparticle Formation

Hydroxyl-terminated PLGA polymer chains were end-modified with a Boc-protected aminooxyacetic acid group (PLGA-Boc) via condensation reaction and PLGA-Boc synthesis was confirmed via NMR. Subsequent deprotection of Boc group to generate PLGA-ONH$_2$ was also confirmed via NMR. PLGA and PLGA-ONH$_2$ microparticle size were measured using dynamic light scattering and average hydrodynamic radius was around 500 nm (Figure A3).
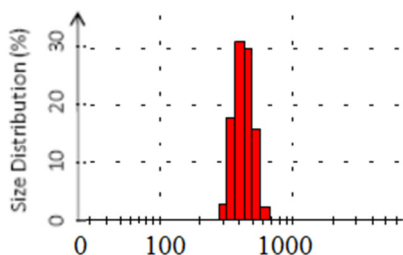

Figure A3. Histogram of PLGA-ONH$_2$ particle sizes based on DLS.

Fab Fragment Transamination

Fab fragment transamination was confirmed by either conjugation of an Alexa 488-ONH$_2$ (Figure A4a) or by conjugation of a 5 kDa PEG-ONH$_2$ (Figure A4b). Densitometry analysis using ImageJ revealed a 38 % conjugation efficiency of transaminated antibody fragments to the PEG alkoxyamine, similar to previously reported values[21].
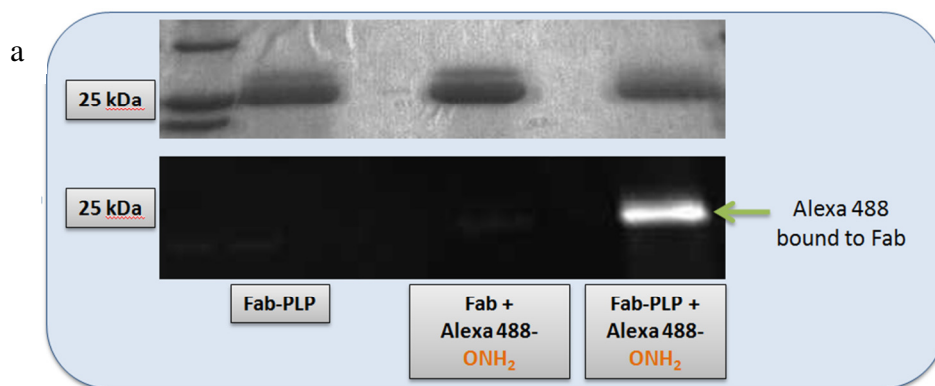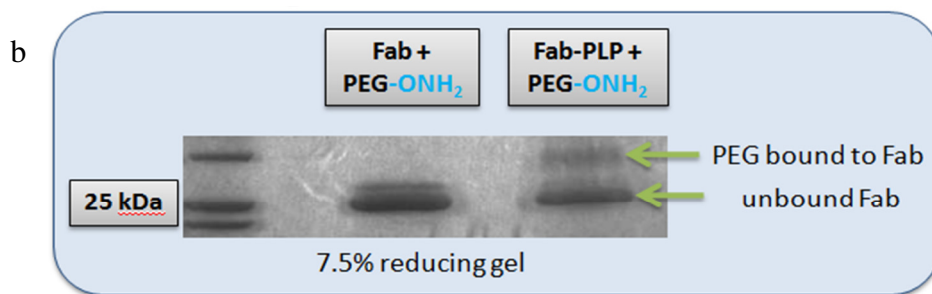
Figure A4. a) Confirmation of Fab fragment transamination through conjugation of Alexa 488-ONH$_2$ (lane 3). PLP-modified Fab (lane 1) and unmodified Fab to which Alexa 488-ONH$_2$ was added (lane 2) show no signal. b) Confirmation of Fab fragment transamination through conjugation of a PEG-ONH$_2$ chain. In lane 1, only the band for unmodified Fab fragments appears, whereas in lane 2, two bands appear, the upper band indicating conjugation of the 5kDa PEG-ONH$_2$.

Conjugation of Antibody Fragments to Microparticles

UV-Vis Spectrophotometry measurements of antibody fragments conjugated to PLGA and PLGA-ONH$_2$ microparticles revealed a greater than 2-fold increase in the number of fragments on PLGA-ONH$_2$ vs. PLGA microparticles (data not shown).

Discussion and Conclusion

Recent work by the Francis group at UC Berkeley has demonstrated the ability to selectively conjugate N-terminally transaminated antibodies, antibody fragments, or proteins to alkoxyamine-functionalized moieties (e.g., polymer chains)[19,21–23]. As the oxime bond formed requires the presence of a ketone or aldehyde (which are not naturally found on proteins), this reaction promotes a unique interaction between the protein and the alkoxyamine-functionalized moiety. We have taken advantage of this chemistry here to chemoselectively conjugate antibody fragments to the surface of PLGA microparticles.

Adsorption or conjugation of antibodies to microparticles for drug delivery or imaging is widespread, though suffers from a number of concerns. Passive adsorption or non-specific conjugation of antibodies (through reaction with any number of lysine amines or carboxylates occurring in most proteins) can lead to improper protein orientation or changes in conformation, leading to decreased targeting efficiency or inactivity[15,17]. In addition, antibody-coated microparticles destined for injection into the circulation may be more rapidly cleared if macrophage-recognized Fc fragments are exposed at their surface[24,25].

We therefore generated Fab fragments from whole IgG antibodies and modified their N-termini to ketones. These N-terminally-transaminated fragments react selectively with alkoxyamine functional groups on the surface of microparticles providing consistent orientation

94

of antibody fragments on the microparticles. This chemosolective conjugation strategy could help increase targeting efficiency of microparticles used for drug delivery or imaging. In addition it can easily be extended to conjugation of peptides or proteins of choice.

Future Work

Originally the antibody-functionalized particles were to be used as transforming growth factor beta 1 (TGF-β1) 'sponges', to remove circulating TGF-β1 from the blood stream. We later discovered that TGF-β1 does not exist in its active form free in the bloodstream, but is in fact inside platelets. The proof-of-principle is still important and such particles – that promote favorable orientation of antibodies – could be adapted for a variety of applications in drug delivery or imaging.

This section will discuss some of the pitfalls of the project and what future work should be completed if a future student decided to continue the project.

Microparticle aggregation and antibody availability

One of the main issues with which we dealt was microparticle aggregation. Although microparticle size was low initially (sometimes under 100 nm), particles aggregated over time due to their hydrophobicity. In general, smaller microparticles have a higher residence time in circulation[24,26]. In addition, hydrophilic, neutrally-charged surfaces also promote longer circulation times[26,27]. The issues with using PLGA could be solved quite simply by moving to a PLGA-polyethylene glycol (PLGA-PEG) nanoparticle system. PEG is hydrophilic and neutrally charged and upon formation of nanoparticles would partition selectively to the surface of the nanoparticles. PEG-coated nanoparticles would be resistant to aggregation based on a number of factors (e.g. hydrophilicity, neutral charge, water structuring, entropic repulsion of compressed chains[27]) and would have increased circulation times. Furthermore, although the conjugation strategy would have to be modified to account for the use of PLGA-PEG, we would gain an additional advantage. Antibodies functionalized to the PEG chains would extend away from the surface of the nanoparticles which would likely improve their antigen accessibility.

Antibody functionality and efficacy

Previous work in the Francis group at UC-Berkeley showed that PLP-modified antibody fragments still retain their ability to recognize and bind their antigen epitopes[21]. After conjugating a specific antibody to the surface of the nanoparticles, their functionality will need to be tested. An assay similar to an ELISA could be performed where the antibody-functionalized nanoparticles are used to bind a certain antigen, and then a second, labeled antibody, specific to the same antigen is introduced (e.g. fluorescent label) and fluorescence is measured after removing any free antibodies or antigen/antibody complexes, for example via dialysis. After the

nanoparticle surface antibodies' ability to recognize and bind antigens is confirmed, future work could examine their efficacy in specific applications, to be defined by the researcher.

Acknowledgments and Funding